Diploma Thesis

Methodic Benchmark for the Characterization of Batterycells and -packs

Michaela Winter

Institute of Electrical Measurement and Measurement Signal Processing
Graz University of Technology
Head of the Institute: Univ.-Prof. Dipl.-Ing. Dr. techn. Georg Brasseur

Supervisor: Univ.-Doz. Dipl.-Ing. Dr. techn. Daniel Watzenig

Advisor: Stephan Kunzfeld, MSc.

Graz, in February 2013

Kurzfassung

Das Thema dieser Arbeit ist der Methodenvergleich zur messtechnischen Charakterisierung von Batteriezellen und -packs.

Als Testobjekt wurde eine A123-Zelle, zylindrischer Form und hoher Leistungsdichte verwendet. Es handelt sich um eine Lithium-Ionen-Batterie, die gute thermische Eigenschaften aufweist. Die zugrunde liegende Lithium-Ionen-Technologie dominiert den Markt in Hinblick auf Kosten und Eigenschaften, besonders wenn es um den Antriebsstrang eines Fahrzeuges geht.

Eine Recherche zu Batterievermessungsmethoden wurde durchgeführt. Das Ziel der Recherche ist die Reduktion der Rechenzeit und die Steigung der Genauigkeit der ermittelten Parameter. Zwei Methoden schienen in diesem Vergleich vielversprechend zu sein. Es handelt sich dabei einerseits um ein Pulsen mit weiterführender Parameterfindung im Zeitbereich und andererseits um die sogenannte Impedanzspektroskopie, welche eine Fourier Transformation der Signale vorraussetzt, um die Parameter aus einem Nyquist-Diagramm zu errechnen. Unter Berücksichtigung der Eigenschaften dieser beiden Methoden wurde eine passende Topologie für das zu parametrierende Ersatzschaltbild gewählt.

Bei der Umsetzung der Methoden konnten die jeweiligen Vor- und Nachteile direkt verglichen werden, wobei auf die Nicht-Linearität, die stationäre Eigenschaft und das dynamische Verhalten der Batterie Rücksicht genommen wurde. Verschiedene Ladezustände wurden vorgegeben, in denen die Spannungsantwort auf die Stromanregung der Methoden gemessen wurde. Im Rahmen der Arbeit wurden alle Messungen bei Raumtemperatur durchgeführt.

Auf die jeweiligen Messwerte wurde die Methode der kleinsten Fehlerquadrate angewandt. Die ermittelten Parameter wurden mittels Matlab Simulink simuliert und das zugehörige Ausgangssignal mit einem gemessenen Spannungssignal verglichen.

Die erfolgversprechendste Methode zum Testen der Batterien für automobile Anwendung ist jene, bei der die Parameterfindung im Zeitbereich erfolgt. In Anbetracht dieses Ergebnisses ist eine Prozedur ermittelt worden, das Ersatzschaltbild für zukünftige Emulation in Testumgebung einfach, effizient und exakt zu erstellen.

Abstract

The subject of this thesis is the comparison of methods for the metrological characterization of battery cells and packs.

A cylindric A123 lithium ion cell of high power density is used, which possesses good thermal characteristics. The underlying technology dominates the market for vehicle propulsion with regards to cost and performance.

Within this thesis a research is carried out. The aim of the research is the reduction of the calculating time and increase of accuracy of the obtained parameters. Two methods are established and subsequently investigated. On the one hand, it is a pulse excitation, where the parameters are determined in the time domain. On the other hand it is the so called impedance spectroscopy, where a Fourier transform of the signals is required, in order to obtain the parameters from the Nyquist plot. Taking the properties of these methods into account, a suitable topology for the equivalent circuit diagram to parameterize is selected.

Testing the two methods, their respective advantages and disadvantages are directly compared. The stationary and the dynamic behavior of the battery as well as its nonlinearity are factored in. Different states of charge are examined when measuring the voltage response for the respective methods' current excitations. All measurements are done at room temperature.

The method of the least squares fit is part of this implementation for each measurement data. Furthermore the resulting parameters are simulated using Matlab Simulink and the output signal is compared with a measured voltage signal.

Moreover the most promising method for testing batteries for the automotive application is the one, where the parameter determination is executed in the time domain. Considering this result, a standard procedure is found so that the equivalent circuit diagram can be acquired easily, efficiently and accurately for future emulation in a testing environment.

Statutory Declaration

I declare that I have authored this thesis independently, that I have not used other than the declared sources / resources, and that I have explicitly marked all material which has been quoted either literally or by content from the used sources.

....
date (signature)

Acknowledgment

I would like to thank all those people who made this thesis possible.

First of all, I would like to express my deepest sense of gratitude to Dr.mont.Alexander Thaler at the Virtual Vehicle Research and Test Center and Dr.techn.Daniel Watzenig at the Institute of Electrical Measurement and Measurement Signal Processing, who supervised me and offered their continuous advice and encouragement throughout the course of this thesis. I thank them for the systematic guidance and great effort they put into training me in the scientific field. I am indebted to Dr.techn.Bernhard Schweighofer, Dipl.-Ing.Manes Recheis and Dipl.-Ing.Harald Brandstätter for their selfless support especially in the matter of measurement.

I would like to express my very sincere gratitude to Dr.techn.Kurt Gschweitl, Stephan Kunzfeld, MSc. and all other colleagues from AVL List GmbH to make this thesis possible. Very special thanks to Ing. Dietmar Niederl for his selfless support.

I am very thankful to Dipl.-Ing.Werner Konrad and Alexander Eder for the support and encouragement whenever I was in need.

Finally, I take this opportunity to thank my parents for their continuous support - both spiritually and materially.

Contents

1. Abbreviations

EV	Electric Vehicle
HV	Hybrid Vehicle
SOH	State of Health
SOC	State of Charge
Li-ion	Lithium Ion
NiCd	Nickel Cadmium
NiMH	Nickel Metal Hydride
EIS	Electrical Impedance Spectroscopy
I	Electric Current
U	Voltage
Z	Impedance
ϕ	Phase Shift
SNR	Signal-to-noise ratio
OCV	Open Circuit Voltage
Q	Electric Charge
Q_{max}	Battery Capacity
ω	Angular Frequency

D	Diffusion
l	Diffusion Length
c	Shape in Nyquist Plot
MC	Measurement Card
DAQ	Data Acquisition
A	Area
T	Length of Period
f_{sine}	Sine Frequency
FFT	fast Fourrier transform
$f_{sampling}$	Sampling Frequency
ϕ_u	Phase Shift of the Voltage
ϕ_i	Phase Shift of the Current
Z_{real}	Real Part of the Impedance
$Z_{imaginary}$	Imaginary Part of the Impedance
R	Resistance
C	Capacitance
Z_{RC}	Impedance of Paralleling R and C
e	Error Constant
a	Weighting Coefficient

LSQ	Least Squares
f_s	Sweep Frequency
C_{sc}	Semi-Circle Capacitance
R_{sc}	Semi-Circle Resistance
Im_{MAX}	Maximum Imaginary Part
L	Inductance
CC	Constant Current
CV	Constant Voltage

2. Introduction

2.1. Motivation

The company, which is the initiator of this diploma thesis, develops electric powertrains as well as instrumentation and test systems. As the simulation or emulation of a battery is desirable, an equivalent circuit diagram is a useful tool to describe a battery. This equivalent circuit diagram is a trade-off between accuracy and computational costs. In addition, it includes no information about the test item's electrochemical behavior. The battery is not stationary, so many parameters have to be found as an input for a proper simulation/emulation. Considerable progress has been made worldwide when it comes to finding circuit diagrams for battery cells. Unfortunately, the automotive industry cannot obtain much information from the measurement of one cell, if the goal is to simulate/emulate the performance of the engine, the inverter or the entire powertrain on the road. The usual component used in a vehicle is a pack, consisting of modules and other hardware, such as the battery controll unit. In addition each module further consists of cells. Therefore, the behavior of the a battery pack with all its components or at least a battery module would be much more significant. The goal of this diploma thesis is to find the most propitious measuring method for a pack or a module. Though the battery types differ, the parameter determination should be as simple, cost-efficient, accurate and quick as possible.

2.2. Content of the Thesis

Papers, books and dissertations serve as a source of information in order to find the most propitious measurement type. Chapter 3: The common elements used in an equivalent circuit diagram are described. A suitable equivalent circuit diagram for this diploma thesis is developed. Some adequate measurement methods are listed with their advantages and disadvantages. Chapter 4: In order to compare the two most promising methods, an A123 cell of high power density, characterized by good thermal behavior, is measured. Further processing is done using Matlab. The developed cell model is validated using measurement data. Chapter 5: The results are summarized and interpreted. Possible future research work is proposed.

2.3. Electric Vehicles

An electric vehicle is driven by electrical energy. The main propulsion elements, which differ from a common fossil fuel vehicle, are the energy storage system, electrical machine and appendant inverter. A hybrid of these two possible power train types is the electric hybrid vehicle. It includes both the electric and the fuel propulsion components. These cars gained importance in recent years. Articles like "The Importance of Electric Vehicles" [Cheesman, 2011], "Study Emphasizes Importance of China's Transition to Electric Cars" [Berman, 2011]

or “Senator Alexander, Nissan and PEW highlight importance of electric vehicles in clean energy economy” [Times, 2011] show that the rising request for electro mobility force vehicle manufacturers worldwide to act: “China’s oil consumption is expected to rise to 11.6 million barrels per day by 2020, from 7.6 million in 2007. Half its oil currently is imported [Berman, 2011].” “In March, the United States spent $39.3 billion on oil imports, the highest level in nearly three years, and net oil imports represented 65 percent of the U.S. trade deficit [Times, 2011].”

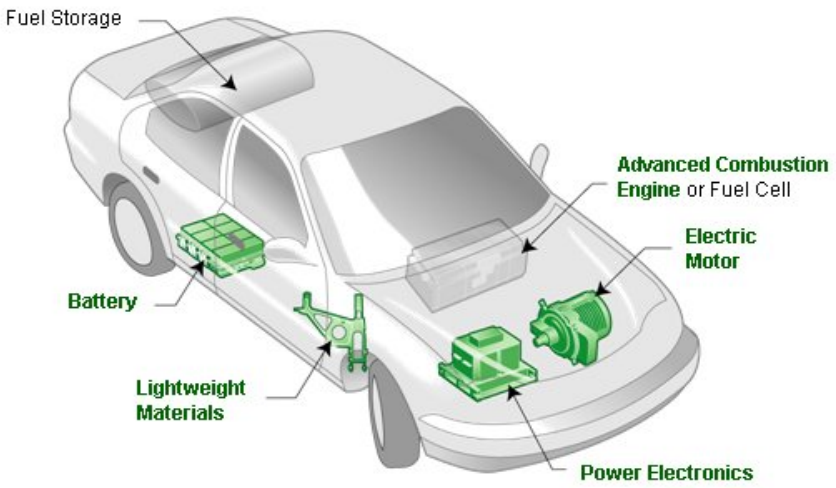

Figure 2.1.: Hybrid Electric Vehicle [Energy, 2013]

However, research concerning electric propulsion is not in its infancy. Already in 1997 the Toyota Prius was introduced in the Japanese market. Nearly 18,000 were sold in the first year [Vehicles, 2011]. As the development proceeded, the constituent parts of the electric drive train became less expensive and more efficient. The development methods became more refined. This is also true for batteries.

2.4. The Challenge of the Efficient Battery

The battery characteristics are a huge part of the challenge concerning electric vehicle development. The general requirements are challenging and there is still no cost-effective solution which would satisfy the average user. Chemical properties are a limitation to the required parameters which are not easily recognizable when testing a battery.

Test specifications were created, some in shape of testing standards in order to support the formation and testing section in evaluating the battery, not underestimating numerous properties, which are so very important in the adoption to the electric propulsion. Some of these properties would be the following:

2.4.1. High Energy Density

Energy density describes the amount of energy which can be stored in a battery in relation to its volume.

The geometry of the electrodes effects the storage capacity and limits the energy density. The power density is also limited by the composition of the electrodes. Their surface affects the reaction rates as well as the aging caused by undesired layers [Wegleiter and Schweighofer, 2012].

2.4.2. High Specific Energy

The specific energy describes the energy which can be saved in the battery in relation to its mass [Wegleiter and Schweighofer, 2012].

It is always necessary to relate the Energy or Power of the battery to the battery's mass and volume. This aspect is important for an electric combustion, because the volume as well as the mass of these storage devices need to be carried in the vehicle. Whether energy or power is the important characteristic of the battery is to be decided with regard to the type of electrification (such as EV (Electric Vehicle), HV (Hybrid Vehicle) as full hybrid or mild hybrid).

2.4.3. Temperature Independence

Temperature is another important parameter when it comes to batteries. Li-Ion batteries for example are sensitive regarding the influence of temperature. Their inner resistance decreases with low temperatures and so does the capability of the battery to serve as an energy source, because the lower voltage limit is then reached sooner. High temperatures cause fast aging. The battery should be as temperature independent as possible. Nowadays, when it comes to electric drive trains, cooling is necessary and not always easy, because every cell needs to be temperated properly. If one single cell is damaged, it may be uneconomically to replace it, it could be irreplaceably attached to the pack, or, even worse, a safety issue. In addition, the cooling equipment is voluminous and heavy in relation to its complexity and has to be carried in the vehicle as well.

2.4.4. Durability

Unfortunately, batteries which are capable of the high performance needed for an electric combustion usually rely on expensive Li-Ion technology [Andre et al., 2010]. All batteries age over time, even if they are not used and of course they age with the number of cycles they have to endure as well. These circumstances make it hard to determine the exact durability of a battery, especially if it is new on the market. The question then has to be how much the cell is actually in use. If there is no data from users (e.g. regular SOH (state of health) measurements or even battery failures) the question must be answered by the laboratory. This regularly results in extrapolation, in order to determine the durability without having to wait for years.

As mentioned above, another aging factor is temperature. In figure 2.2 the aging of a Li-ion cell can be seen as the remaining cell capacity decreases over time. Each point was obtained as an average over 3 tested cells. Furthermore, four different temperatures were set, so that

not only the time-, but also the temperature influence can be seen when it comes to aging effects.

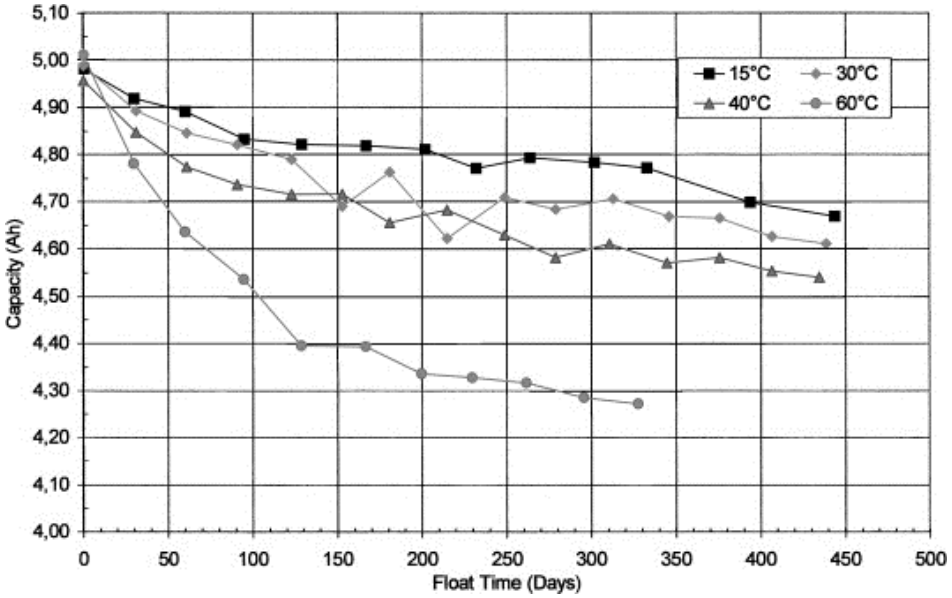

Figure 2.2.: Durability [Broussely et al., 2001]

Capacity decreases are often taken as an indicator for the battery's SOH in %. The SOH is 100% at the time of manufacture. There are more indicators for the SOH though, such as internal resistance, voltage, self-discharge and ability to accept a charge.

The cycle life of Li-Ion batteries depends on its chemistry and is maximal 10 000 in number. There are, however, considerations to integrate the Li-Ion battery packs into the electrical grid (while they are plugged) as soon as they are numerous enough to count as an additional source, compensating when the demand for current is high. So the commercial aim would be to make the battery less expensive and increase its durability as much as possible [Wegleiter and Schweighofer, 2012].

As a battery ages, its behavior change as well. In this thesis, the SOH shall not be regarded further. The measurement data is accurate though, because the battery does not age in the short time the measurements were performed. As a consequence, there is no inconsistency in the data deliverables.

2.4.5. Safety

Safety is always a big issue with new technologies.

The Li-ion pack in the car can be counted as a new technology. While accidents involving Li-Ion cells often feature prominently in the news, statistics show that this technology is as safe as others. Temperature limits causing thermal runaway are about 150°C for cobalt cathodes and 250°C for mangan cathodes [Buchmann, 2012]. Short circuitry within a cell is an effect which could warm it up. It occurs when microscopic metal particles come in contact with other areas of the battery. As the maximal energy density for the known chemistry

seems to be nearly reached, the manufacturers focus on these circumstances so that accidents due to short circuitry are continuously declining.

So the Li-ion chemistry is as safe as others and it still dominates in regards to cost and performance compared to alternatives (such as the fuel cell, flywheel mass or supercap).

2.5. The Li-ion Battery

The above mentioned properties are the reason why the Li-ion battery is used for testing.

A Li-Ion Battery is characterized by the lithium ions which move from the negative electrode to the positive electrode when discharging and backwards when charging. So "Li-ion battery" serves as an umbrella term for all batteries with lithium ion basis. Proven chemistries would be $LiFePO_4$ or $LiMn_2O_4$. Today's battery experts are still researching the underlying chemistry of the lithium ion technology in a quest for even more desirable properties. An example for this would be the effort where air was used in a composite electrode. Prototypes reach an energy density of 2500 Wh/kg and an endurance of more than 15 years. The usual voltage of a Li-ion cell is 2-4.3 volt. The electrolyte of a Li-Ion cell is not aqueous, an aqueous electrolyte would decompose because of the high voltage values. The limitation for aqueous electrolytes would be 2.2 V. Examples are secondary cells, which are not on Li-Ion basis, such as NiCd (1.2 V), Lead Acid (2 V) and NiMH (1.2 V) [Wegleiter and Schweighofer, 2012].

Li-Ion batteries require low maintenance, they show no memory effect and have no need for scheduled cycling to ensure durability [Buchmann, 2012].

2.5.1. Battery Testing

The more battery testing becomes a common procedure, the more obvious it is that for testing other components, the real battery may be just another source of inaccuracy in the testing environment. Influenced by temperature, SOH and fabrication variances above others, the real battery should not be part of the testing equipment of an inverter or an electrical engine. For the purpose of reliable data collection, the battery needs to be emulated. A power source of sufficient accuracy and power, where current, voltage and power can be set arbitrarily may be an alternative.

The emulation of the battery is just one example to prove the necessity of the equivalent circuit diagram to describe this energy storage device. Once obtained properly, there are much more possibilities to apply the data.

Finding the fitting equivalent circuit diagrams and the methods to obtain their parameters, is the challenge concerning further emulation.

3. Battery Model Determination

The principal properties of batteries make characterizations difficult. Batteries are not stationary, highly nonlinear, and their dynamical behavior depends on different parameters like temperature, SOC (state of charge) or short term history. Therefore, a suitable method has to be found, where comparability of the data deliverables to the real battery meets the cost- and time-efficiency of the cycling. This is why methods are compared in this chapter in order to find a fitting one. Afterward, an equivalent circuit diagram needs to be chosen, which is then parameterized using this method.

3.1. Methods

A possibility to characterize a battery is to disassemble it into its components. A battery cell is manufactured under certain conditions, so the main disadvantage of this method is that the disassembly of the unit undergoing the test is irreversible and as a consequence the battery is lost. In addition, for the understanding of a battery and its behavior it is desirable to test it as a whole. Fortunately, many experts already put much effort into developing methods for battery testing, which do not require destroying the test unit. These methods treat the battery as a system, where some input, such as current or voltage, results in an output. So the behavior of the battery to a certain signal delivers information about its composition. Further on, the behavior is a good indicator of what the battery's output is in general.

There are two popular computing environments for such methods, the time domain and the complex variable domain.

3.1.1. Time Domain

The methods described in this chapter refer to the ones evaluated in the time domain. This means that the evaluation's underlying data is characterized by its time series. As the measured raw data usually provides a time series, no transformation into another computation environment is needed for the evaluation in the time domain. Figure 3.1 shows signals for such a method whose basis is the time domain. In the case of a battery, the input is a current signal and the output is a voltage signal. The battery is the system whose characterization is desired.

The input current can be a signal of different shapes. A step function is such a signal which is close to the battery's application in typical use.

3.1.1.1. Step Function

In figure 3.2 the principle of a step function is illustrated. In the case of a battery measurement, it will not endure infinitely and the height varies with the cells' properties and the purpose of the testing. The data procedure is done as follows: After current pulsing, the resulting voltage traces, transient and stationary, are being measured for further parameter

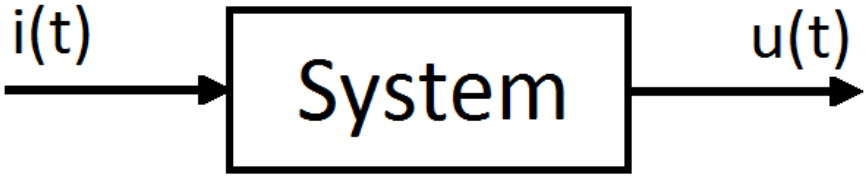

Figure 3.1.: System of the Time Domain

determination. A simple equivalent circuit diagram needs then to be chosen, so that the parameterization can be done by reverse calculating the step response using basic electric rules, such as a system matrix.

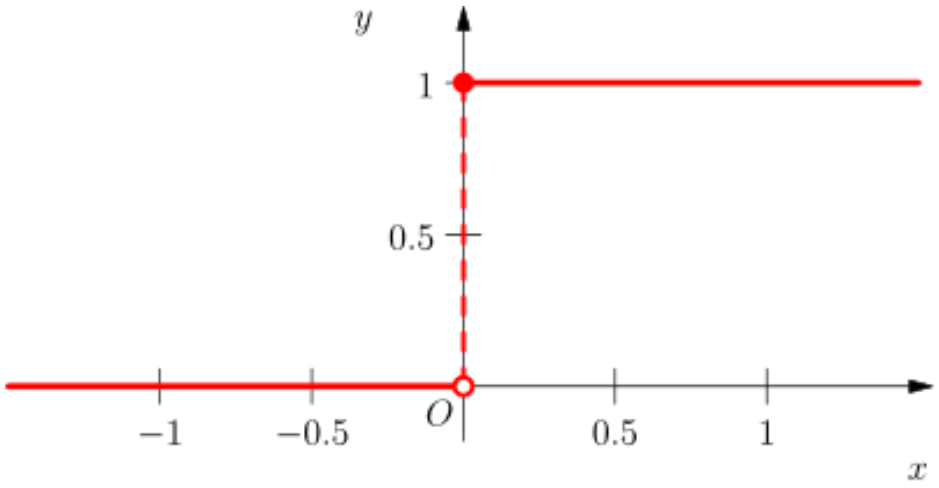

Figure 3.2.: Step Function

3.1.1.2. Advantages

The data acquisition requires no FFT or other transformation into another computation environment. It is experimentally easily accomplished.

3.1.1.3. Disadvantages

The equivalent circuit is mathematically restricted to simple elements like the RC-element and the inner resistance. Implementation of additional components like the Warburg impedance or the Zarg element [Buller, 2005] are common tools when it comes to the EIS (Electrical Impedance Spectroscopy), but not for the step function evaluated in the time domain. These elements are described in more detail in chapter 3.2.

3.1.2. Complex Variable Domain

The methods described in this chapter refer to the ones evaluated in the so-called complex variable or frequency domain. This means that the evaluation's underlying data is complex. Such a diagram does not have a time axis, but a real and an imaginary part of the complex variable as x- and y- axis.

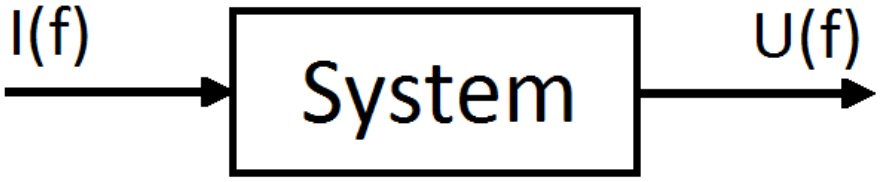

Figure 3.3.: System of the Complex Variable Domain

The system in figure 3.3 is the unit under test. In this case it is a battery cell. A current signal is chosen and the resulting voltage is measured. In order to obtain the values for a Nyquist plot from the current and the measured voltage response, both signals are transformed into the complex variable domain using the Discrete Fourier Transforms to determine the battery's impedance [Thele, 2008]. In order to obtain useful data, a wide frequency range, which reaches from about 1 mHz to 1 kHz [Buller, 2005], needs to be covered by determining the impedance for each frequency, while the distance between these chosen frequencies has to be sufficiently small, so that the evaluation of the resulting Nyquist plot is possible.

The different possibilities to obtain the Nyquist plot for the calculation of the parameters for the equivalent circuit diagram are as a matter of principle limited. In the required frequency range, the voltage response needs to be obtained sufficiently accurately.

3.1.3. Impedance Spectroscopy

In the case of the EIS, the excitation signal is a sine. The current and voltage amplitudes and the phase shift are required for further calculation.

$$\mid Z \mid = \frac{U}{I} \tag{3.1}$$

$$Real\ part = \mid Z \mid \cdot cos(\phi) \tag{3.2}$$

$$Imaginary\ part = \mid Z \mid \cdot sin(\phi) \tag{3.3}$$

In equation 3.1, I is the current amplitude, U the voltage amplitude, Z is the impedance and ϕ is the phase shift between current and voltage.

Contrary to a capacitor, a battery's voltage is never 0 V. So there is a OCV, even if the battery is fully discharged and without load. The OCV is a function of the SOC, so it changes during charge or discharge [Thele, 2008]. Z = dU / dI is not equal to the quotient U / I. Hence, the AC current excitation has to be small compared to typical battery currents. The battery is nonlinear, but if the current amplitude is small, it can be pseudo-linear. Nonlinear voltage response can be recognized by undesirable harmonics of its excitation frequency, because the voltage response is then significantly affected by the SOC change during half a period.

SOC-calculation: The formula for Q, the electric charge is

$$Q = \int I dt \tag{3.4}$$

Q is the electric charge of the battery in general, but the maximum charge quantity of a battery is referred to as Q_{max} in As. This is the so called battery's capacity, the SOC represents the percentage of Q_{max} the battery is capable to store. For instance, 10% SOC means the batteries charge is $1/10$ of its Q_{max}.

Another reason for the limitation of the signal excitation is that using a higher current amplitude causes a strong influence on the spectrum (the curve seems to shrink), because the cell endures an increased cell temperature [Andre et al., 2010]. In this paper a 4°C difference in temperature was measured using a 1A amplitude, observing a cylindrical cell.

A current as low as 0.5 C is usually used.

In principle there were two measurement types [Sauer, 2006b]: The galvanostatic type, where a current signal is impressed, and the potentiostatic type, where a voltage signal is impressed. For the potentiostatic type, the amplitude could be controlled in case of reaction. However, in the case of a battery, the galvanostatic type is to choose. In regard to the potentiostatic type, the SOC may drift because of the asymmetric charge-/discharge reaction, as the SOC depends on the current, which is then a result of the voltage. In case of the galvanostatic type, however, the charge would be guaranteed. Additionally, it is much easier to overlay the measurement signal with the test signal, as it is a current. As mentioned before, high currents, which would occur in potentiostatic measurement types, only have undesirable effects on the data deliverable. The potentiostatic type would be modified if the amplitude of the current is adjusted in such a way that the voltage remains constant on a desirable level. Then voltage limitation and the above mentioned charge can be part of this modified method.

3.1.3.1. Advantages

The availability of measurement instruments as well as the accurate signal generating devices make it easier to use this technology [Barsoukov and Macdonald, 2005].

The SNR (signal-to-noise ratio) is better than using other methods (higher accuracy, clear differentiation between different frequencies).

3.1.3.2. Disadvantages

The data collection is slow because every frequency needs to be measured separately [Thele, 2008]. For p = 3 periods per measured frequency and N = 8 frequencies, a formula to calculate the duration of the measurement of a complete impedance spectrum TSPK is TSPK = 12 / fmin [Sauer, 2006b].

A justified question may be whether the above mentioned limitations of the currents' amplitudes/offset values might be a limitation when it comes to emulation of a high power application.

3.1.4. Band Limited Noise Response

Another possible signal shape is white noise. The white Gaussian distributed noise is characterized by different low amplitudes over a certain frequency range. There is no hint of the location of possible harmonic waves. White noise is a random signal with a flat power spectral density. In reality, the frequency bandwidth of white noise is always limited. White noise can be generated as an input current which contains the required frequency range for the Nyquist plot. The result is that for one Nyquist plot only one measurement is necessary.

3.1.4.1. Advantages

There is a short measuring period as there is only one signal [Barsoukov and Macdonald, 2005].

3.1.4.2. Disadvantages

Requires Gaussian distributed white noise and the need to carry out a Fourier analysis for a high signal-to-noise ratio which is highly inaccurate [Barsoukov and Macdonald, 2005]. Therefore, it is impossible to obtain a Nyquist plot from such data. In addition, fast data collection would be needed in order to obtain data for high frequency behavior.

3.1.5. Step Function

The step function is explained above for the time domain method. The shape of this signal is therefore in execution a pulse whose value is dependent on the application as well. The difference is that with this method the data is transformed to the frequency domain, basically disassembling the pulse into its frequency components.

3.1.5.1. Advantages

It is experimentally easily accomplished [Sauer, 2006a].

3.1.5.2. Disadvantages

The requested rise time of the input signal, measurement accuracy and time sampling rate (logarithmic) are challenging in comparison to other measurement methods [Bessler, 2007]. The higher the rise time, the more information can be obtained in the high frequency range. Therefore, the measurement also needs to be fast. The accuracy in evaluation of each measurement value may not be equal because the SNR differs using different frequencies [Barsoukov and Macdonald, 2005]. Additional information of one frequency is overlapping in appearance of harmonics with information belonging to other frequency data. As a consequence, one signal would not carry all frequency data, even if logarithmic and accurately measured. Because of the noise and the above mentioned overlapping, a maximum of 3 to 4 frequencies can be measured in order to guarantee the required accuracy. Thus, in comparison with other methods, measurement time cannot be significantly reduced.

3.1.6. Resulting Methods

Two methods were chosen to be compared by measurement and data acquisition. The EIS nowadays is a proven tool which is also accurate. The step function in time domain is simple in every regard and accurate. In terms of automotive application, a step function as a current excitation is practical. These two methods strongly differ in execution and shall be compared further by testing them in practice in chapter 4. As the measurement methods were chosen, a fitting equivalent circuit diagram needs to be found.

3.2. Possible Elements for an Equivalent Circuit Diagram

As the used elements are correlated –if possible– to chemical cell processes, empirical models should be simple and should consist only of few elements. The Nyquist plot of a Li-ion cell in principal is illustrated in figure 3.4. It is broken down into 5 sections which are defined by their underlying properties.

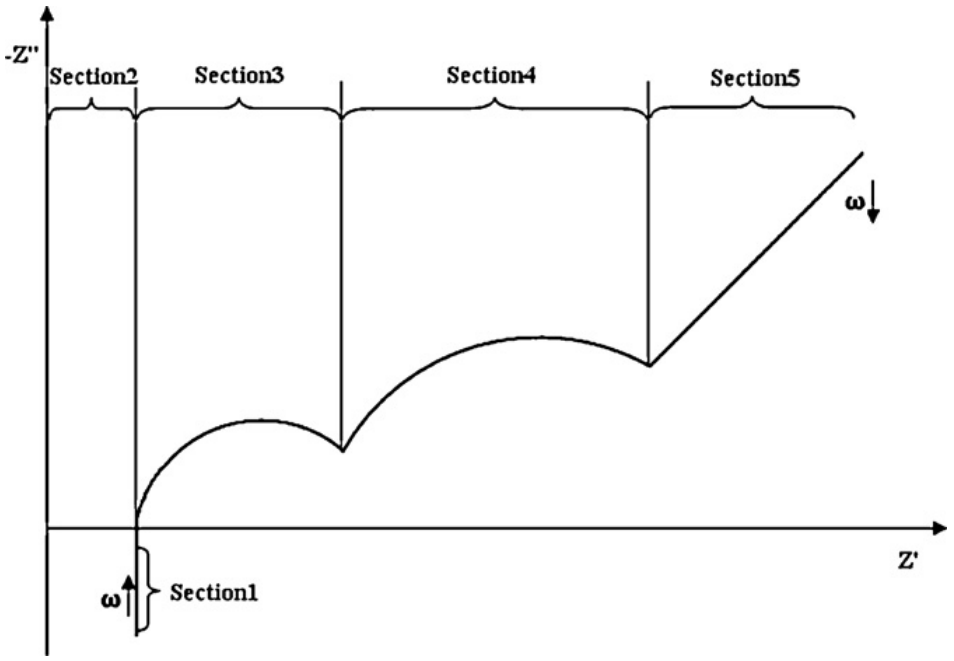

Figure 3.4.: Sections in Nyquist [Andre et al., 2010]

Section 1 is the inductance of the battery.
Section 2 ends with the intersection of the curve with the x-axis and represents the inner resistance of the battery.
Section 3 and 4 are in principle a semi-circles, which in a Nyquist plot is each a resistance in parallel to a capacitance.
Section 5 can be expressed as the so called Warburg impedance, which basically consists of a number of paralleled resistances and capacities [Wegleiter and Schweighofer, 2012]. For an angular frequency converging to 0, there would only be a capacity left. The section's underlying chemistry is further explained below.

3.2.1. Chemistry

The equivalent circuits consist of an internal resistor R_i, an inductor L, a double layer capacitor C_{dl} and the nonlinear charge-transfer resistor R_{ct}. The inductance is caused by the metallic connectors between the poles and the electrodes of the battery. The ohmic resistor R_i represents the limited conductance of the contacts, the inter-cell connections, the grids, the active masses and the electrolyte. R_i depends on SOC, age and temperature of the battery. The parallel connection of the capacitor C_{dl} and the nonlinear resistor R_{ct} represents the double layer capacitance and the charge-transfer resistance, respectively [Thele, 2008].

Double layer capacitance: The zone between the electrode and the electrolyte is called electrolytic double layer. As for the double layer interface, the nonuniform distribution of particles and charges occurring can be regarded as the double layer capacitance [Karden, 2001].

An additional semicircle may arise. It is usually associated with the solid electrode interface and can be found during cycling [Andre et al., 2010].

All above mentioned chemical properties of the cell can be expressed as simple electric components or particularly as RC-elements.

3.2.2. Zarg and Warburg

3.2.2.1. CPE

The CPE (constant phase element) can be used to model the properties of a stretched semicircle [Thele, 2008]. This is a possibility for a more accurate equivalent circuit diagram. The disadvantage is that it can never be physically a real component of an equivalent circuit diagram. The CPE is part of the Zarg element.

3.2.2.2. ZARG

The Zarg element can be expressed as a number of RC elements. It consists of a CPE paralleling a resistance [Thele, 2008].

3.2.2.3. WARBURG

The Warburg impedance is the holy grail when it comes to section 5 in figure 3.4. With this mathematical approach, the straight line is represented more accurately. As mentioned for the Zarg-element, the Warburg impedance does not seem to be a real component when it comes to physics either, but the line is actually formed by a defined number of RC-elements. The parameters of these RC-elements are mathematical interdependent, so that once determined, they can be simply described by a few values [Wegleiter and Schweighofer, 2012].

$$Z_\omega = \frac{c}{\sqrt{j\omega D}} \cdot tanh(\frac{1}{\sqrt{D}} \cdot \sqrt{j\omega}) \tag{3.5}$$

In equation 3.5, ω is the angular frequency, D the diffusion, l the diffusion length and c is an additional constant, basically describing the the appearance of the Warburg impedance in the Nyquist plot. This back-transformation provides evidence that, as mentioned above, a large amount of RC-elements does not require the same amount of variables to describe them.

$$R_i = \omega_i \cdot \frac{cl}{D} = \omega_i R_\omega \tag{3.6}$$

$$C_i = \frac{l}{2c} = C_\omega \tag{3.7}$$

$$\omega_i = \frac{8}{(2n-1)^2\pi^2} \tag{3.8}$$

3.3. Equivalent Circuit Diagrams

Figure 3.5 shows an example for a possible topology for the equivalent circuit diagram. One element is missing, though: the OCV dependence. Frequently a capacitance is used to describe the OCV in the equivalent circuit diagram. In this thesis, regarding the method in the time domain, the OCV is subtracted for equivalent circuit diagram parameterization and added afterward for the purpose of simulation. Regarding the method in the frequency domain, the SOC is changing by 1% at the most, so nothing is subtracted or suffering a loss of accuracy.

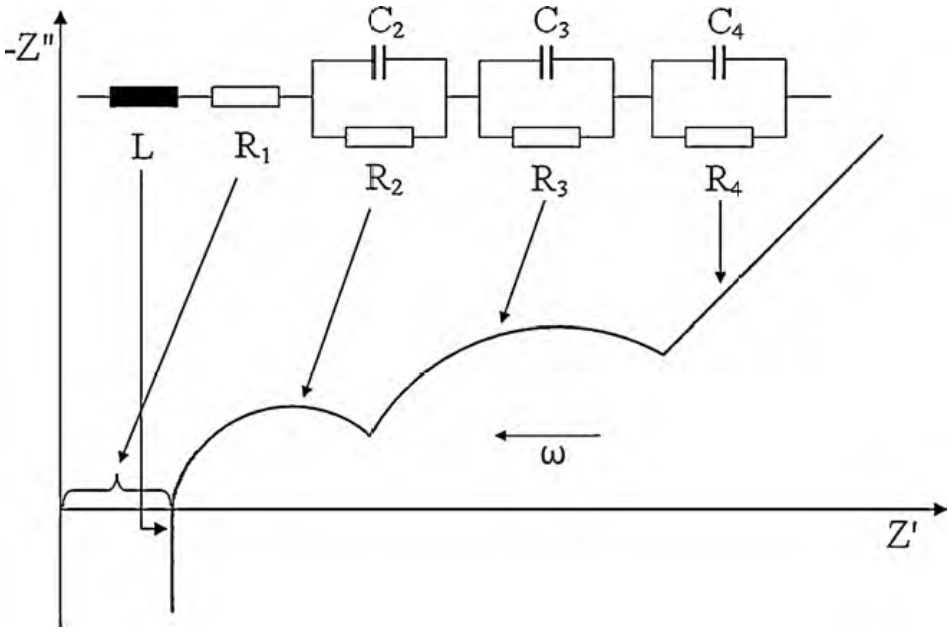

Figure 3.5.: General Topology [Andre et al., 2010]

The possibilities of elements combined in the equivalent circuit diagram to describe the data deliverables would be indefinite, not only in the frequency domain but also in the time domain. Figure 3.6 shows topologies which could result in one similar Nyquist plot if the parameters are chosen well (two semi-circles delayed on the x-axis). This is representative

for the numerous possibilities. The correlation between elements of the equivalent circuit diagram and the Nyquist plot are explained in detail in chapter 4.

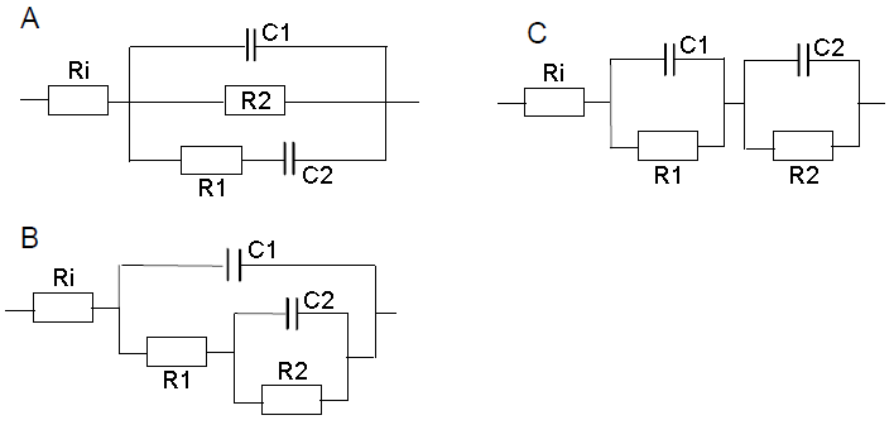

Figure 3.6.: Different Topologies Representing the Input/Output Behavior of Li-ion Cells

3.4. Examples of Use

In figures 3.7, 3.8, 3.9 and 3.10 possible equivalent circuit diagrams are depicted. They include the components described in 3.2. The classic and famous diagram of Randles [Tröltzsch, 2005] is illustrated in figure 3.7.

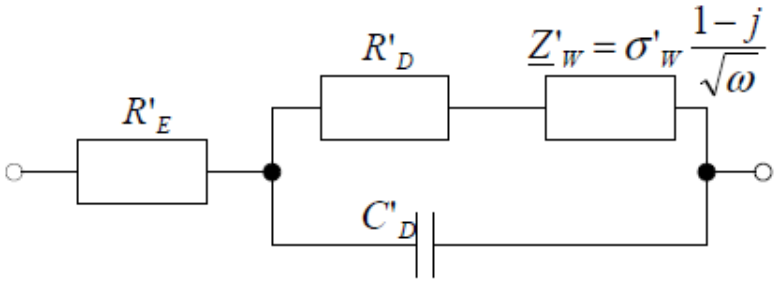

Figure 3.7.: Equivalent Circuit Diagram [Tröltzsch, 2005]

The equivalent circuit diagram in figure 3.8 is basically the same as the one depicted in figure 3.7. An inductance is added, which means that the inductive behavior occurring using a signal of high frequencies, were taken into account.

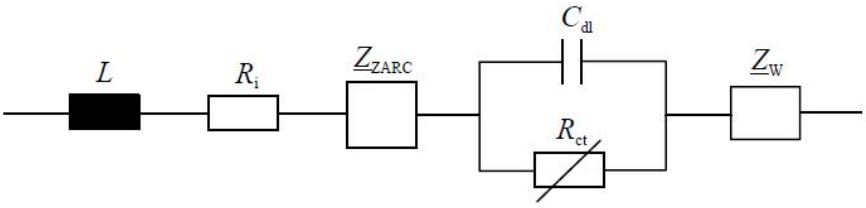

Figure 3.8.: Equivalent Circuit Diagram [Buller, 2003]

In figure 3.9 the positive and the negative electrodes circuit diagrams were modeled separately, in order to describe each electrodes chemistry further. Even tough the creator of this equivalent circuit diagram used the one of Randles as basis, the two diagrams would not include a Warburg impedance if they were combined.

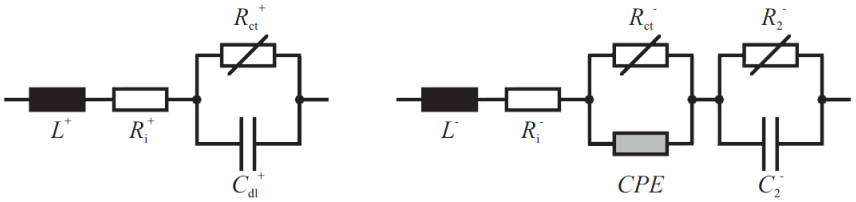

Figure 3.9.: Equivalent Circuit Diagram [Thele, 2008]

As the Zarg element and the Warburg impedance were adapted to the complex variable domain by their inventors, they cannot be used for the step function computation in the time domain. This is why, for comparison reasons, this thesis uses simple RC elements (2 or 3 in number) and an inner resistance, as shown in figure 3.10.

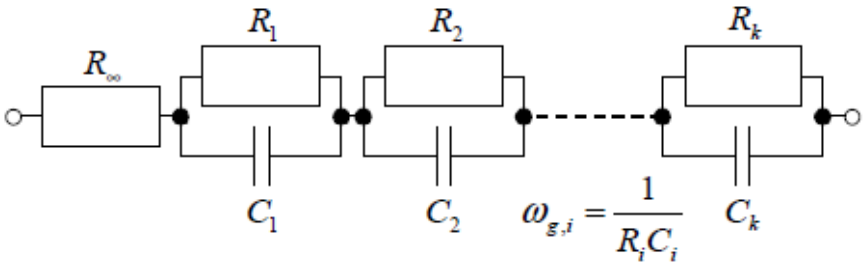

Figure 3.10.: Equivalent Circuit Diagram [Tröltzsch, 2005]

3.5. Resulting Equivalent Circuit Diagram

L, R_i and the double layer RC-element seem to be proven standard components for common battery equivalent circuit diagrams. The inductance is not of importance in the automotive sector where constant current or power excitations usually are the signals of choice. The controlling of an emulator is not usually as accurate, so that the inductance, occurring with very high frequency, does not matter for emulation. It might be critical, though, when it comes to the emulation on the inverter testbed later on, because the inverter changes load in the velocity of kHz. As the transient time of the usual test equipment is not close to the kHz range, the inductance shall be disregarded here in the final results.

4. Measurements and Results

In the following, the test assembly and its components are described. The unit under test was a Li-ion cell. As described in chapter 3, measurements were done for the two most auspicious methods, so that after data evaluation the whole procedure can be compared directly.

4.1. Test Assembly

All measurements were performed at room temperature. Consequently, the battery was set to room temperature before testing. The surrounding temperature during testing was also room temperature. Additionally, a PT100 served as a temperature monitor.

4.1.1. Unit Under Test

As a unit under test served a A123 high power Li-ion cell with nanophosphate technology. It has, according to the manufacturer, the capability of very high power, long cycle and calendar life as well as an excellent abuse tolerance.

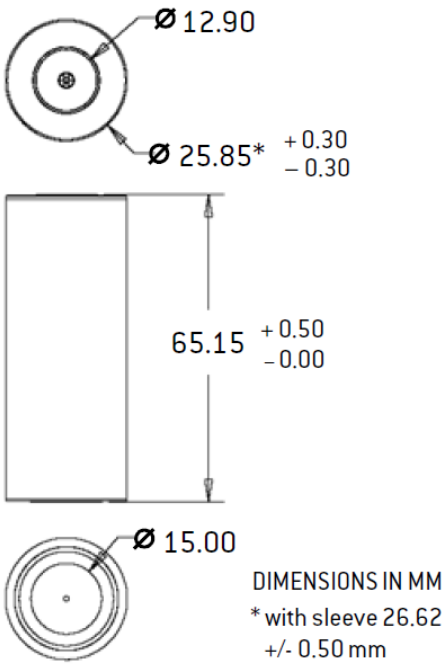

Figure 4.1.: Unit Under Test

It is a Li-ion cell of the type $LiFePO_4$. This type was chosen because it is used in the automotive area and because of its high power performance which still provides thermal safety. In figure 4.2 the thermal behavior is visualized by normalized heat flow over temperature. As technologies such as $LiNi_0.8Co_0.16Al_0.05O_2$ and especially $LiMn_2O_4$ show a typical, so called thermal runaway behavior, the $LiFePO_4$ cell's heat flow remains intact. Principally, the $LiFePO_4$ technology is known for its high specific power density and intrinsic safety. Its cycle stability is also remarkably high and it is inexpensive compared to other energy storage devices based on Li-ion technology.

The characteristics of this particular cell type, e.g. voltage plateaus (see chapter 4.2) or the Nyquist plot showing just a small semi-circle, make it hard to determine its parameters for the equivalent circuit diagram.

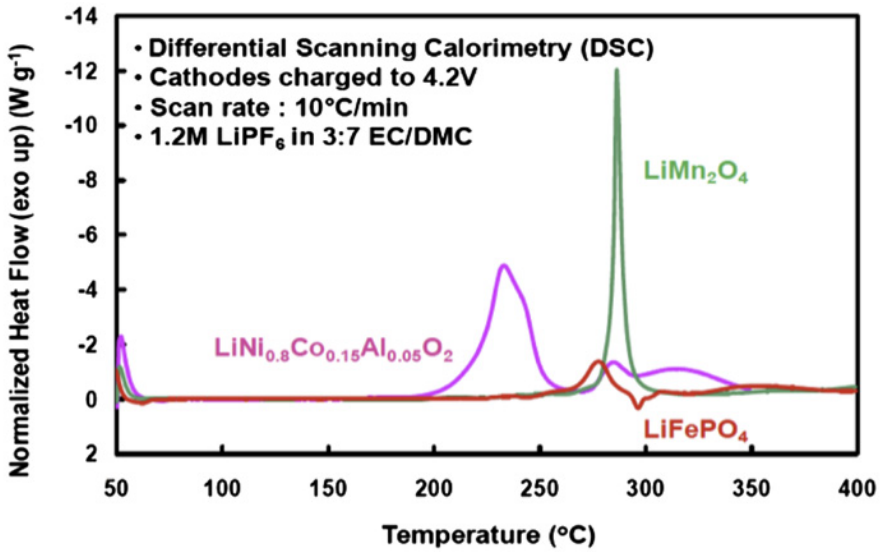

Figure 4.2.: Comparison Thermal Safety of Different Li-ion Cell Types [Zaghib et al., 2012]

4.1.2. Potentiostat

The Wenking HP96 is a signal generator whose output is suitable for the purpose of pulse- or sine excitation up to 4 kHz. The controlled current source can provide up to 96 V and 20 A with an accuracy of 0.5 mA.

4.1.3. Relays

The inaccuracy of the potentiostat is causing a 0.5 mA current even if the set current would be 0 A. For this reason, a relay is part of the test assembly 4.3 to prevent a falsification of the SOC during rest periods. It is controlled by the PC and is also controlled by cell voltage monitoring.

4.1.4. Measurement Box

Two parameters are measured by means of the measurement box: the electric current through the battery and the resulting cell voltage. The current is measured via a precision shunt. The advantages of the precision shunt compared to other methods such as current clamp are the thermal stability and the zero point accuracy. The measurement ranges are ±20 A and ±2 A. Depending on the application, one of these ranges is then converted to a voltage of ±10 V. The voltage signal allows an accurate readout for the analog input. The voltage measurement is provided via impedance converter, so that the measurement is of high resistance (M to G Ω range). Otherwise there would be a remarkable self-discharge noticeable, caused by a small resistance to the analog input. In order to increase resolution, the OCV for one particular SOC is measured and then subtracted from voltage output during excitation. In this case 40 mV are converted to 4 to 5 V for a more precise output. A computer adapter serves as power supply for the measurement box.

A second measurement box is used which is connected to the PC and provides 3 features: The analog output sets the voltage for the potentiostat. One digital output controlls the relay. Another digital output provides a rectangle for the watchdog which monitors if the test run is currently active.

4.1.5. PC Impedance Spectroscopy

The dSpace hardware is used as a workstation PC. Its usual test environment is in the area of fast prototyping. The resolution of 16 bit is standard for each channel. A functionality is included that if one of the 32 analog I/O channels fails, it automatically takes a value predefined by the user. A filter can be implemented directly for filtering the data beforehand.

4.1.6. PC Pulsing

The PXI-National Instruments hardware is used as a workstation PC for pulsing. Its resolution is 12 bit. The pulse measurement is precise enough (up to 10-30 kHz pulses possible) using the PXI-National Instruments.

4.1.7. Software

Matlab, installed in a proper windows operating system environment was used to implement and automate the required test runs. Using the data acquisition toolbox, it supports some digital- and analog output hardware.

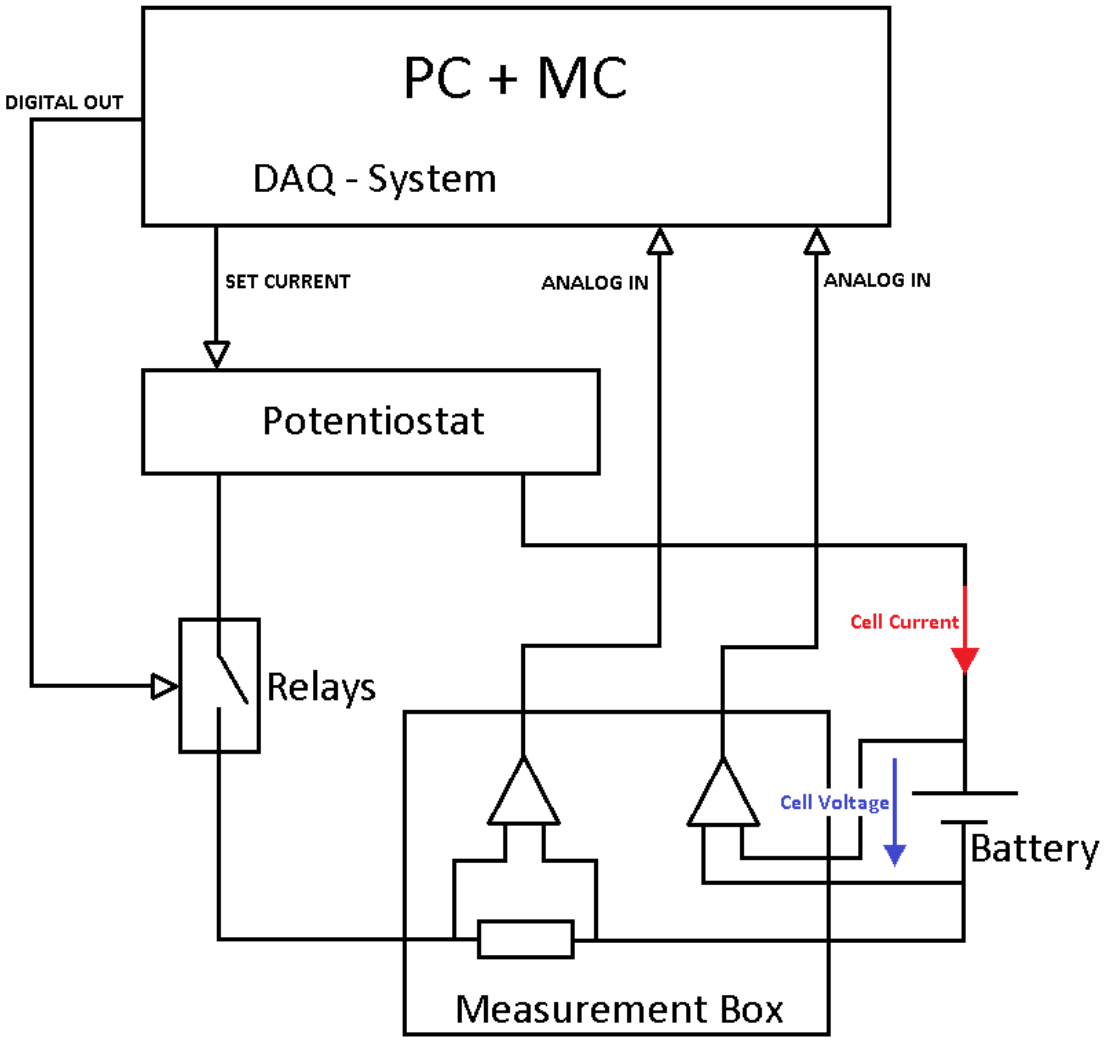

Figure 4.3.: Test Assembly

4.2. Complex Variable Domain

This chapter describes the evaluation of the method executed in the complex variable domain via Matlab computation. The Matlab program outputs the circuit diagram's parameters for each computed SOC value.

The measured data includes excitation current, resulting voltage, frequency of each sine signal and SOC of each measurement point. The time relation was not recorded because knowing the sine frequency, all additional data can be determined anyway.

Table 4.1 shows which SOC points were used as set points. The method for setting the SOC was to fully load the cell to 3.6 V and then discharge it using constant current excitation.

Number	SOC Set Points [%]
1	5
2	15
3	25
4	35
5	45
6	55
7	65
8	75
9	85
10	95

Table 4.1.: SOC Set Points

Table 4.2 shows which sine frequencies were used for current excitation for each computed SOC value. In order to perform a test as accurately as possible it is essential to include a rest period after setting the SOC by current excitation.

As only whole sine periods were cut of the measured data beforehand, windowing is not necessary in further processing.

4.2.1. Matlab Computation

The available data, which is the result of the measurements, is saved as .mat-files. Two are 'cell'-files, where every value saved in a vector contains another vector. These 'cell'-files each represent the current and the voltage of one SOC in each cell, where 24 different input frequencies were applied.

As mentioned in chapter 3, the battery is highly nonlinear and therefore there is no offset in the excitation current. Additionally, the value of the signal's amplitude was chosen to be 0.5C, so as not to influence the SOC during one period's half-shaft. As the current flow rises with the duration of a half-shift, the SOC change during half a period is frequency dependent. This is the reason why, for very low frequencies, the amplitudes were reduced such that the response is sufficiently accurate. In this case the exact SOC change allowed for one half shift is 1%. The nominal capacity of the battery is 2.3 Ah, so 1% 0.023 Ah is equivalent to 82.8

Number	Frequencies each Set Point [Hz]
1	4.167e+03
2	2.083e+03
3	1.042e+03
4	5.208e+02
5	2.604e+02
6	1.302e+02
7	65.104
8	32.552
9	16.276
10	8.138
11	4.069
12	2.035
13	1.017
14	0.509
15	0.254
16	0.127
17	0.0636
18	0.0318
19	0.0159
20	0.00795
21	0.00397
22	0.00199
23	0.000993
24	0.000497

Table 4.2.: Frequencies each Set Point

As. The area between half the sine wave and the x-axis equals the electric charge because $Q = \int Idt$. The computation of the capacity in dependence of the sine amplitude is as follows:

$$A = I \int_0^{\frac{T}{2}} sin(\omega t)dt \tag{4.1}$$

$$A = I(\frac{-cos(\omega \cdot \frac{T}{2})}{\omega} + \frac{-cos(\omega \cdot 0)}{\omega}) \tag{4.2}$$

$$A = \frac{I}{\omega} \cdot (1 + 1) \tag{4.3}$$

$$I = 82.8 \cdot \pi \cdot f_{sine} \tag{4.4}$$

In equation 4.1, A is the area between curve an x-axis, I is the current amplitude, ω is the angular frequency, T is the length of the period and f_{sine} is the current's sine frequency.

Figure 4.4 illustrates the resulting current amplitudes of each frequency from high to low frequencies as listed in table 4.2.

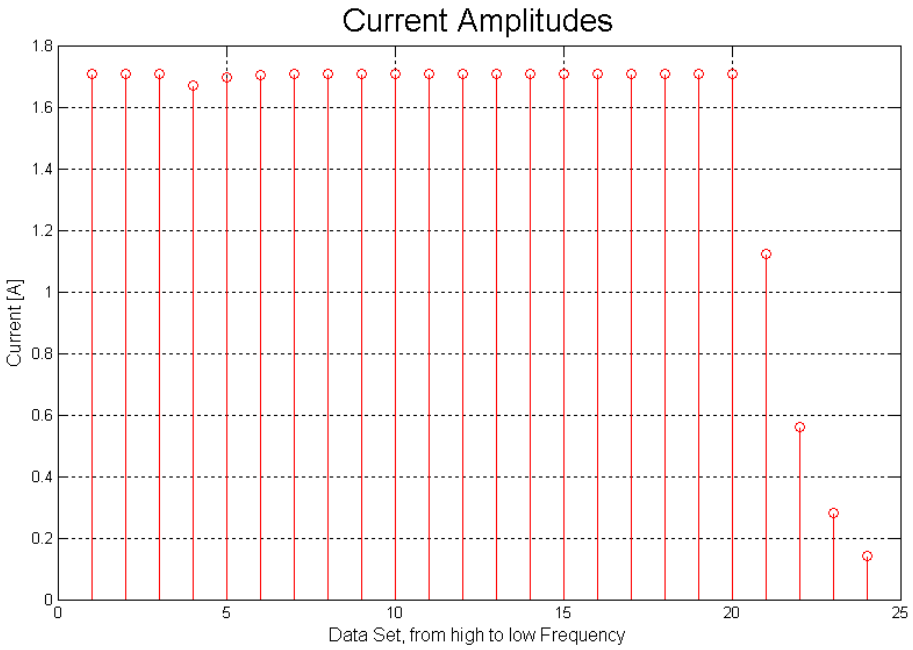

Figure 4.4.: Current Amplitudes

Figure 4.5 shows the resulting voltage amplitudes of each frequency.

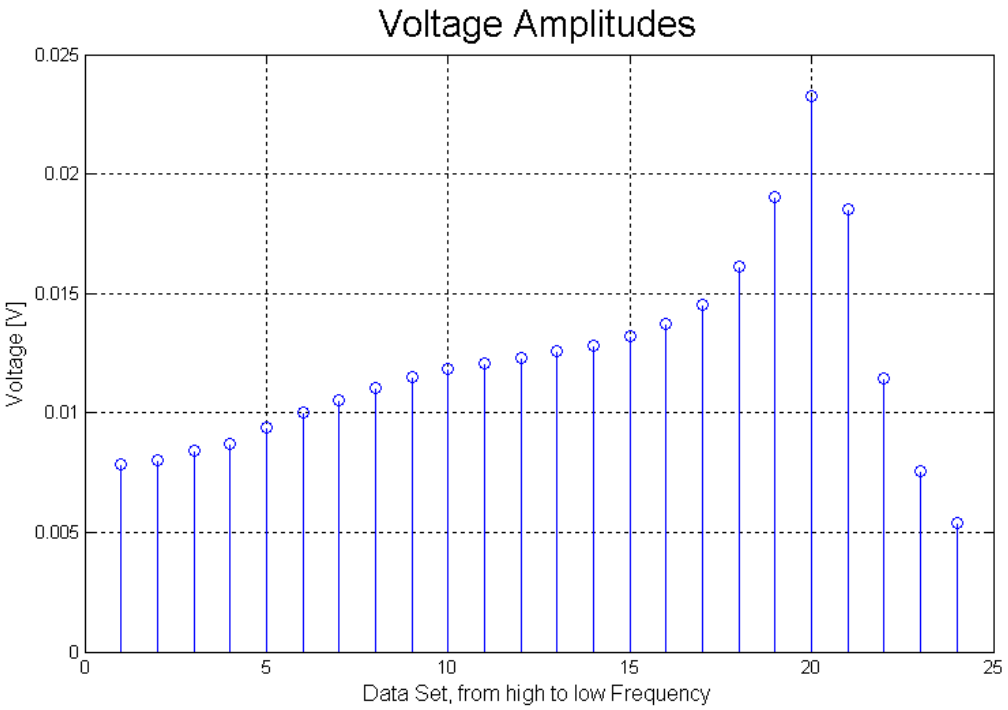

Figure 4.5.: Voltage Amplitudes

4.2.1.1. Fast Fourier Transform Resulting in Nyquist Diagram

As the parameters of the equivalent circuit diagram in impedance spectroscopy are usually obtained from the Nyquist plot, the impedance needs to be obtained in advance in order to obtain this Nyquist plot from the available data. It requires the phase shift between current and voltage signal and the amplitudes of both signals.

In figure 4.6 these values can be seen for the measurement at 260.4 Hz at the set point of 55% SOC.

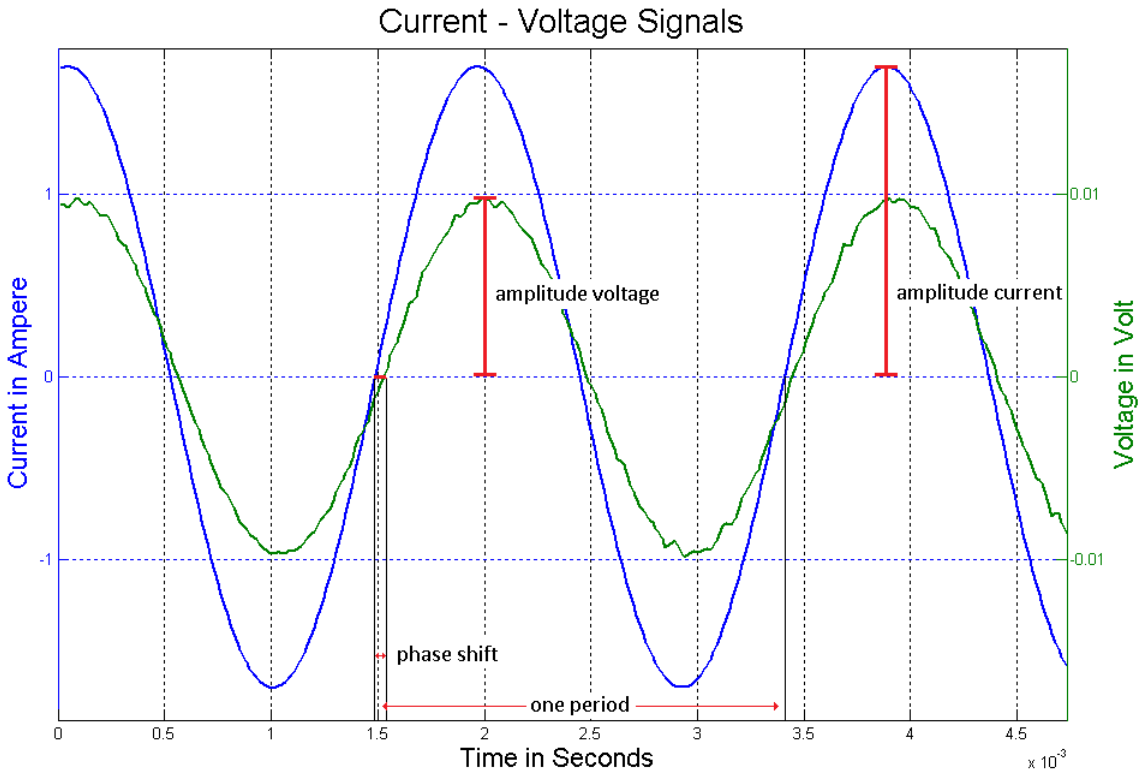

Figure 4.6.: Parameters to be determined via Fast Fourier Transform

For the time discrete measurement points, a discrete Fourier transform can be used to evaluate the required data accurately. Matlab provides the FFT (fast Fourier transform) operation which is basically resulting in the same data as the discrete Fourier transform but is mathematically more efficient.

First the FFT is done for the current and voltage output. As the values obtained from the FFT usually are complex, its absolute value is equivalent to the amplitude of the sine signal. The results need to be normalized, otherwise the value for the amplitude would just be a sum of all measurement points.

The normalization requires the sampling rate.

$$f_{sampling} = f_{sine} \cdot 2^{2 \cdot NumberOfSetFrequency} \tag{4.5}$$

In equation 4.5, $f_{sampling}$ is the sampling frequency, f_{sine} is the signals sine frequency and n is the frequency's number according to 4.2. The formula above shows the interdependence between sampling rate and signal frequency until the 12th frequency was set. It results from dividing the signal frequency in half every time a new frequency is set, as the overall sampling rate remains the same. Figure 4.7 illustrates the overall number of measurement points which remains the same until the 12th set frequency and is then diminished proportionally to the signal's frequency. So from the 12th frequency setting onwards, the measurement points per frequency remain at 16384.

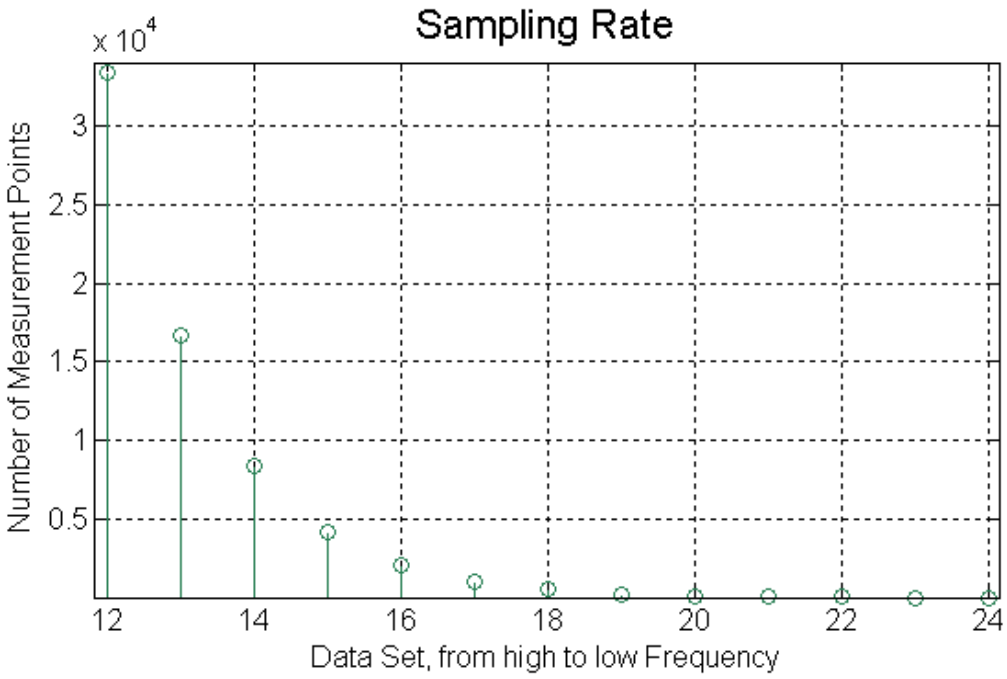

Figure 4.7.: Sampling Rate

For the highest frequencies, the measurement is the most inaccurate. The signal can be identified entirely, though. The smallest number of points per period is 4 and according to the Shannon theorem, more than 2 points per period are sufficient. Figure 4.8 shows the sine calculated by the FFT (amplitude and phase shift) for the highest measurement frequency and it fits perfectly.

Figure 4.9 shows the current amplitude response for the signal in figure 4.6. The amplitudes of each occurring frequency component are delivered. In this case the signal's frequency is 260.4 Hz.

It can clearly be seen that as the current excitation has only one sine frequency there is exactly one amplitude for this particular frequency.

As a consequence, the one amplitude can be extracted from the dataset easily, for example by using the maximum. As for the voltage output, the average value needs to be subtracted beforehand, so that the correlation between voltage and current amplitude is right.

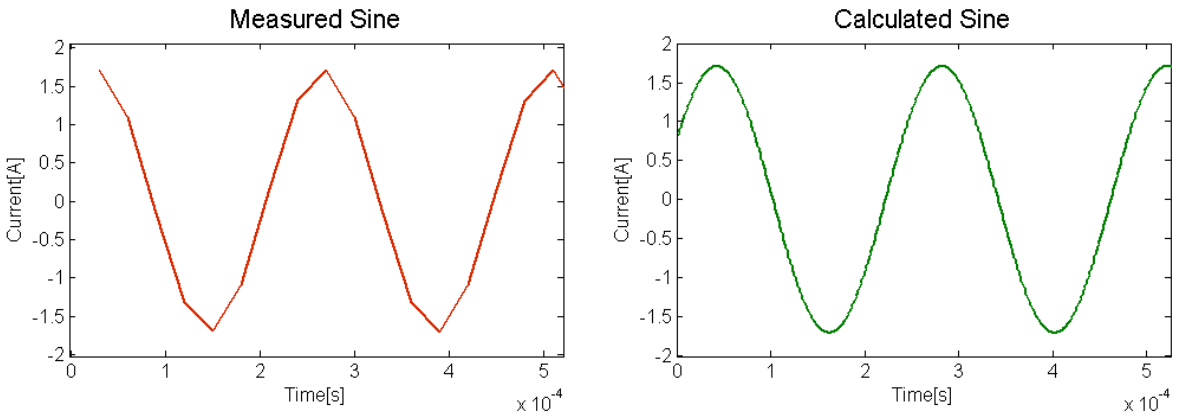

Figure 4.8.: Shannon for Highest Frequency

$$U_{resulting} = U_{measured} - U_{mean} \tag{4.6}$$

The steps to obtain the voltage amplitude are then the same as the ones used above. The absolute value of Z can then be computed as follows:

$$\mid Z \mid = \frac{U}{I} \tag{4.7}$$

The angle of the Fourier transform shows the phase shift of the whole transform. Theoretically there would be one phase shift for every (not really) occurring frequency.

In order to determine the phase shift between current and voltage only for the one dominating sine frequency, the corresponding measurement frequency is used again. The angle values are taken in the corresponding data point, where the amplitudes were found. The phase shift ϕ can then be computed as follows:

$$\phi = (\phi_u - \phi_i) \tag{4.8}$$

In equation 4.8, ϕ is the phase shift between current and voltage, ϕ_u is the phase shift of the voltage and ϕ_i is the phase shift of the current. The imaginary and the real part of Z are then calculated as:

$$Z_{real} = \mid \underline{Z} \mid \cdot cos\phi \tag{4.9}$$

$$Z_{imaginary} = \mid \underline{Z} \mid \cdot sin\phi \tag{4.10}$$

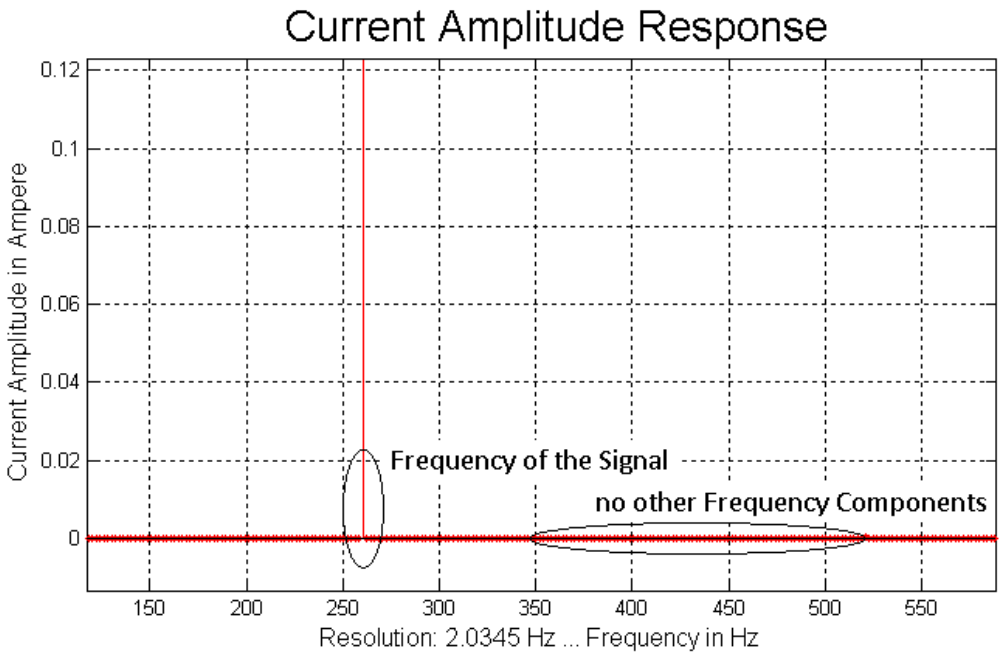

Figure 4.9.: Current Amplitude Response Zoom

In equation 4.9, Z_{real} is the real part of the impedance and in equation 4.10, $Z_{imaginary}$ is the imaginary part of the impedance. The values of the imaginary and the real part for each SOC data set are then found by repeating the upper computation for all 24 sine frequencies.

4.2.1.2. Parameter Determination

The impedance of R and C as a parallel element is computed as follows:

$$Z_{RC} = \frac{R \cdot \frac{1}{j\omega C}}{R + \frac{1}{j\omega C}} \tag{4.11}$$

In equation 4.11, R is the resistance, C is the capacitance and Z_{RC} is the impedance of paralleling R and C.

In order to create the equivalent circuit diagram, some RC elements and one inner resistance are combined by summing up these elements. The next step is to calculate the equivalent circuits so called start parameters manually and then compare their Nyquist curve on the loop to the measured Nyquist curve. For this purpose a function is written A.2 in which a variable represents the squared difference between value of measured data and calculated value. The loop terminates if either a defined amount of loops (10 billion) has been performed or a defined difference value of 1e-10 has been undershot. After every try the parameters are changed iteratively in order to converge on the optimal solution. Theoretically, an infinite number of solutions would be possible for every equivalent circuit diagram. In order to avoid physically unrealistic dimensioned components in the equivalent circuit diagram, the start values need to be chosen as close to the actual values as possible. The LSQ (least squares) fit also is more accurate if less variables need to be fitted.

The calculation would not be as accurate if every point was compared in the same manner, because the values of the real part as well as the imaginary part get higher and therefore, the difference between measured value and start value would preponderate. This is why a weighting coefficient is included into the equation [Boukamp, 1985]. In the loop the difference between the values is then expressed as:

$$e = e + a \cdot ((Re_{measured} - Re_{calculated})^2 + (Im_{measured} - Im_{calculated})^2) \tag{4.12}$$

Where e is the difference between measured value and squared weighted value, as is common for a LSQ fitting method. a is the weighting coefficient, defined as:

$$a = \frac{1}{Re^2_{calculated} + Im^2_{calculated}} \tag{4.13}$$

Additionally to the above mentioned methods for increasing the accuracy, the start variables are normalized. A coefficient for each parameter is established which actually has the initially calculated start value, but is not changed during the LSQ fitting. The parameters which are changed are all normalized to the number 1 because the size of all parameters would otherwise differ too much and hence affect the overall accuracy.

Once determined, the start parameters in the Nyquist plot of a SOC set point is then given by the resulting parameters of SOC set point next to the other. The reason is that the value of the parameters does not differ that much for the SOC closest to the next one and therefore the resulting values then qualify as start values.

The distance between the intersection of x- to y-axis to the intersection of the data with

the x-axis is the inner resistance of the battery.

Figure 4.10 shows the RC element in a Nyquist plot. For a RC parallel element, the diameter of the semi-circle is the resistance. The capacity can be obtained by finding the lowest measured value for the y-axis (imaginary part) of the semi-circle. The sine frequency for this particular measurement is also part of the equation. So the capacity C of a RC parallel element is determined as followed:

$$C_{sc} = \frac{1}{2\pi \cdot R_{sc} \cdot f_s} \tag{4.14}$$

In equation 4.14, f_s is teh sweep frequency, C_{sc} is the semi-circle's capacitance and R_{sc} is the semi-circle's resistance.

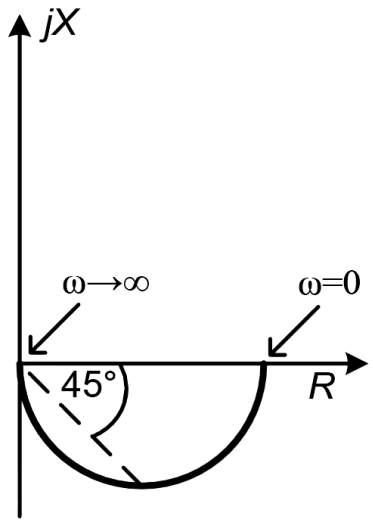

Figure 4.10.: Calculation of the RC-elements parameters in Nyquist [Bösch et al., 2012]

The data which shows the inductive behavior of the cell for high frequencies can be taken into account by including the inductance in the equation by simply determining its value, which is the highest measured value for the y-axis (imaginary part), not disregarding the angular frequency as shown below.

$$Im_{MAX} = \omega L \tag{4.15}$$

In equation 4.15, Im_{MAX} is the maximal imaginary part, ω is the angular frequency and L is the battery's inductance. Figure 4.11 illustrates the angle to inductive dependence in a Nyquist plot. R_s is the resistance value at the intersection to the x-axis and L_s is the inductance, resulting in the imaginary part of the Nyquist plot.

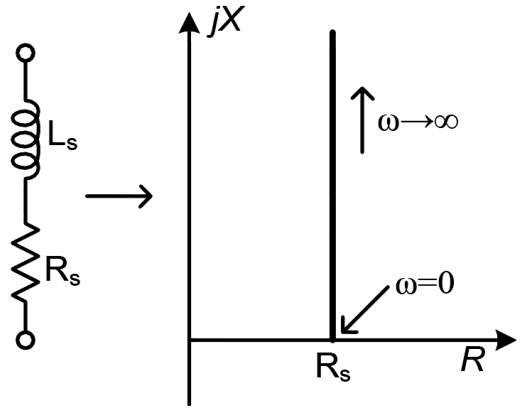

Figure 4.11.: Calculation of the inductive parameter in Nyquist [Bösch et al., 2012]

4.2.1.3. Manual Calculation

Figure 4.12 shows the approach for the RC elements in semi-circles, as well as the location of R_i and L. It can be clearly seen that the inaccuracy in such an approach lies in the semi-circles, not only because of the fact that the measured values do not from exact semi-circles, but also because of the overlap of these elements.

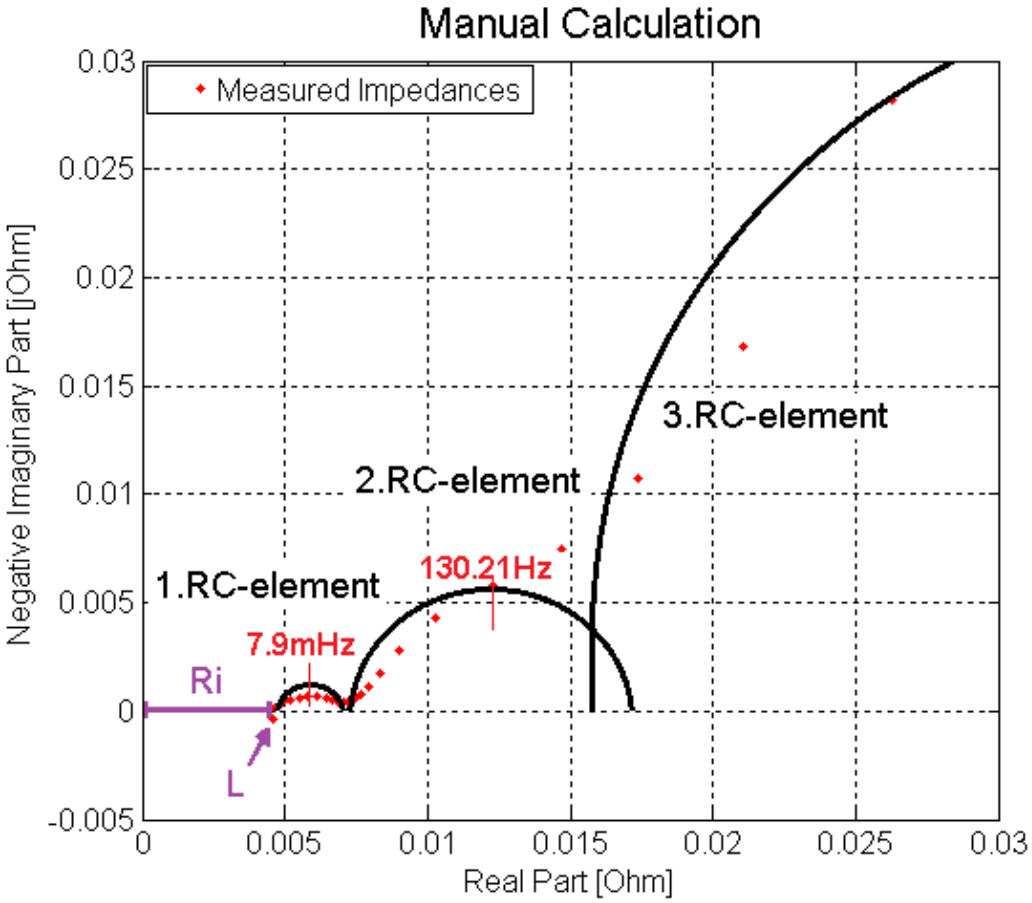

Figure 4.12.: Manual Calculation

Inner Resistance:

$$R_i = R_{intersection} \tag{4.16}$$

$$R_i = 4.652 \cdot 10^{-3}\Omega \tag{4.17}$$

Inductance:

$$L = \frac{Im_{MAX}}{\omega} \tag{4.18}$$

$$L = \frac{0.3 \cdot 10^{-4}}{2\pi 4.1667 \cdot 10^{-3}} = 7.2 \cdot 10^{-9} H \tag{4.19}$$

First RC element:

$$R_1 = R_{x1} - R_i \tag{4.20}$$

In equation 4.20, R_{x1} is the resistance at the second intersection of the belonging semi-circle with the x-axis.

$$R_1 = 7 \cdot 10^{-3}\Omega - 4.7 \cdot 10^{-3}\Omega = 2.3 \cdot 10^{-3}\Omega \tag{4.21}$$

$$fg_1 = 130.21 Hz \tag{4.22}$$

$$C_1 = \frac{1}{\omega \cdot R_1} \tag{4.23}$$

$$C_1 = \frac{1}{2\pi 2.3 \cdot 10^{-3} \cdot 130.21} = 0.5314 F \tag{4.24}$$

Second RC element:

$$R_2 = R_{x3} - R_{x2} \tag{4.25}$$

In equation 4.25, R_{x2} is the resistance at the first intersection of the belonging semi-circle with the x-axis and R_{x3} is the resistance at the second intersection of the belonging semi-circle with the x-axis.

$$R_2 = 17 \cdot 10^{-3}\Omega - 7.5 \cdot 10^{-3}\Omega = 9.5 \cdot 10^{-3}\Omega \tag{4.26}$$

$$fg_2 = 0.0079 Hz \tag{4.27}$$

$$C_2 = \frac{1}{\omega \cdot R_2} \tag{4.28}$$

$$C_2 = \frac{1}{2\pi 9.5 \cdot 10^{-3} \cdot 0.0079} = 212.07F \tag{4.29}$$

Third RC element:
The third semi-circle cannot be determined accurately enough manually, so the parameters for this semi-circle were estimated:

$$R_3 = 1\Omega \tag{4.30}$$

$$C_3 = 2000F \tag{4.31}$$

Figure 4.13 shows the first approach using the manually calculated start parameters. The red curve shows the Nyquist diagram which came from the measurement data. The blue line results from plotting a Nyquist diagram for the start parameters, covering the same frequency range which was used for measurement.

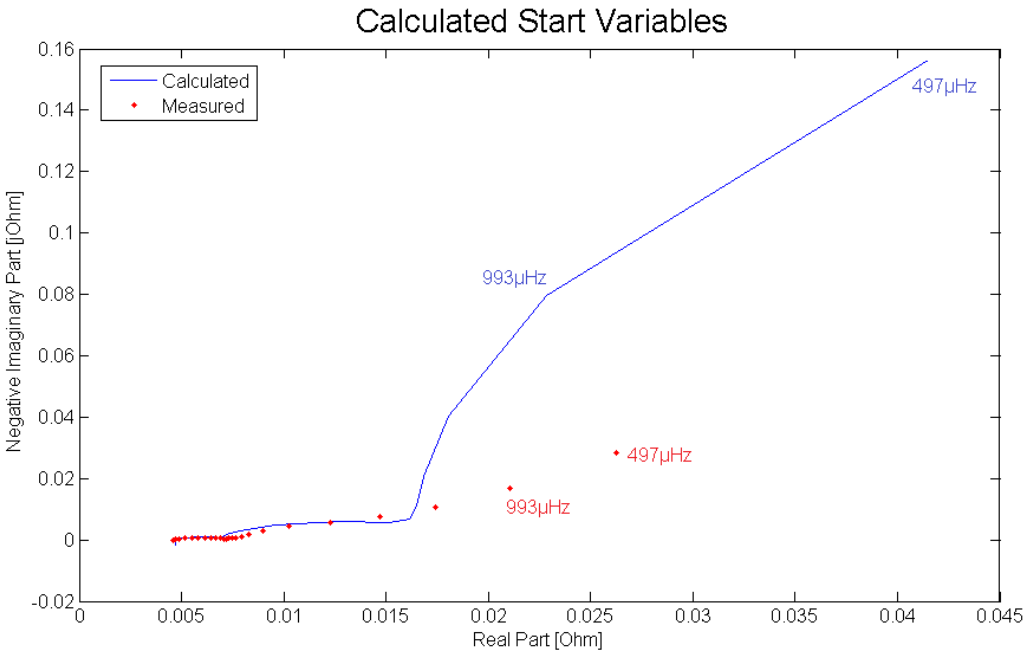

Figure 4.13.: Nyquist Plot for Start Parameters

The influence of the manually not exactly calculable third semi-circle can be clearly seen as the calculated curve differs significantly from the measured one, especially concerning frequencies lower the mHz range. With some frequency points added, the weak point of this

first approach is revealed even clearer as it becomes obvious that there is not only a difference between the imaginary parts, but also between the real parts of the compared data. Figure 4.14 shows the LSQ fitted curve. The red line represents the measured and the blue line the calculated one. Unfortunately, during the fitting process, the clearly determinable inner resistance R_i, the intersection of the x-axes slided, to serve the overall fit.

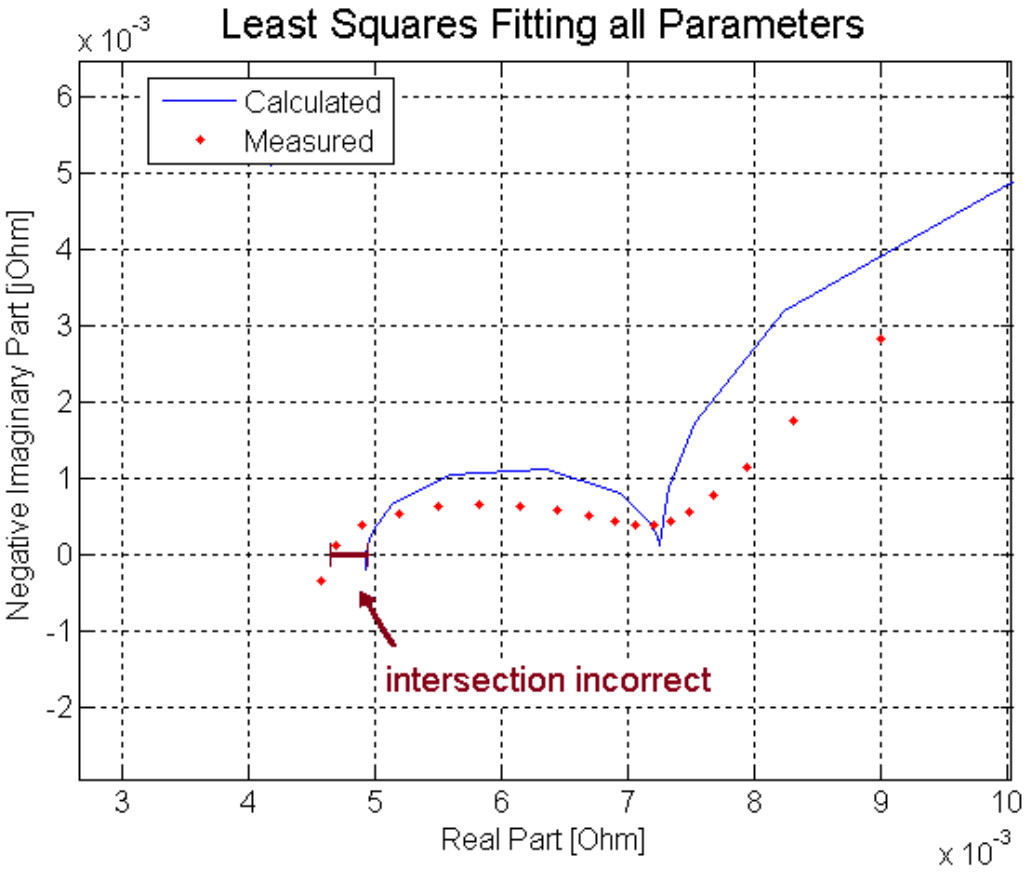

Figure 4.14.: Nyquist Plot after Least Squares Fit

The resolution for this problem is to determine the intersection by Matlab in advance and include the unchangeable R_i into the LSQ fit. The resulting curve can be seen in figure 4.15.

The parameters obtained for each SOC are illustrated in table 4.3 and 4.4. L as a parameter is added for a more accurate curve fit. Because of the frequency area (very high frequency) it is not relevant for the elevation of the battery, as mentioned in chapter 3.

The stationary impedance for 2 and 3 RC elements is compared in table 4.5. It is determined by adding all resistances. A further conclusion is made in chapter 5.

In figure 4.16 the OCV is depicted. It has two so called voltage plateaus which means that the SOC is difficult to determine by its voltage in this area. Fortunately, as the SOC is known for each measurement, it is not necessary to obtain the SOC from the voltage value. In case of application, other indicators needed to be found to evaluate the SOC such as its

SOC [%]	R_i [**mΩ**]	R_1 [**mΩ**]	R_2 [**mΩ**]	R_3 [**mΩ**]	C_1 [**F**]	C_2 [**F**]	C_3 [**F**]	L [**H**]
05	4.7	3.0	9.2	1024.8	0.64	1249.2	2126.2	9.54e-9
15	4.7	2.8	9.5	280.4	0.62	1255.9	4431.8	1.12e-8
25	4.7	2.9	9.3	207.5	0.59	1510.8	6144.1	9.98e-9
35	4.7	3.0	9.3	128.9	0.57	1546.2	6768.9	8.90e-9
45	4.7	2.7	9.0	76.6	0.58	1596.8	8081.7	1.02e-8
55	4.7	2.5	8.2	73.4	0.58	1624.9	9304.7	1.17e-8
65	4.7	2.6	8.5	96.2	0.56	1645.5	8842.5	1.17e-8
75	4.7	2.6	9.2	115.2	0.56	1573.9	7698.1	9.95e-9
85	4.7	2.6	8.7	55.1	0.54	1545.1	8956.9	9.90e-9
95	4.7	2.6	8.6	80.1	0.53	1564.2	8280.0	9.86e-9

Table 4.3.: Parameters Complex Variable Domain

SOC [%]	R_i [**mΩ**]	R_1 [**mΩ**]	R_2 [**mΩ**]	C_1 [**F**]	C_2 [**F**]	L [**H**]
05	4.6	3.0	18.7	0.57	876.55	1.05e-8
15	4.6	2.8	11.3	0.52	1.10e+3	1.25e-8
25	4.6	2.9	9.7	0.49	1.14e+3	1.14e-8
35	4.6	2.9	9.0	0.47	1.16e+3	1.05e-8
45	4.6	2.7	8.3	0.47	1.23e+3	1.18e-8
55	4.6	2.5	7.7	0.47	1.28e+3	1.34e-8
65	4.6	2.6	7.9	0.45	1.28e+3	1.35e-8
75	4.5	2.6	8.9	0.42	1.19e+3	1.24e-8
85	4.5	2.6	8.0	0.41	1.21e+3	1.23e-8
95	4.5	2.6	8.4	0.40	1.23e+3	1.23e-8

Table 4.4.: Parameters Complex Variable Domain with only 2 RC elements

SOC [%]	**Sum** R **for 3 RC-elements** [**mΩ**]	**Sum** R **for 2 RC-elements** [**mΩ**]
05	1041.7	26.3
15	297.4	18.7
25	224.4	17.2
35	145.9	16.5
45	93.0	15.6
55	88.8	14.8
65	112.0	15.1
75	131.7	16.0
85	71.1	15.1
95	96.0	15.5

Table 4.5.: Comparison Overall Stationary Impedance - Frequency Domain

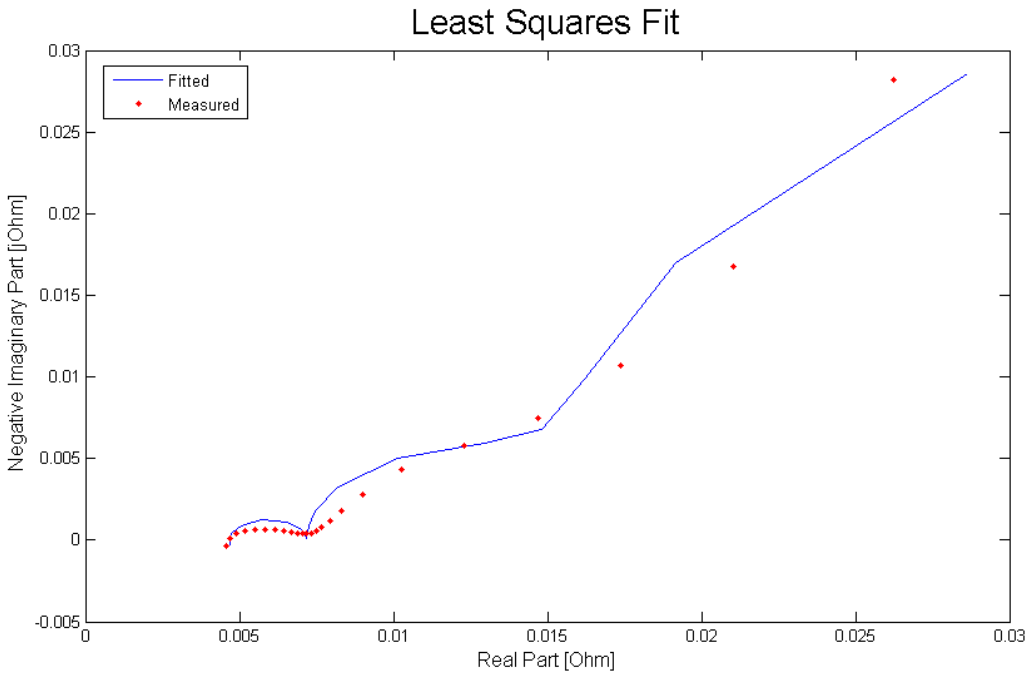

Figure 4.15.: Nyquist Plot for Start Parameters

correlation to $\int Idt$, which is described in chapter 4.2.

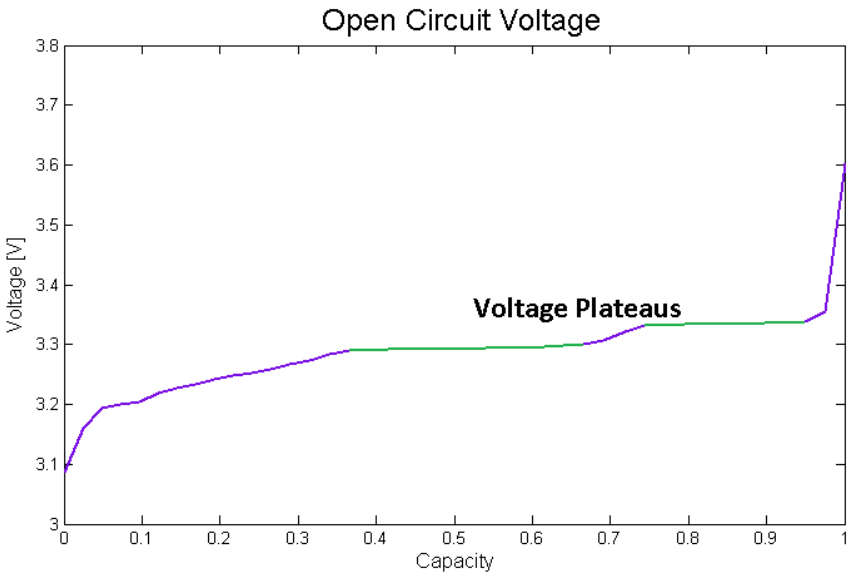

Figure 4.16.: Voltage Plateaus in OCV Curve

4.3. Time Domain

This chapter describes the evaluation of the method, executed in the time domain via Matlab computation. The Matlab program outputs all corresponding equivalent circuit diagram parameters for each entered SOC value.

4.3.1. Calculation

As mentioned in chapter 3, a simple calculation like the one shown below is needed for the LSQ fit in the time domain.

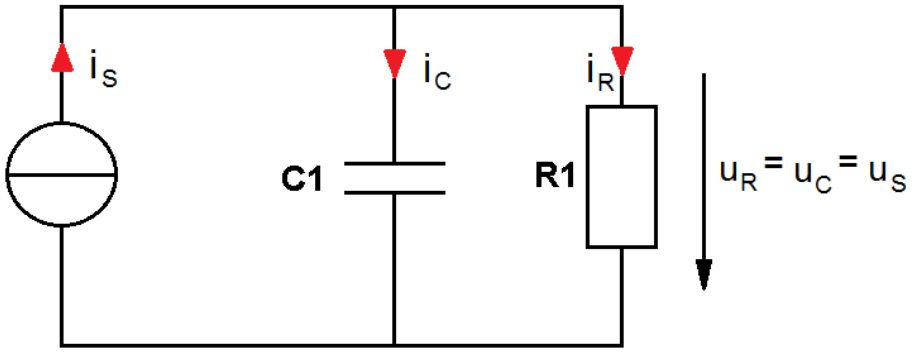

Figure 4.17.: RC Element

Hence the current for one RC element would be:

$$i_S = i_R + i_C \tag{4.32}$$

$$C_1 u' + \frac{1}{R_1} u - i_S = 0 \tag{4.33}$$

For solving the differential equation, several steps are mandatory. The voltage consists of a homogeneous and a particular part. As soon as the homogeneous part is determined as an approximate value, it is possible to calculate the particular part. The solution for the variable k can be found in the end.

Homogeneous:

$$-\lambda k e^{-\lambda t} + \frac{1}{R_1 C_1} k e^{-\lambda t} = 0 \tag{4.34}$$

$$\tau = \frac{1}{\lambda} = -R_1 C_1 \tag{4.35}$$

τ is the time constant, in this case a product of the resistance and the capacitance. It indicates the time course during charging.

Resulting in:

$$u_h = k e^{-\frac{1}{R_1 C_1} t} \tag{4.36}$$

Particular:

$$u_p = A \tag{4.37}$$

$$u' + \frac{u}{R_1 C_1} - \frac{i_S}{C_1} = 0 \tag{4.38}$$

Resulting in:

$$u_p = i_S R_1 \tag{4.39}$$

k:

$$u(0) = k e^0 + i_S R_1 \tag{4.40}$$

$$k = u(0) - i_S R_1 \tag{4.41}$$

Solution:

$$u(t) = (u(0) - i_S R_1) e^{-\frac{1}{R_1 C_1} t} + i_S R_1 \tag{4.42}$$

In this case it would be easy to insert the circumstance of a charged capacitor into the calculation. Unfortunately if there are two RC elements in series, there is no hint about which capacitor accounts for what load. If empty capacitors are a measurement precondition, the equation can still be done right without solving this problem. For u(0) = 0 it would be:

$$u(t) = i_S R_1 - i_S R_1 e^{-\frac{1}{R_1 C_1} t} \tag{4.43}$$

The further equation for a resistor serial with two RC elements would then be:

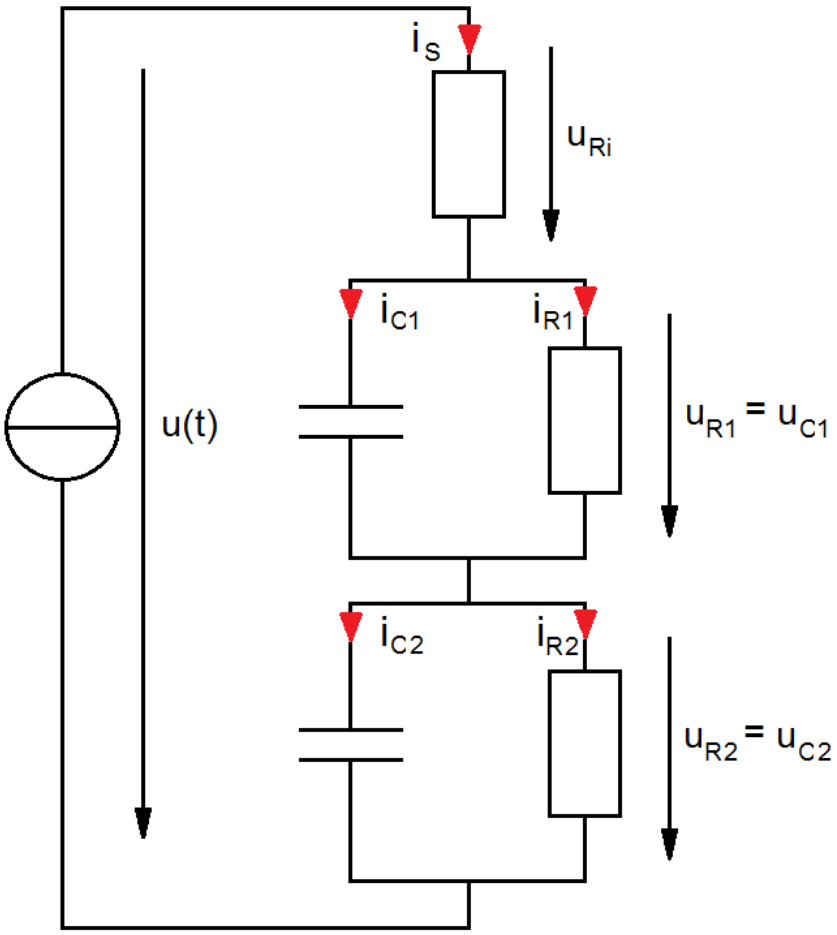

Figure 4.18.: ECD for R and two RC Elements

$$u_{Ri} = i_S R_i \tag{4.44}$$

$$u_{RC1} = i_S R_1 - i_S R_1 e^{-\frac{1}{R_1 C_1} t} \tag{4.45}$$

$$u_{RC2} = i_S R_2 - i_S R_2 e^{-\frac{1}{R_2 C_2} t} \tag{4.46}$$

$$u(t) = i_S R_i + i_S R_1 - i_S R_1 e^{-\frac{1}{R_1 C_1} t} + i_S R_2 - i_S R_2 e^{-\frac{1}{R_2 C_2} t} \tag{4.47}$$

As mentioned above, this formula is only valid if the capacitors are empty, so the relaxation time has to be sufficient long, before the battery is cycled, only then the variables can be obtained by a pulse of constant current.

4.3.2. Matlab Computation

The available data, which is the result of the measurement, is saved as .mat-files. Two files were made, one contains current and voltage and the other the time instants. Contrary to the EIS there was only one measurement where the entered SOC points were reached one after another. The overall measurement time was 15.65 hours. Each entered SOC point was reached by fully charging the battery and then discharging to the entered points, starting with the highest SOC of 95%. The entered SOC points were the same as used for the EIS, shown in table 4.1. For every entered point a current excitation in shape of squares was performed. This current curve was repeated for every SOC. It is illustrated in figure 4.19. Two current values were measured as illistrated in 4.19: 1.28A and 12.76A. The first value lies near one of the measured sine waves in 4.2. The other is 10 times higher and will not be considered for the further investigations.

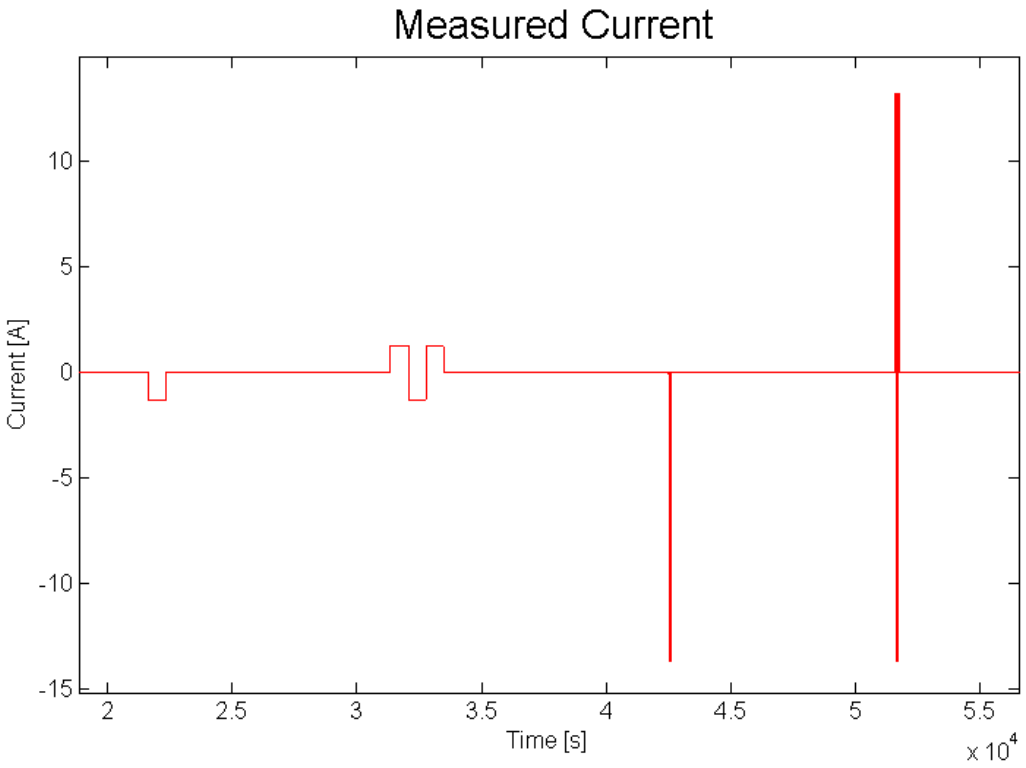

Figure 4.19.: Measured Electric Current

As figure 4.20 shows, the measurement was aborted at 5% SOC because the lower voltage limitation of the cell was reached. CC-CV fully charged means that the cell was first charged with the excitation of a CC (constant current) and then CV (constant voltage). This is a common charge method when it comes to batteries.

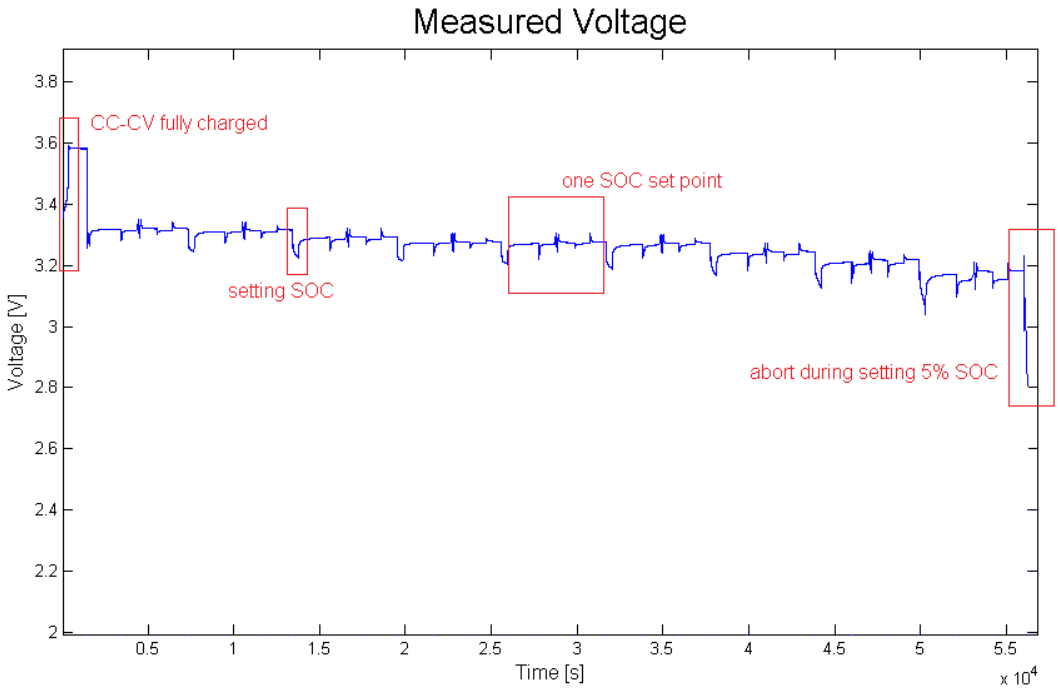

Figure 4.20.: Measured Voltage

Every time a square is performed, the SOC changes. Therefore, the OCV curve needs to be determined and subtracted from the measured voltage for the LSQ fit in the required areas. This curve can easily be evaluated by using the voltages before and after the event of the square. But for both voltages the cell needs to have rested so that the obtained voltage matches the actual OCV. In figure 4.21 the measured voltage and its belonging OCV curve are depicted for the original entered SOC point of 95%.

Figure 4.22 shows the result of the subtraction.

The curve fitting principally works like the one demonstrated in chapter 4.2. The LSQ fit, though, evaluates the minimal gap on the y-axes. The formula used for the LSQ fit is the one calculated beforehand as shown in the subsection calculation above. The data deliverables are illustrated in tables 4.6 and 4.7.

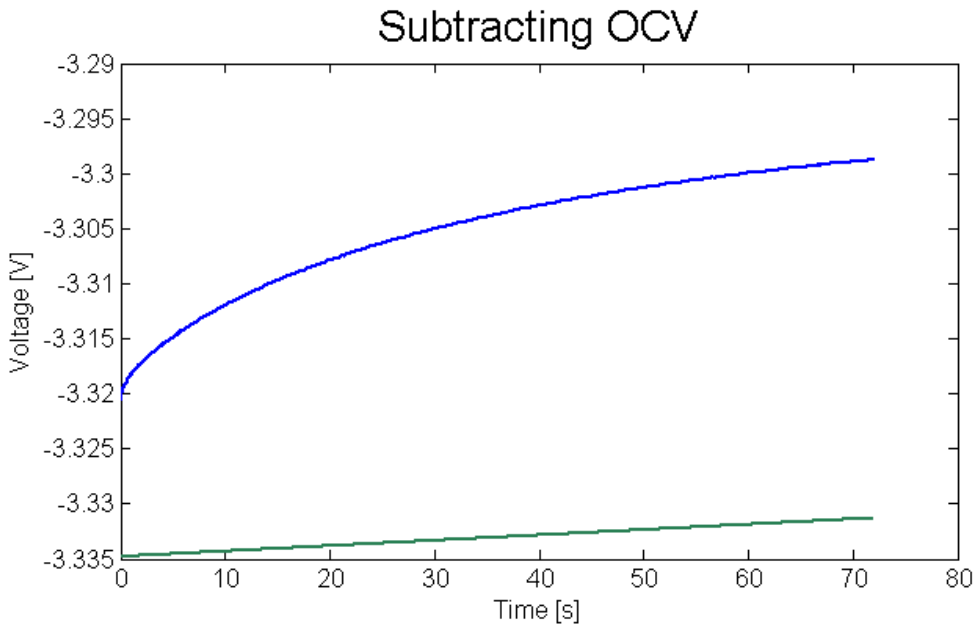

Figure 4.21.: Subtracting OCV

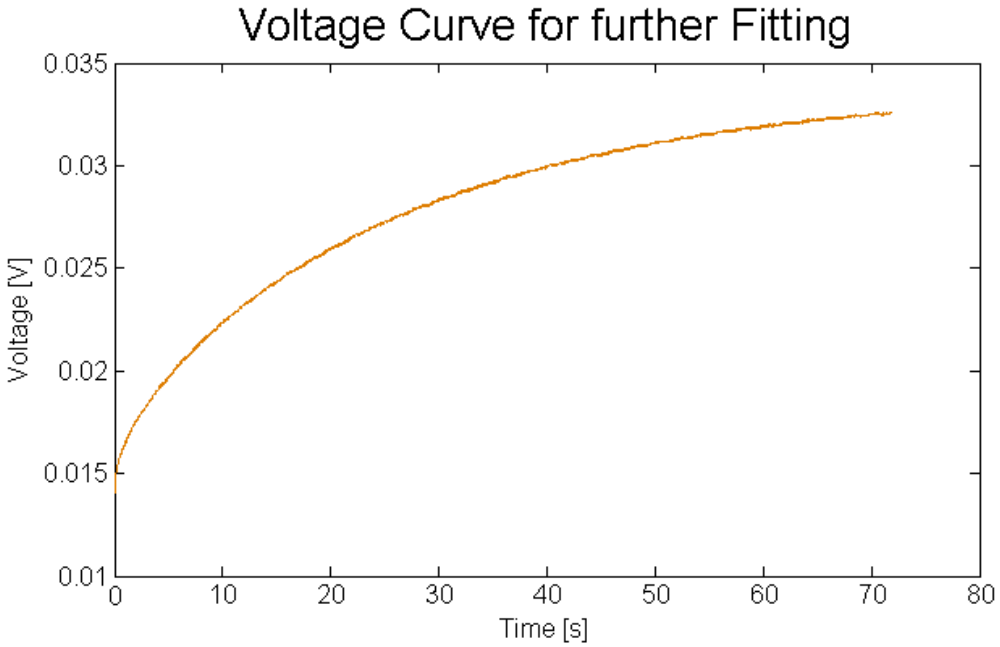

Figure 4.22.: Curve for further Fitting

SOC [%]	R_i [**mΩ**]	R_1 [**mΩ**]	R_2 [**mΩ**]	R_3 [**Ω**]	C_1 [**F**]	C_2 [**F**]	C_3 [**F**]
15	10.3	2.8	33.3	8.86e-4	2.29e+3	2.82e+3	9.81e-15
25	9.0	2.6	23.0	8.46e-4	1.91e+3	1.87e+3	5.23e-15
35	9.4	2.6	18.4	6.70e-4	2.20e+3	1.44e+3	0.13
45	9.4	3.0	19.4	7.51e-4	2.55e+3	1.55e+3	2.23e-13
55	9.2	2.6	17.1	6.80e-4	2.41e+3	1.36e+3	0.13
65	8.6	2.4	14.8	2.47e-4	2.45e+3	1.51e+3	0.62
75	8.6	2.1	12.8	6.21e-4	2.04e+3	629.62	0.06
85	8.8	2.9	18.1	8.54e-4	2.67e+3	1.55e+3	1.02e-13
95	8.6	2.0	12.7	1.88e-15	2.06e+3	921.54	0.74

Table 4.6.: Parameters Time Domain

SOC [%]	R_i [**mΩ**]	R_1 [**mΩ**]	R_2 [**mΩ**]	C_1 [**F**]	C_2 [**F**]
15	10.3	5.7	52.7	1.35e+3	3.11e+3
25	9.2	2.7	23.1	938.91	1.80e+3
35	9.8	2.6	18.5	1.09e+3	2.13e+3
45	10.0	2.9	19.4	1.42e+3	2.50e+3
55	9.9	2.6	17.1	1.36e+3	2.41e+3
65	8.8	2.4	14.8	1.51e+3	2.45e+3
75	9.2	2.1	12.8	629.62	2.040e+3
85	9.7	3.0	18.1	1.58e+3	2.68e+3
95	8.2	2.2	12.8	579.29	2.01e+3

Table 4.7.: Parameters Time Domain

The stationary impedance for 2 and 3 RC-elements is compared in table 4.8. It is determined by adding all resistances. Further conclusion is made in chapter 5.

The capacitance of the third RC element are very low for 15, 25, 45 and 85% SOC. Additionally all resistances in the third RC element are in the $\mu\Omega$ range. These parameters represent not only τ, but the respective resistance is also a factor which is weighting the RC element's part in the curve fit regarding the stationary part. If the product of the RC element's parameters is very low it means that the result would not differ without taking into account the mentioned element. The opposite might be the case. If only C is very low, the appendant R would actually be part of the inner resistance if the RC elements would have been left out of the fit. In figure 4.23 such a correlation is illustrated. It can be seen that the third RC element is in this case replaceable by one with a slightly higher inner resistance value. Even for high frequencies no additional information could be obtained of it, because the sampling rate was only 100 Hz.

A LSQ fit for 2 RC elements clearly provides an accuracy, which seems to be equal to a fit with 3 RC elements, as depicted in figure 4.24. The accuracy is discussed further in chapter 5.

SOC [%]	Sum R for 3 RC elements [mΩ]	Sum R for 2 RC elements [mΩ]
15	47.3	68.7
25	35.4	35.0
35	31.1	30.9
45	32.6	32.3
55	29.6	29.6
65	26.0	26.0
75	24.1	24.1
85	30.7	30.8
95	23.3	23.2

Table 4.8.: Comparison Overall Stationary Impedance - Time Domain

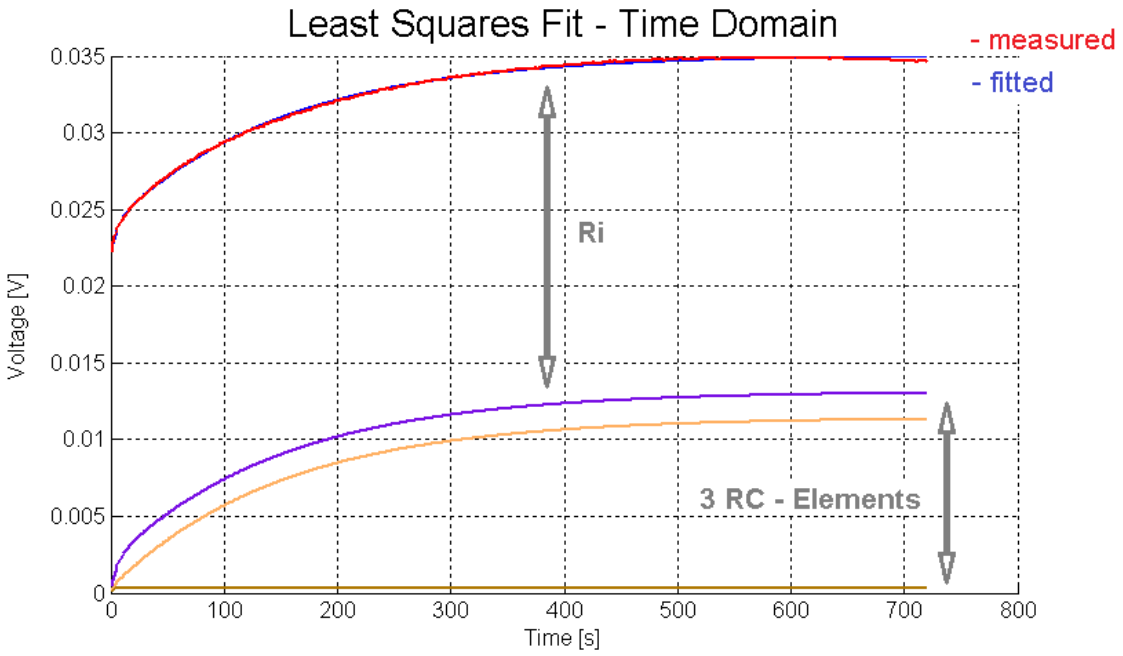

Figure 4.23.: Least Squares Fit in Time Domain for 3 RC Elements

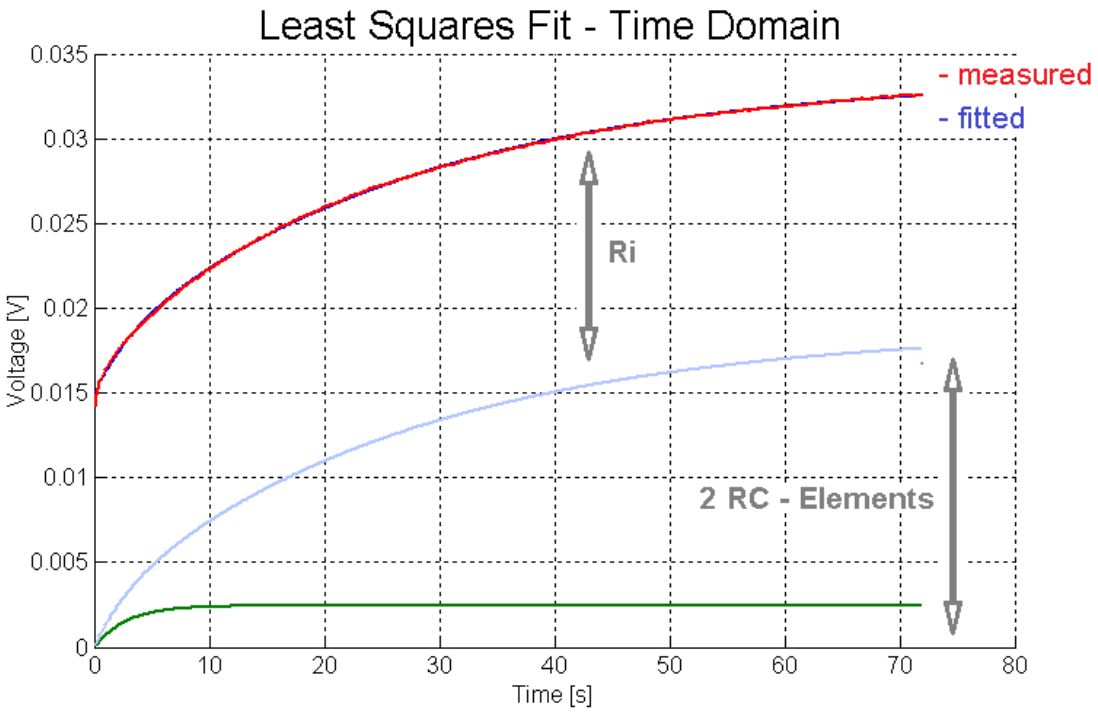

Figure 4.24.: Least Squares Fit in Time Domain with only 2 RC Elements

4.4. Simulation of Results

4.4.1. Computation

In Matlab Simulink the evaluated parameters are simulated. For this, a matrix has to be determined. For one RC element, if the voltage is x_1, the correlation is

$$i = C_1 \cdot \frac{dx_1}{dt} + \frac{x_1}{R_1} \tag{4.48}$$

$$\frac{dx_1}{dt} = \frac{i}{C_1} + \frac{x_1}{R_1 \cdot C_1} \tag{4.49}$$

If i is the input signal u, the matrix of the shape

$$\frac{dx}{dt} = Ax + bu \tag{4.50}$$

is then

$$\frac{dx}{dt} = \begin{pmatrix} -\frac{1}{R_1 \cdot C_1} & 0 \\ 0 & -\frac{1}{R_2 \cdot C_2} \end{pmatrix} x + \begin{pmatrix} \frac{1}{C_1} \\ \frac{1}{C_2} \end{pmatrix} u \tag{4.51}$$

The result is the sum of the voltages of the two RC elements and the voltage applied to R_i

$$u_{output} = i \cdot R_i + x_1 + x_2 \tag{4.52}$$

The output signal, the overall voltage for two RC elements of the shape

$$y = c^T x + du \tag{4.53}$$

is then

$$y = \begin{pmatrix} 1 & 1 \end{pmatrix} x + (R_i)u \tag{4.54}$$

4.4.2. Simulink

In figure 4.25 one RC element is shown according to the previously mentioned matrix. In order to simplify the model, the input current is set as negative.

For the inner resistance, the negative current needs to be taken into account as well, as illustrated in figure 4.26.

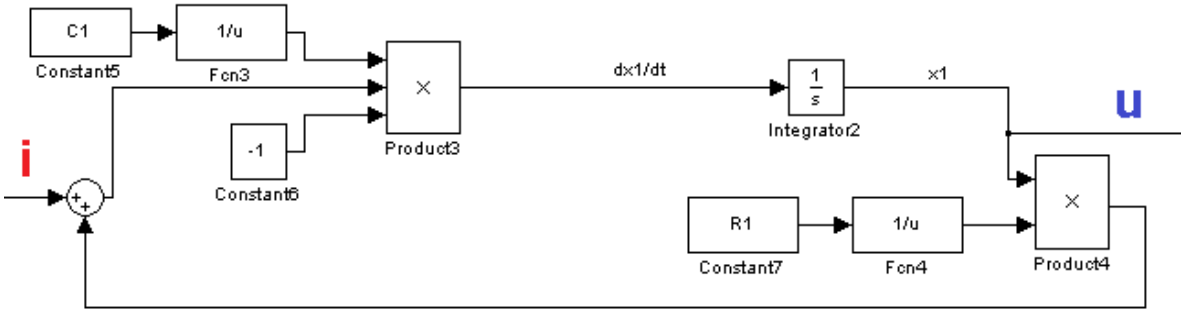

Figure 4.25.: One RC element in Simulink

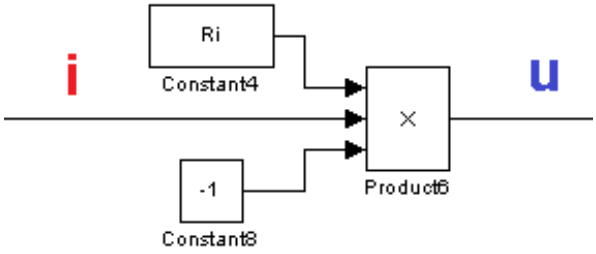

Figure 4.26.: The inner Resistance in Simulink

A signal builder was used as source to generate the current signal used in the original measurement, as is shown in figure 4.27.

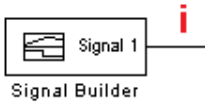

Figure 4.27.: Simulink Source

The negated signal generated by the source is inverted in the display for better understanding. It is illustrated in figure 4.28.

The sum of these three voltages does not include the OCV of the cell. One more branch is then added to the simulation. Figure 4.29 shows that branch.

First the current is inverted again. In order to obtain the capacity change during charge or discharge, the current is integrated. The according SOC amount is then found by dividing the capacity change by the rated capacity of the cell. Then a value is added which represents the initial SOC value. The OCV value is then found by connecting the SOC value to the appendant OCV. The lookup table was generated by using the OCV values, obtained from

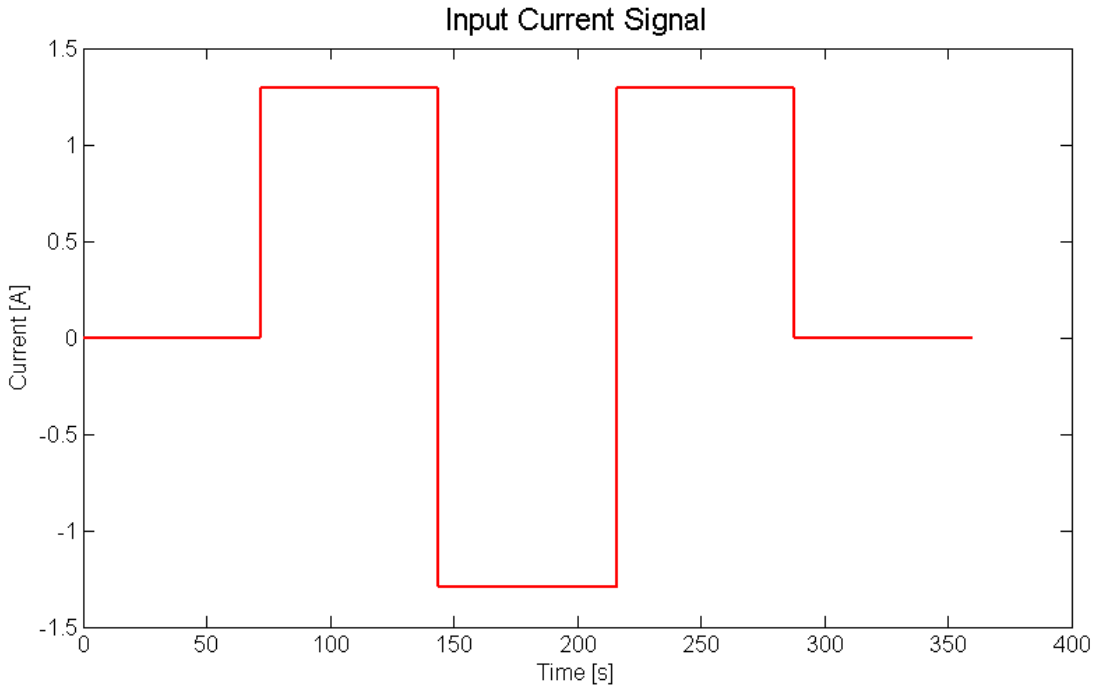

Figure 4.28.: Current Signal for Simulation

the measured voltages in the pulse measurement, the same values which were used to subtract the OCV value for the LSQ fit in the time domain. In figure 4.30 the resulting exemplary OCV curve for a simulation at 55% SOC is illustrated.

The complete Simulink Model is illustrated in figure 4.31. The fixed step size of the solver (ode3) used for simulation is 0.001s.

The following simulations were done with the initial SOCs of 25, 55 and 85% and the appendant parameters. As can be seen by comparing figures 4.32 and 4.35, the difference between 2 and 3 RC elements is significant for the complex variable domain. Further explanation can be found in chapter 5.

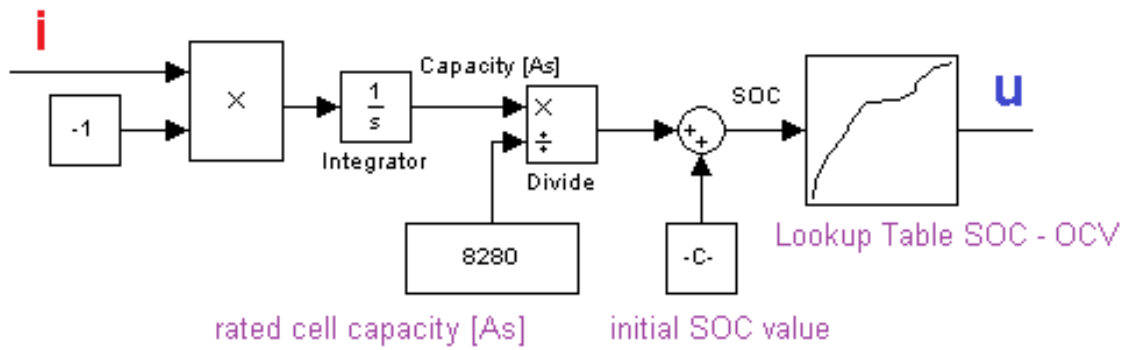

Figure 4.29.: OCV in Simulink

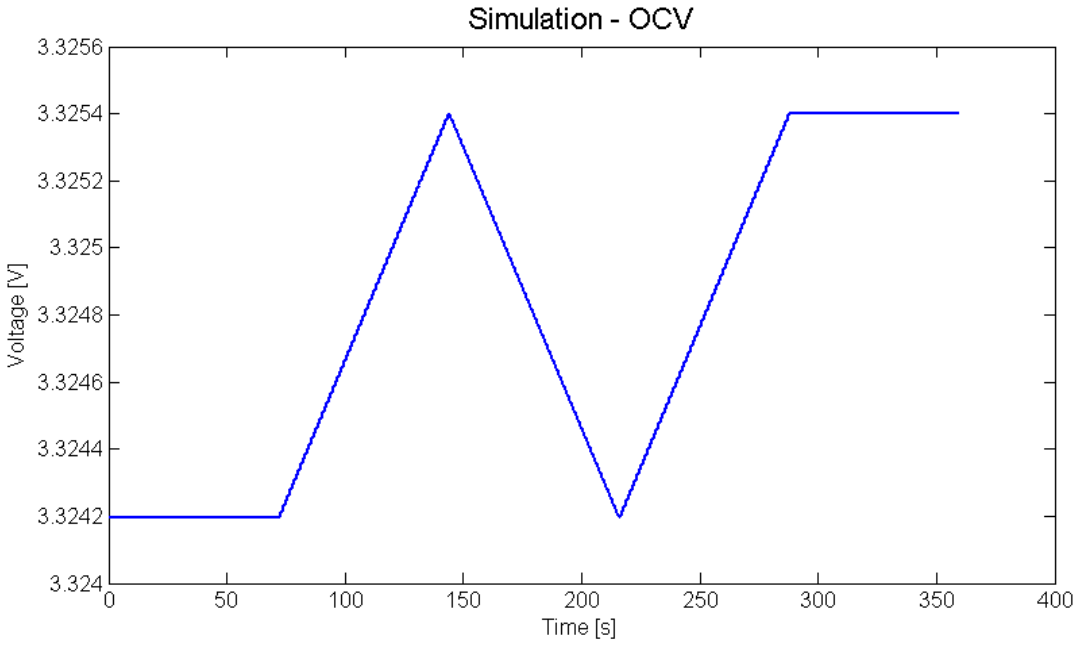

Figure 4.30.: Exemplary OCV Curve

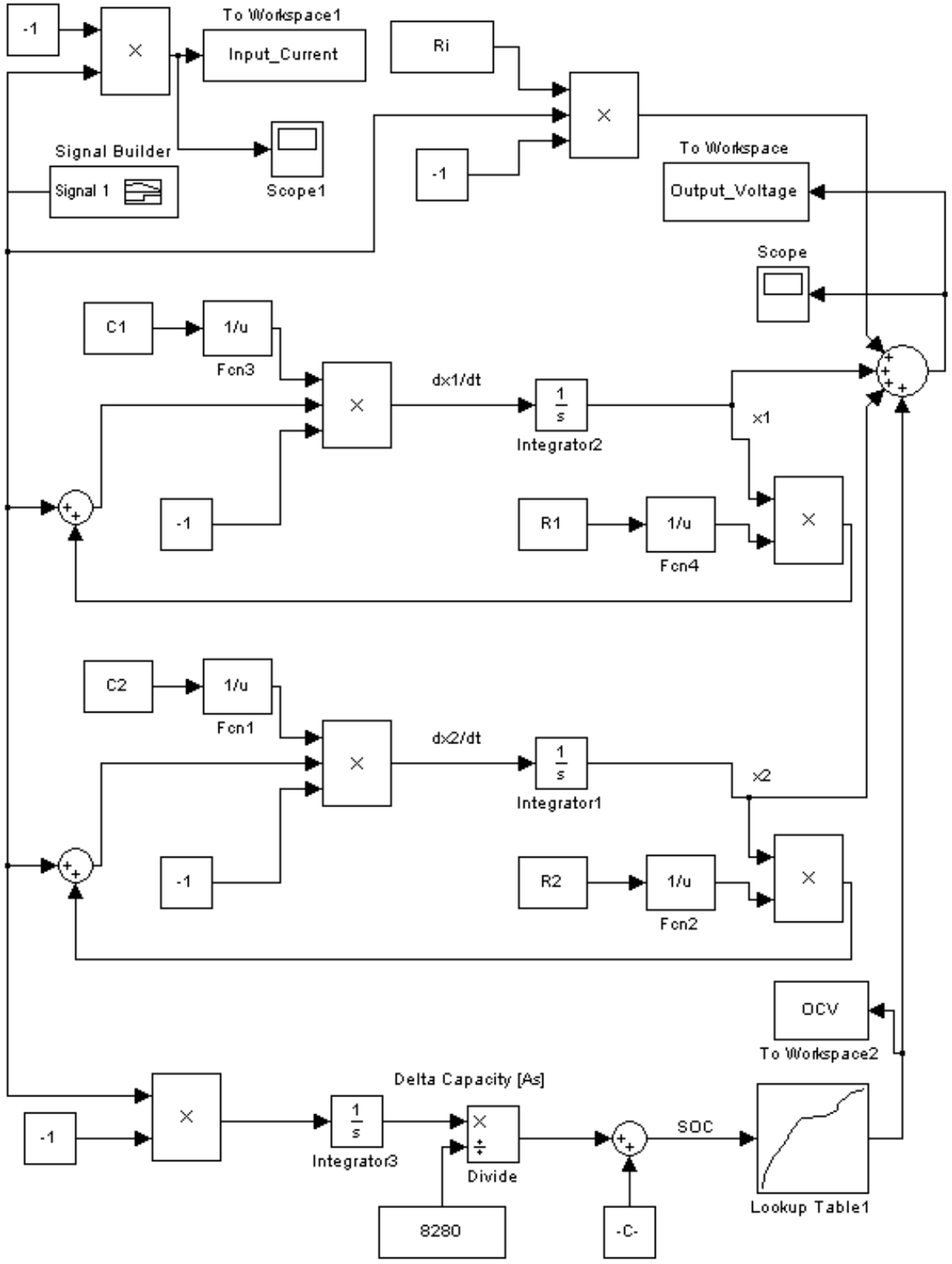

Figure 4.31.: Simulink Model

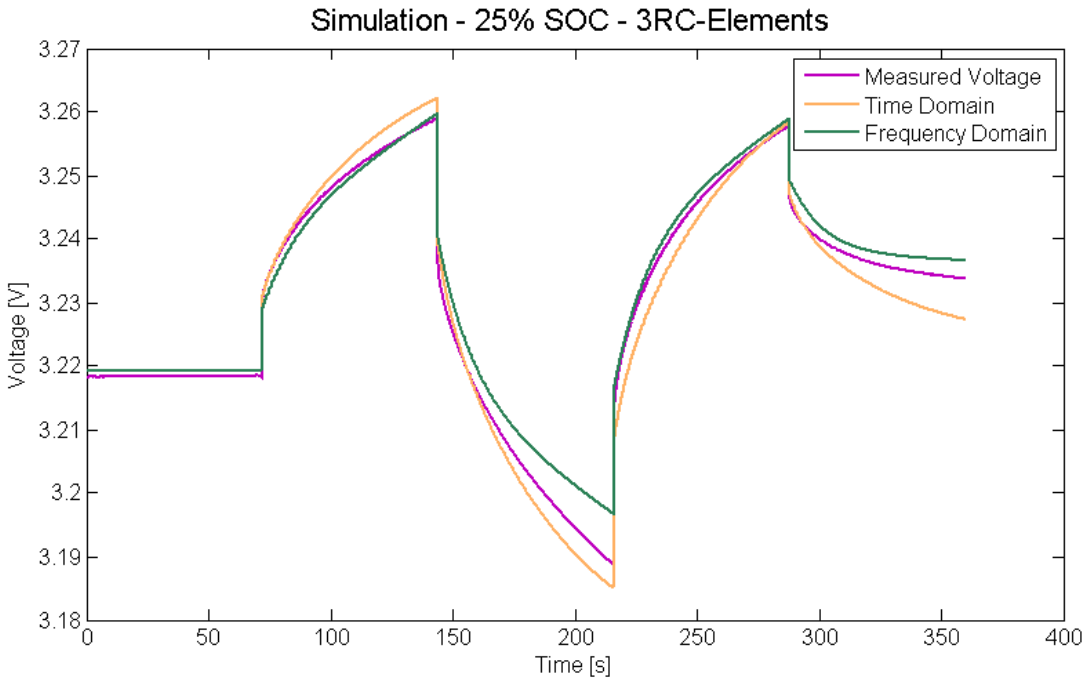

Figure 4.32.: Simulation for 3 RC Elements at 25% SOC

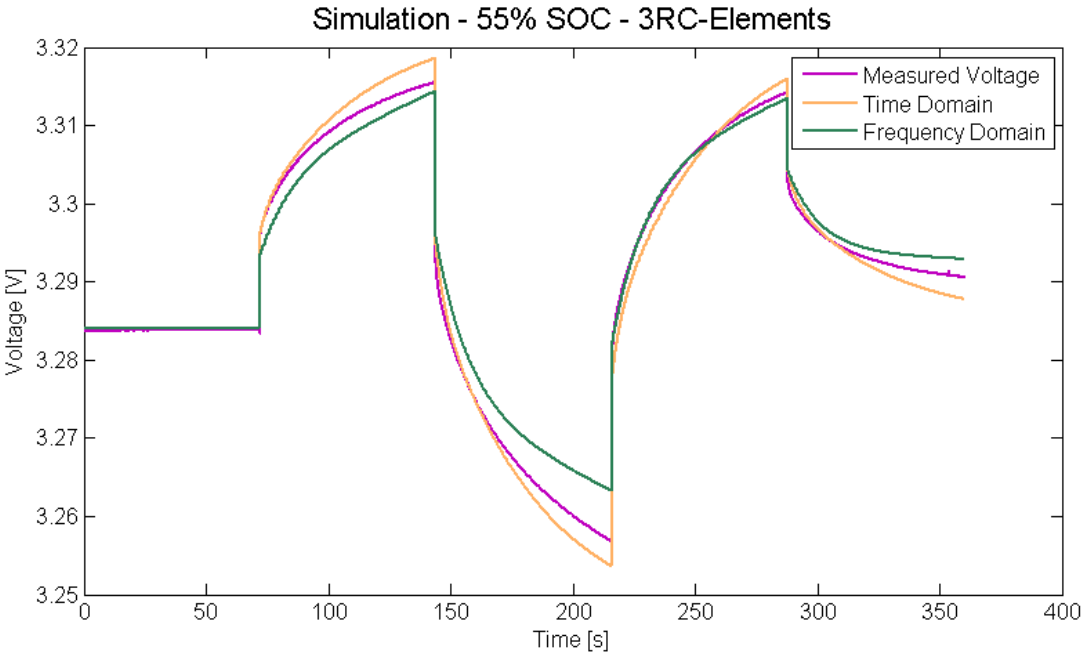

Figure 4.33.: Simulation for 3 RC Elements at 55% SOC

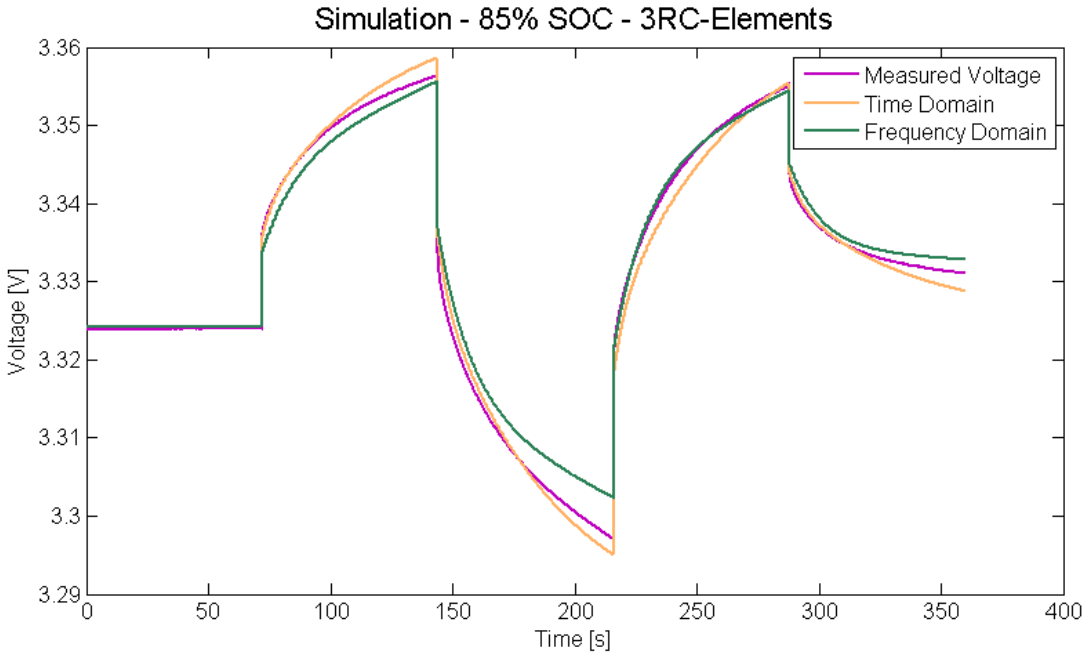

Figure 4.34.: Simulation for 3 RC Elements at 85% SOC

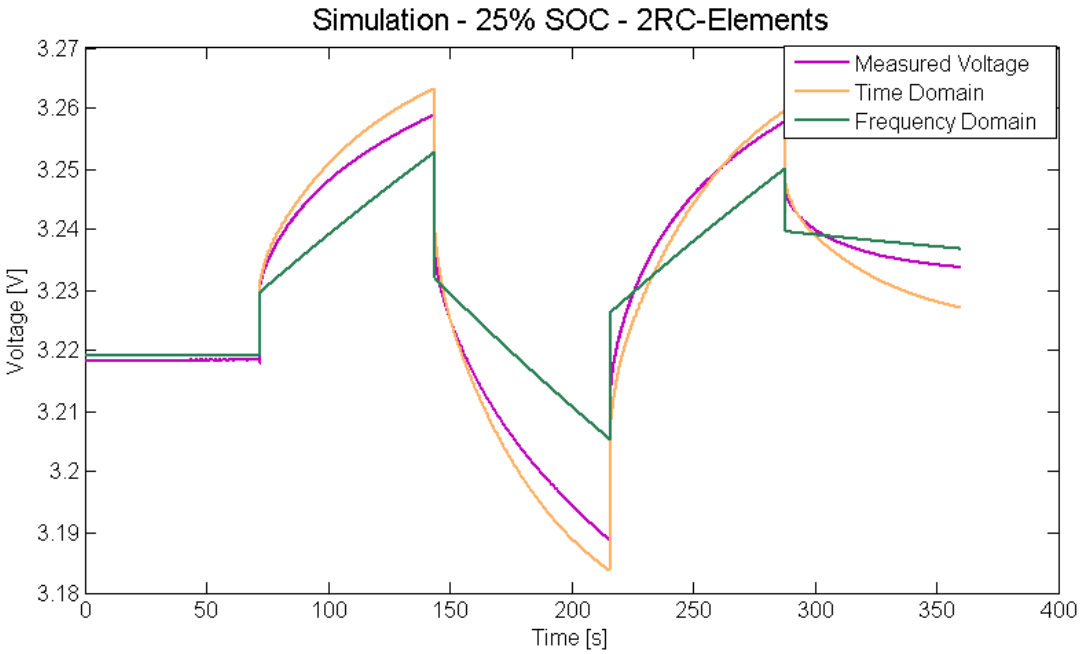

Figure 4.35.: Simulation for 2 RC Elements at 25% SOC

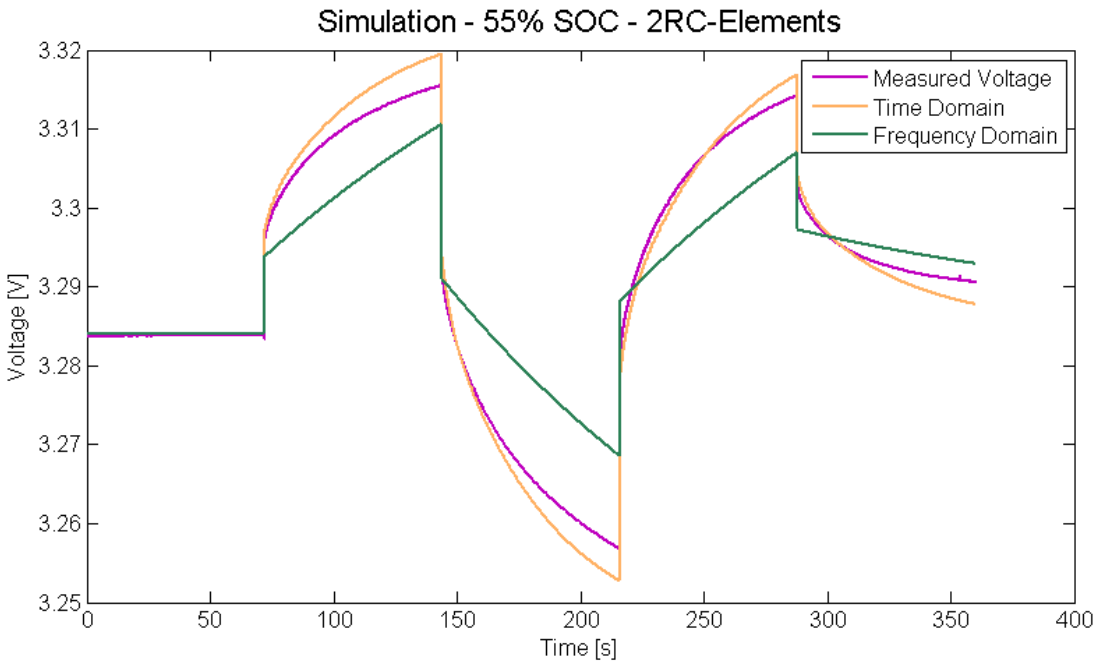

Figure 4.36.: Simulation for 2 RC Elements at 55% SOC

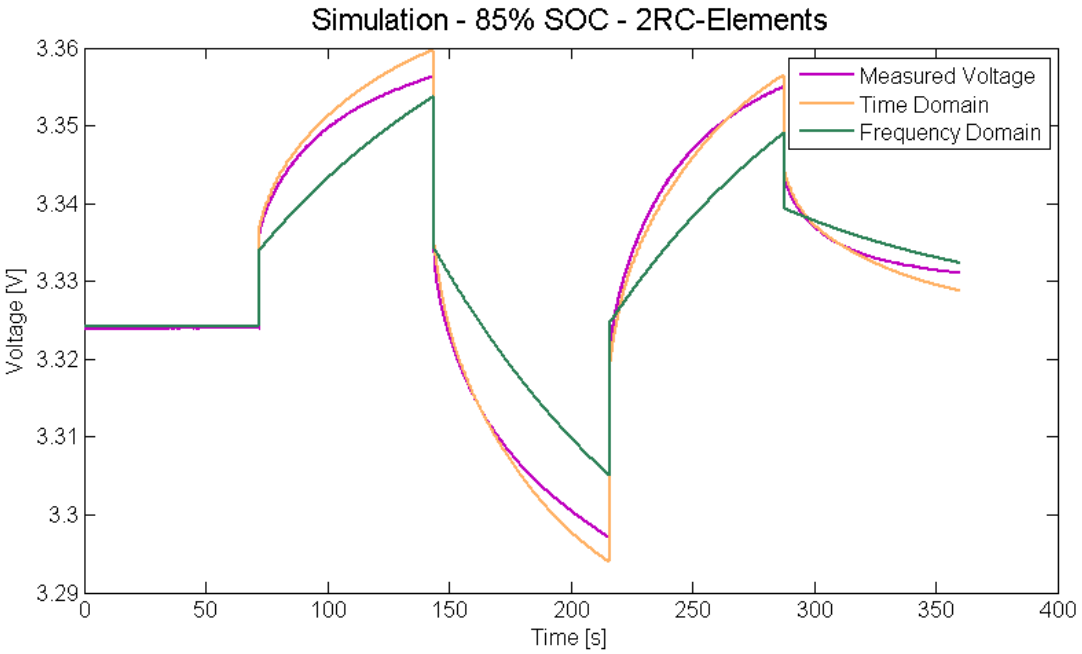

Figure 4.37.: Simulation for 2 RC Elements at 85% SOC

4.5. Cell vs Module

Usually, as the current output of Li-Ion technology is sufficient, cells are connected in a serial manner in order to obtain a higher output voltage. So what would that mean for the measurement of a battery module or pack?

4.5.1. Parameter Calculation

As the equivalent circuit diagram is easy to set up, its different elements can simply be added. The assumption is that the cells equivalent circuit diagrams are defined by the same variables. The cells are equal. For a large amount of cells this approach is acceptable, because the manufacturing variance is then neutralized. This is why the simplified approach was made with similar cells. Without this simplification, the cells resistances and capacitances would have needed to be summed up manually.

Therefore the inner resistance of one cell can be multiplied with the number of the cells, serialized in the module, to obtain the inner resistance of the whole module.

Ohm's law in principal allows to add serial impedances. For the RC element a calculation proves the interdependence in cell number and parameterization of the modules equivalent circuit diagram regarding the cells.

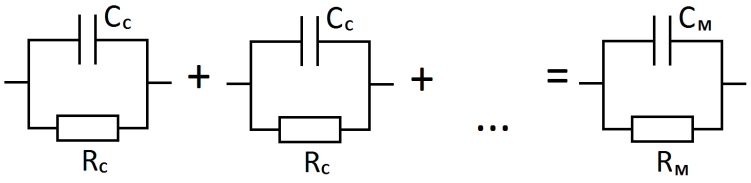

Figure 4.38.: Cell to Module Calculation

The equation is as follows:

$$n \cdot \frac{R_C}{R_C \cdot jwC_C + 1} = \frac{R_M}{R_M \cdot jwC_M + 1} \tag{4.55}$$

$$\frac{n}{C_C} - j \cdot n \cdot R_C = \frac{1}{C_M} - j \cdot R_M \tag{4.56}$$

$$C_M = \frac{C_C}{n} \tag{4.57}$$

$$R_M = n \cdot R_C \tag{4.58}$$

R_C is the resistance parameter of the cell, C_C is the capacitance parameter of the cell, R_M is the resistance parameter of the module, C_M is the capacitance parameter of the module and n is the number of cells.

Knowing this interdependences, a first approach can be made when it comes to the parameterization of a battery module.

4.5.2. Taking into account the Pack Related Hardware

In figure 4.39 a very simplified view of a pack is displayed. These components are used for electric vehicles and all kinds of hybrids. The preload contactor sits parallel to one main contactor. A resistance is added to its circuit. A high dimensioned capacitor is always situated at the interface to the inverter . Would the main contactors close, ignoring that circumstance, a current would flow whose charge is comparable to the one of a short circuit current, causing damage to the component. The purpose of the preload circuit is to limit the current provided by the battery, so that the current peak during ignition is decreased significantly. For every pluggable version, such as electric vehicles or plug-in hybrids, a charge relay is part of the hardware. It may be part of the external equipment, though, and would therefore be left out in the pack hardware itself. Usually, a pack's voltage is about 350 V to 450 V. It should be mentioned that up to 60 V voltage, one main relay is known as a sufficient hardware resolution.

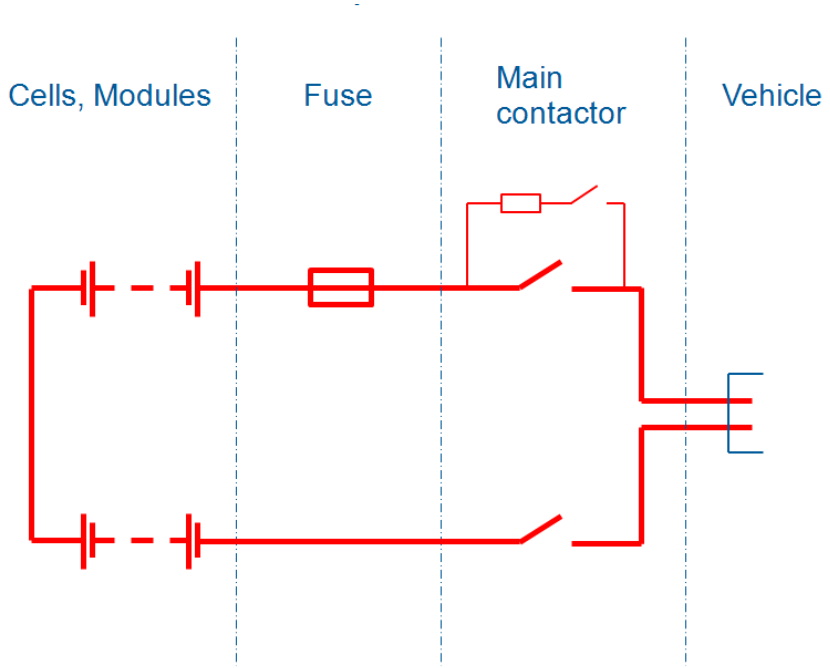

Figure 4.39.: Simplified Schematic view of a Pack

A pack not only consists of the components themselves. The cells of the packs are interconnected by screwing, welding or even clinching. As shown in figure 4.40, parts of the pack

are usually also two main contactors, the above mentioned preload contactor as well as a fuse and in some cases a charge contactor. Other elements would be busbars between batteries and interfaces, as well as interfaces to the vehicle. Cables are needed, pressed-in-pins and additional screwed connections.

A pack was estimated where the resistances served as approximation basis. 150 cells were chosen as a starting point. In figure 4.41 the elements of this example pack are visualized except the cells themselves in regard to their influence on a possible equivalent circuit diagram as resistances. Busbars are named by their location. E.g. the busbar connecting the batteries is referred to as busbar HV. Cell contacts are the interconnections between the cells. The other components are mentioned above.

The cabling and the fuse have the largest resistances in the chart, whereas the cell contactors, despite being numerous only account for 3.16 % resistance of all pack-related hardware.

Comparing the cell resistances to those of the other hardware of the pack, it is clearly not the additional hardware which preponderates. The proportion of resistance of the entire additional hardware to all cells is 50:1, if one cell's resistance is set to 1 mΩ. The ohmic approach for the entire pack is then 100 mΩ.

It should be mentioned that the length of the overall hardware causes an inductive behavior. Additionally, there are capacitive characteristics between cell circuit and ground. These phenomena are difficult to measure and evaluate and differ from pack to pack.

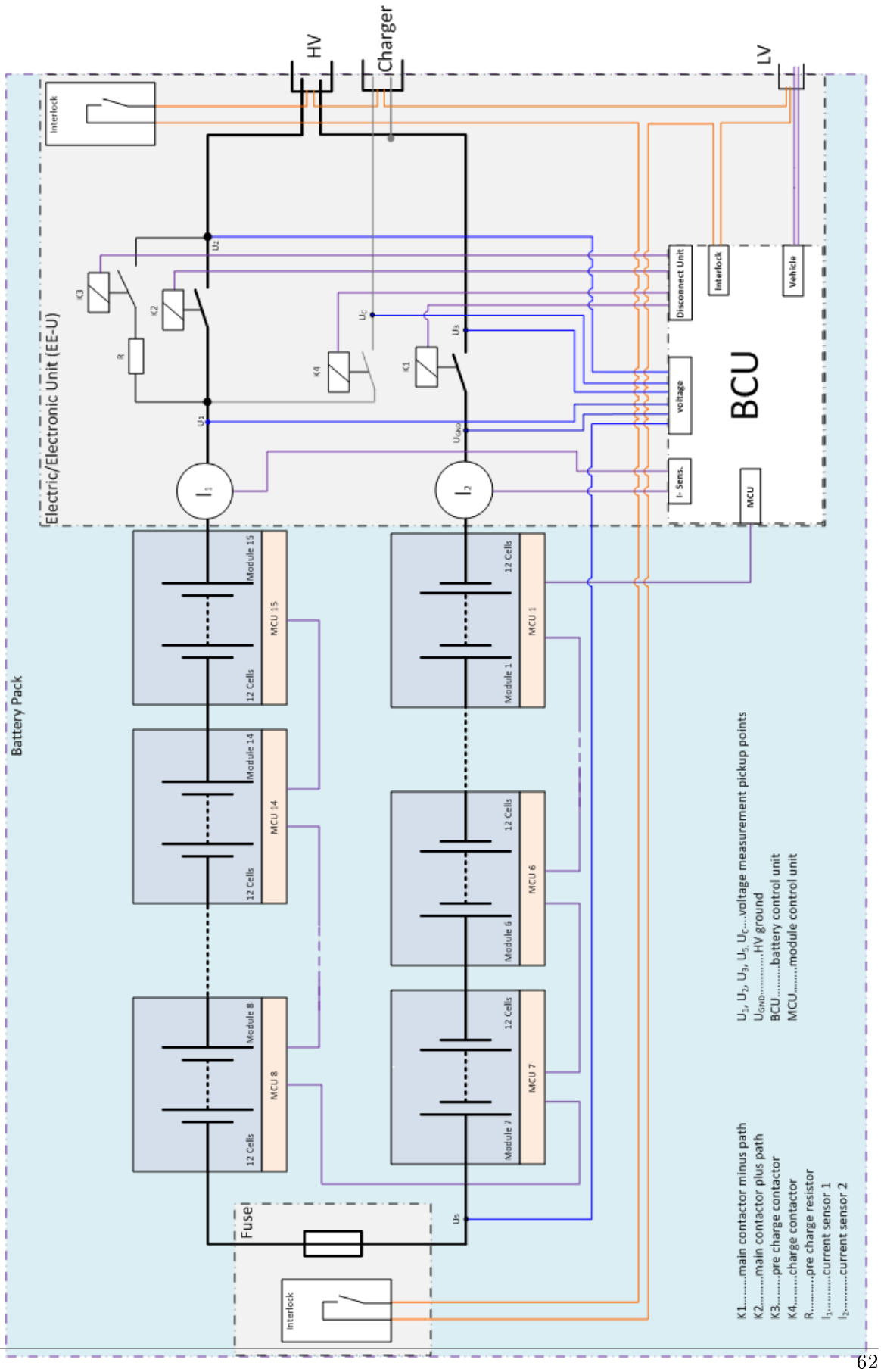

Figure 4.40.: Modular View of a Pack

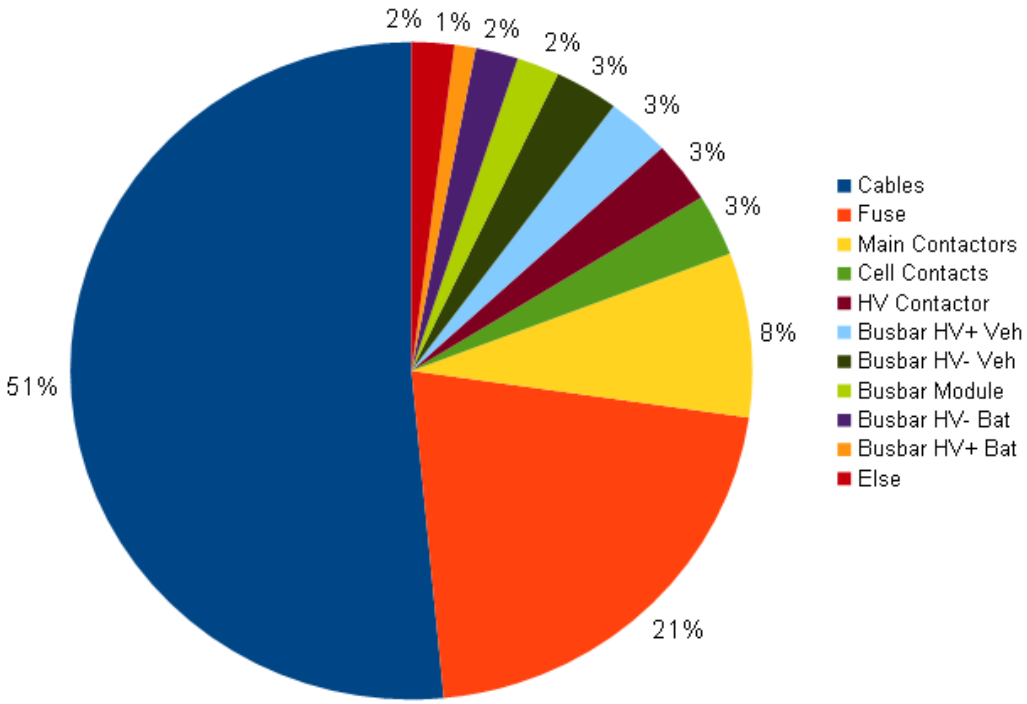

Figure 4.41.: Pack Related Resistances

5. Conclusion and Further Work

5.1. Conclusion

By comparing the methods, executed in the frequency and time domain, it turned out that they are very similar in terms of execution. Significant differences can be seen in the number of elements in the equivalent circuit diagram and the application area of each method.

5.1.1. Number of RC Elements

The reason, for the different results in simulating the equivalent circuit diagram for 2 and 3 RC elements for the results of the frequency domains method, is that as illustrated in figure 5.1 the least squares fit in the Nyquist plot for 2 RC elements cannot be as accurate as would be desirable. The parameters are especially inaccurate for the frequency range used in the simulation. So unfortunately, the frequency domain and the time domain parameters cannot be compared directly. The frequency range for the frequency domain reaches from 0.5 kHz to 0.5 mHz and for the time domain it reaches from 100 Hz to 10 mHz. In chapter 4 the least squares fit for 3 RC elements can be seen in figure 4.15. For the simulated range its accuracy is sufficient.

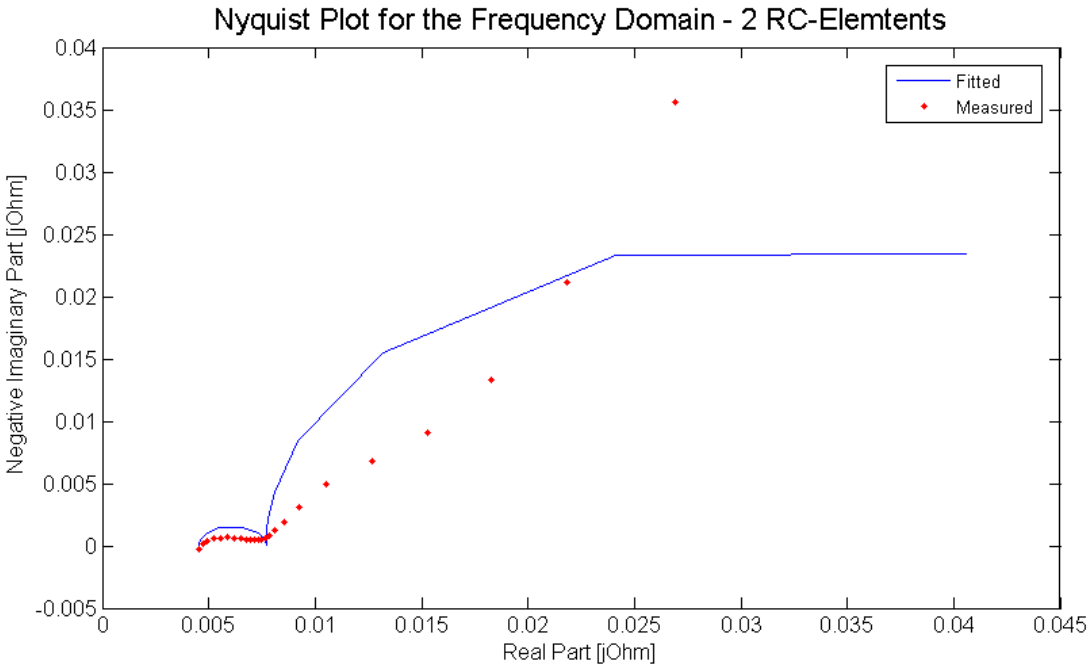

Figure 5.1.: 2 RC Elements Least Squares Fit at 75% SOC

The time domain's equivalent circuit diagram with 2 RC elements leads to the same simulation results and the same overall resistance. As described in chapter 4, even for high frequencies no additional information could be obtained from a third RC element, because the sampling rate was 100 Hz and a third element would be informative, when it comes to modeling the first seconds behavior of the cell, including the inductance, which is clearly calculable by measuring at least with 1 kHz. In addition, as the simulation is accurate enough as it is for the underlying purpose, a third element providing further information, e.g. a higher sampling rate, is simply not necessary. Therefore, two RC elements are fitting for this method.

Compared to the parameters obtained from the time domain's least squares fit, where the resistances of the third RD element is in the $\mu\Omega$ range, the ones determined using the method, executed in the frequency domain, are in average higher by the factor 1000. The reason is that the SOC change in the frequency domain is visible in the Nyquist plot for low frequencies from about 5 mHz on and contrary to the time domain, the OCV difference in each sine wave was not subtracted in advance. This difference would then result in a capacitance, in series to the equivalent circuit diagram. Therefore, as depicted in figure 5.2 the ohmic resistance of one RC element turned out to be very high, so that only the capacity remained.

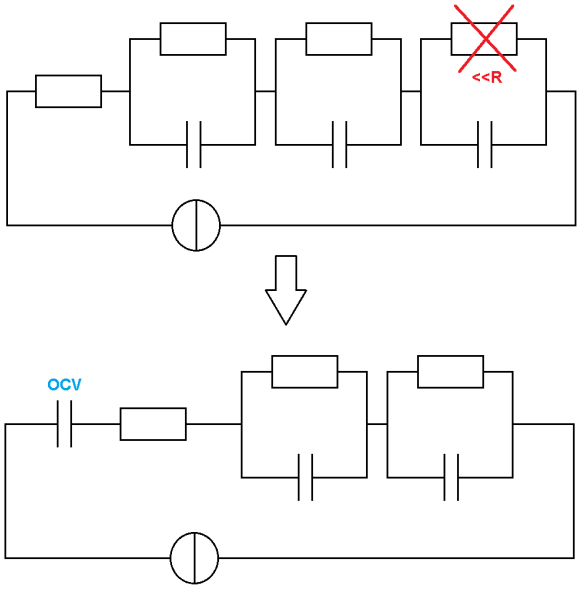

Figure 5.2.: Equivalent Circuit Diagram - Frequency Domain

The parameters obtained by the EIS are for a wider frequency range (1 mHz to 1kHz). Additional information can be found, depending on the chemistry of the battery. More RC elements or a Warburg impedance may actually cause an overlapping fit with the measured voltage in the simulation. The EIS becomes far less accurate, with high currents, if the inner resistance is nonlinear.

As shown in table 5.1, the parameters obtained by the time domains method are equal accurate to the ones determined by the method using the Nyquist plot. The table displays

the average difference between simulated and measured value in mV. Therefore time domains method is accurate enough for the automotive industry. Possible non-linearities are simple to remove mathematically. In the first second of excitation, the dynamic behavior would obtain further information. But the least squares fit would require taking it weighted into account, by e.g. executing a second fit only for the area of the first second. So a second fit and a higher sampling rate would be necessary to simulate the double layer capacity. The current strength, the endurance of a pulse and the sampling rate can and should be as close to the further application as possible. If necessary, high currents can then be emulated accurately, even if the inner resistance is nonlinear.

Method	**Average Difference at 55% SOC [mV]**
Frequency Domain – 2RC Elements	5.4
Tine Domain – 3RC Elements	2.1
Frequency Domain – 3RC Elements	1.8
Time Domain – 2RC Elements	1.6

Table 5.1.: Accuracy in Simulation

5.1.2. Cost-Efficiency

For the same frequency range, both methods require the same hardware and are even equal in complexity (sampling rate, amplifier).

5.1.3. Duration

The measurement duration is equal. For both methods, the SOC and the temperature are set under the same boundary conditions. Each measurement requires at least the duration of the lowest frequency which is then used in further emulation. Even if the time domain is more processor-intensive in data analysis (many more data points in least squares fit), one curve fitting still is done in seconds on a PC equipped with an i7 Core processor and 6 GB RAM.

The conclusion is to use pulsing, followed by a least squares fit in the time domain for efficient accurate parameterization for further emulation.

5.2. Further Work

As the current strength, the temperature dependence as well as the SOH dependence were not part of this thesis, the results still need to be verified accordingly. Additionally, the relation of the cell's equivalent circuit diagram to the one of a module or a pack needs to be ascertained correctly. In particular the impedance spectroscopy with its high accuracy in terms of cells is not necessarily very accurate for modules and packs as well.

5.2.1. Module/Pack Testing

The method, which is basically proven in regard to cell testing needs to be verified in the automotive application for modules and packs. Therefore, the measurement equipment needs to be advanced for higher power application.

5.2.2. Current Magnitude

A current excitation of higher currents would prove the above mentioned accuracy of this method for all current strengths.

5.2.3. SOH Dependence

Using batteries of different, but defined age may result in new parameter sets for each SOH.

5.2.4. Temperature Dependence

The reliability of the method needs to be tested for different temperatures. It would seem that for the frequency domain, possible inaccuracies due to a change in temperature are proven:

As shown in figure 5.3, low cell temperatures cause higher impedance values in the Nyquist diagram [Andre et al., 2010].

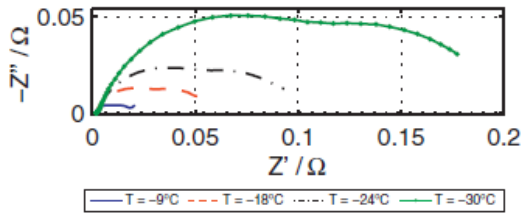

Figure 5.3.: Nyquist of Low Temperature [Andre et al., 2010]

Not only are the chemical processes slower, causing higher impedance for the first two semi-circles (ion movement), but also the diffusion processes are dependent on the temperature, which is represented by the diffusion coefficient in Fick's law:

$$J = -D\frac{\delta\gamma}{\delta x} \tag{5.1}$$

D is the diffusion coefficient, J the diffusion flux, γ the concentration and x the position. Consequently, there is no calculable parameterization in the Nyquist plot of low temperatures. In the case of high temperature, as shown in figure 5.4, the semi-circles merge, the ohmic resistance is decreasing. The time constants converge.

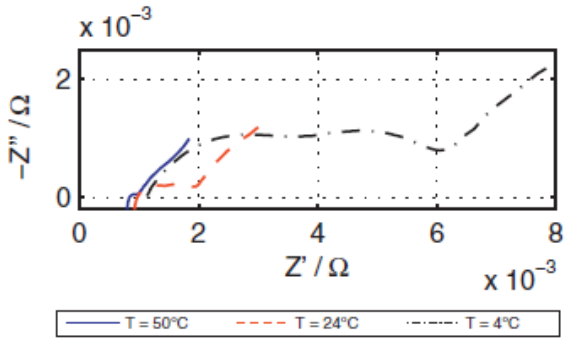

Figure 5.4.: Nyquist of High Temperature [Andre et al., 2010]

And yet the variables for the parameterization of an equivalent circuit diagram can still be accurately obtained from a mid temperature measurement where the semicircles are well-defined in the Nyquist diagram.

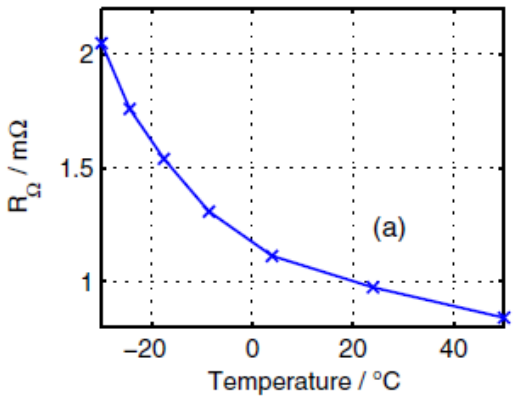

Figure 5.5.: Diagram of Temperature-Resistance Dependence [Andre et al., 2010]

As shown for the ohmic resistance in figure 5.5, at 20°C and above, the measurement is reliable. For temperatures below, Arrhenius law is causing an exponential rise of the resistance. It defines the dependency between temperature and chemical reactions:

$$k = A \cdot e^{-} \frac{Ea}{RT} \tag{5.2}$$

k is the rate constant, T the temperature, Ea the activation energy, A is the pre-exponential factor and R is the universal gas constant.

If temperature dependence causes problems for a single cell there are all the more reasons to test it for modules and packs. As the above mentioned temperature inaccuracy is only proven for the Nyquist plot, the time domains dependence still needs to be tested further.

Bibliography

D. Andre, M. Meiler, K. Steiner, Ch. Wimmer, T. Soczka-Guth, and D.U. Sauer. Characterization of High-Power Lithium-Ion Batteries by Electrochemical Impedance Spectroscopy. I: Experimentalinvestigation. *Journal of Power Sources*, 2010.

E. Barsoukov and J. R. Macdonald. Impedance Spectroscopy: Theory, Experiment, and Applications. *John Wiley & Sons*, 2005.

B. Berman. Study Emphasizes Importance of China's Transition to Electric Cars. Website, 2011. URL `www.NYtimes.com`. retrieved: 20.04.2011.

W. G. Bessler. Rapid Impedance Modeling via Potential Step and Current Relaxation Simulations. *Interdisciplinary Center for Scientific Computing (IWR)*, 2007.

B. A. Boukamp. A Nonlinear Least Squares Fit Procedure for Analysis of Imittance Data of Electrochemical Systems. *Elsevier Science Publishers B.V. - North-Holland Physics Publishing Division*, 1985.

M. Broussely, S.Herreyre, P. Biensan, K.Nechev, and R.J.Staniewicz. Aging mechanism in Li Ion Cells and Calendar Life Predictions. *Journal of Power Sources, Volumes 97-98. pp. 13-21*, 2001.

W. Bösch, M. Gadringer, and I. Russo. Grundlagen der Hochfrequenztechnik. 2012.

I. Buchmann. Safety Concerns with Li-Ion. Website, 2012. URL `http://batteryuniversity.com/learn/article/safety_concerns_with_li_ion`. retrieved: 29.10.2012.

S. Buller. Impedance-Based Simulation Models for Energy Storage Devices in Advanced Automotive Power Systems. *Aachener Beiträge des ISEA, Band 31, Februar 2003, p. 52*, 2003.

S. Buller. Impedance-Based Simulation Models of Supercapacitors and Li-Ion Batteries for Power Electronic Applications. *IEEE Transactions on Industry Applications, Vol. 41, No. 3, May/June*, 2005.

G. Cheesman. The Importance of Electric Vehicles. Website, 2011. URL `www.care2.com`. retrieved: 13.06.2011.

US Department Energy. Hybrid Electric Vehicles. Website, 2013. URL `www1.eere.energy.gov`. retrieved: 09.01.2013.

E. Karden. Using Low-Frequency Impedance Spectroscopy for Characterization, Monitoring, and Modeling of Industrial Batteries. 2001.

D. U. Sauer. Impedanzspektroskopie - Eine Methode, Viele Anwendungen. *Technische Mitteilungen, pp. 7-11*, 99 Heft 1/2, 2006a.

D. U. Sauer. Grundlagen der Impedanzspektroskopie für die Charakterisierung von Batterien. *Technische Mitteilungen, pp. 74-80*, 99 Heft 1/2, 2006b.

M. Thele. A Contribution to the Modelling of the Charge Acceptance of Lead-Acid Batteries - Using Frequency and Time Domain Based Concepts. *Shaker Verlag GmbH*, 2008.

IB Times. Senator Alexander; Nissan and PEW Highlight Importance of Electric Vehicles in Clean Energy Economy. Website, 2011. URL `http://uk.IBtimes.com`. retrieved: 21.07.2011.

U. Tröltzsch. Modellbasierte Zustandsdiagnose von Gerätebatterien. 2005.

History Hybrid Vehicles. History of Hybrid Vehicles. 13.06.2011, 2011. URL `www.hybridcars.com`. retrieved: 13.06.2011.

H. Wegleiter and B. Schweighofer. Entwurf und Modellierung mobiler Energiespeichersysteme. 2012.

K. Zaghib, J. Dubé, A. Dallaire, K. Galoustov, A. Guerfi, M. Ramanathan, A. Benmayza, J. Prakash, A. Mauger, and C. M. Julien. Enhanced Thermal Safety and High Power Performance of Carbon-Coated $LiFePO_4$ Olivine Cathode for Li-Ion Batteries. *Journal of Power Sources 219, pp. 36-44*, 2012.

List of Figures

List of Tables

A. Appendix

A.1. Battery Cell Data Sheet

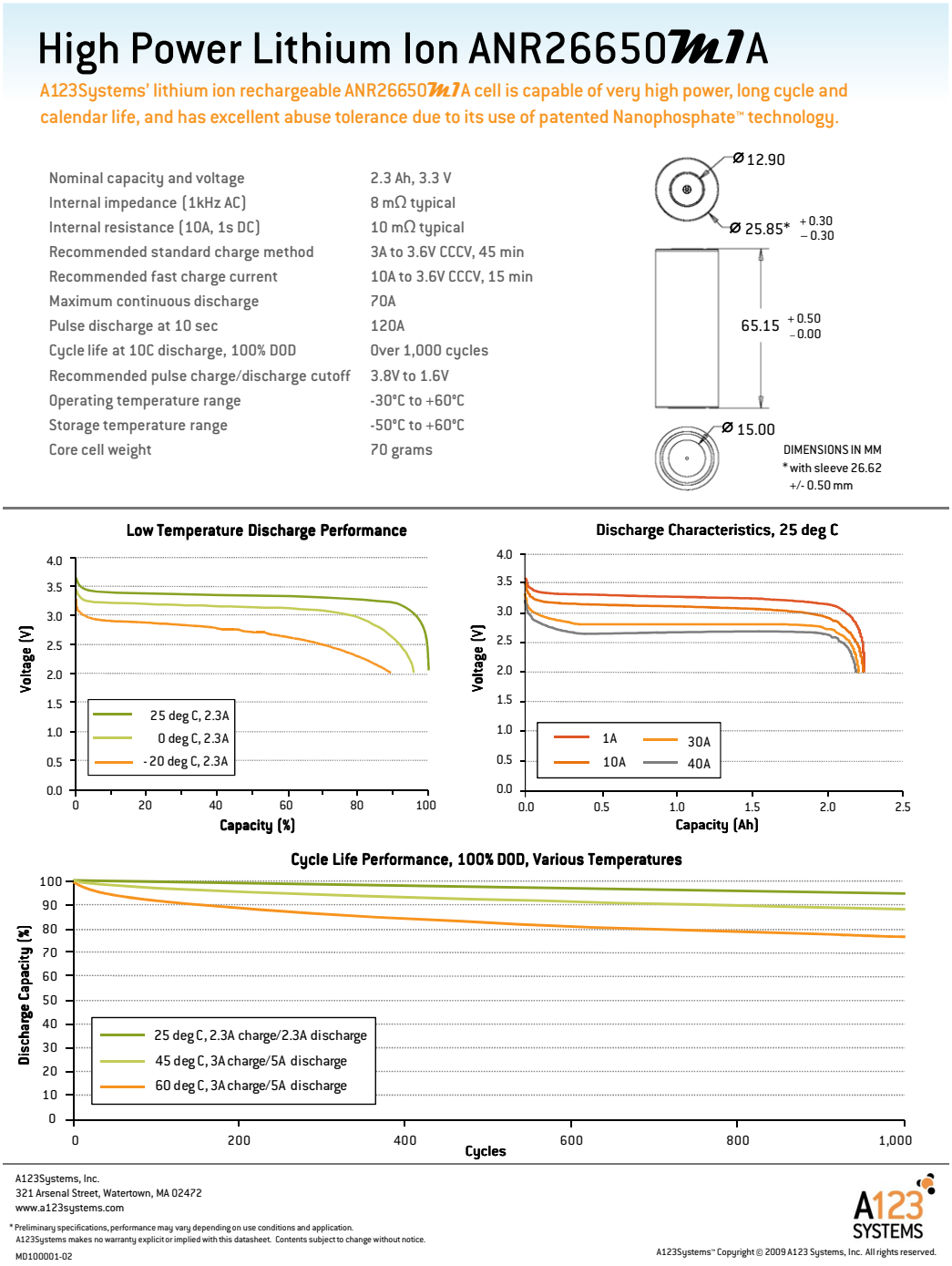

Figure A.1.: Battery Cell Data Sheet

A.2. Matlab Computation Frequency Domain

```
clear all variables
close all

load ('8')


global cnt1 speicher_frequenz

startmeas = 1;
endmeas = 24;

for cell = startmeas:endmeas

N = length(speicher_strom{:,cell});

% fft current
I = fft(speicher_strom{:,cell},N);
amplI = abs(I);
angleI = angle(I);

%fft voltage
Umean = mean(speicher_spannung{:,cell});
    if cell > 1
    Umeanaverage = (mean(speicher_spannung{:,cell-1}) +
mean(speicher_spannung{:,cell}))/2;
    else
    Umeanaverage = mean(speicher_spannung{:,cell});
    end
Usignal = speicher_spannung{:,cell} - Umean;
U = fft(Usignal,N);
amplU = abs(U);
angleU = angle(U);

%sampling rate
if 1 <= cell && cell <= 11
    fa = speicher_frequenz(cell)* 2^(2+cell);
    y(cell) = 2^(2+cell);
    x(cell) = speicher_frequenz(cell)* 2^(2+cell);
end
if cell >= 12
    fa = speicher_frequenz(cell)*16384;
    x(cell) = speicher_frequenz(cell)*16384;
    y(cell) = 16384;
end
df = fa/N;
fn = fa/2;
```

Figure A.2.: Matlab Frequency Domain for 2RC-Elements

```
x_fa = 0 : df : fa-df;
x_fn = 0 : df : fn-df;

amplitudengangI = [amplI(1)/N amplI(2:N/2)/(N/2)]; % DC-Bin to
N normalized
% stem(x_fn, amplitudengangI, 'b.-')
% title('Amplitude Response')
% ylabel('Amplitude')
% xlabel(['Resolution: ',num2str(df),' Hz Frequency in Hz'])
% grid

amplitudengangU = [amplU(1)/N amplU(2:N/2)/(N/2)]; % DC-Bin to
N normalized
% stem(x_fn, amplitudengangU, 'b.-')
% title('Amplitude Response')
% ylabel('Amplitude')
% xlabel(['Resolution: ',num2str(df),' Hz Frequency in Hz'])
% grid

Imax = max(amplitudengangI);
Umax = max(amplitudengangU);

Imaxcheck = max(speicher_strom{:,cell});
Umaxcheck = max(speicher_spannung{:,cell});

%computation Z
Z_absolute = sqrt(Umax^2 / Imax^2);

%computation phi
i=0;

for i=1:N
    if amplitudengangI(i) > 0.1
        break;
    end
end

phi = (angleU(i) - angleI(i)) *180/pi;

%check solution
% for i=1:N
%     Isin(i) = Imax*sin(2*pi*speicher_frequenz(cell)*i);
% end

Zreal1(cell) = Z_absolute * cos(phi*pi/180);
Zimg1(cell) = Z_absolute * sin(phi*pi/180);
```

Figure A.3.: Matlab Frequency Domain for 2RC-Elements

```
end

%PLOT ONE SIGNAL

fa = speicher_frequenz(7)* 2^(2*5);
ta = 1/fa; %sampling rate

%x-axes
for i = 1:length(speicher_strom{:,5})
    time(i) = i*ta;
end

Umean = mean(speicher_spannung{:,5});
Usignal = speicher_spannung{:,5} - Umean;

Fontsize = 20;
%figure1 = figure();
[haxes,hline1,hline2] =
plotyy(time,speicher_strom{:,5},time,Usignal,'plot');
grid
title('Current - Voltage Signals')
axes(haxes(1))
ylabel('Current in Ampere')
axes(haxes(2))
ylabel('Voltage in Volt')
xlabel('Time in Seconds')

%check as plot
% plot(Zreal1,-Zimg1,'r.')
% title('Nyquist Plot')
% ylabel('Negative Imginary Part')
% xlabel('Real Part')

% Computation Ri
found=0;
Ri=0;
for i=startmeas:endmeas
    if (Zimg1(i)<=0 && found==0)
    Ri = ((Zreal1(i) - Zreal1(i))*(-Zimg1(i-1))) / (Zimg1(i)-
Zimg1(i-1)) + Zreal1(i-1);
    found=1;
    end
end


global Ri KR1 KR2 KC1 KC2 KL
```

Figure A.4.: Matlab Frequency Domain for 2RC-Elements

```
global Zimg1 Zreal1
cnt1 = 0;
No_Coeff = 5; % 8 Coefficients are unknown ...
C1,C2,R1,R2,Ri ...

optims=optimset('fminsearch');
optims.MaxIter = 10000000000;
optims.MaxFunEvals = 10000000000;
optims.TolX=1e-10;
optims.TolFun=1e-10;

start=[1;1;1;1;1];

%Initial Seed
KR1=0.0033;
KR2=0.007;
KC1=0.5314;
KC2=2050;
KL=1.1459e-013;

parameters=repmat(start,1,endmeas);

parameters(:,1) =
fminsearch('impedanz10112RC',parameters(:,1),optims);


% plot of the result
imagt=zeros(1,endmeas);
realt=zeros(1,endmeas);


for i=startmeas:endmeas
    w=speicher_frequenz(i)*2*pi;
    R1=parameters(1,1);
    R2=parameters(2,1);
    C1=parameters(3,1);
    C2=parameters(4,1);
    L =parameters(5,1);
Z1 = (Ri);
Z2 = ((R1*KR1)/(1i*w*(C1*KC1)))/((R1*KR1)+1/(1i*w*(C1*KC1)));
Z3 = ((R2*KR2)/(1i*w*(C2*KC2)))/((R2*KR2)+1/(1i*w*(C2*KC2)));
Z5 = 1i*w*(L*KL);
zg = Z1 + Z2 + Z3 + Z5;
realt(i) = real(zg);
imagt(i) = imag(zg);
end
```

Figure A.5.: Matlab Frequency Domain for 2RC-Elements

```
    Ri
    R1=(parameters(1,1))*KR1
    R2=(parameters(2,1))*KR2
    C1=(parameters(3,1))*KC1
    C2=(parameters(4,1))*KC2
    L =(parameters(5,1))*KL

figure
 plot (parameters(1,:))
figure
plot(realt(startmeas:endmeas),-imagt(startmeas:endmeas))
hold
plot(Zreal1,-Zimg1,'r.')
```

Figure A.6.: Matlab Frequency Domain for 2RC-Elements

```
function e=impedanz10112RC(p)

global speicher_frequenz Zimg1 Zreal1 cnt1


R1=p(1);
R2=p(2);
C1=p(3);
C2=p(4);
L =p(5);


global Ri KR1 KR2 KC1 KC2 KL


e = 0;

for cnt1 = 1:24

w = speicher_frequenz(cnt1)*2*pi;
Z1 = (Ri);
Z2 = ((R1*KR1)/(1i*w*(C1*KC1)))/((R1*KR1)+1/
(1i*w*(C1*KC1)));
Z3 = ((R2*KR2)/(1i*w*(C2*KC2)))/((R2*KR2)+1/
(1i*w*(C2*KC2)));
Z5 = 1i*w*(L*KL);
zg = Z1 + Z2 + Z3 + Z5;
realteil = real(zg);
imagteil = imag(zg);
a = 1/((Zreal1(cnt1))^2 + (Zimg1(cnt1))^2);


e = e + a * ((realteil-Zreal1(cnt1))^2+(imagteil-
Zimg1(cnt1))^2);
end
```

Figure A.7.: Matlab Frequency Domain for 2RC-Elements - Least Squares Fit

```
clear all variables
close all
clc

load ('2')


global cnt1 speicher_frequenz

startmeas = 1;
endmeas = 24;

for cell = startmeas:endmeas

%cell = 3;
N = length(speicher_strom{:,cell});

% fft current
I = fft(speicher_strom{:,cell},N);
amplI = abs(I);
angleI = angle(I);

%fft voltage
Umean = mean(speicher_spannung{:,cell});
    if cell > 1
    Umeanaverage = (mean(speicher_spannung{:,cell-1}) +
mean(speicher_spannung{:,cell}))/2;
    else
    Umeanaverage = mean(speicher_spannung{:,cell});
    end
Usignal = speicher_spannung{:,cell} - Umean;
U = fft(Usignal,N);
amplU = abs(U);
angleU = angle(U);

% Plot Angle

% if cell == 5
% figure1 = figure();
% [haxes,hline1,hline2] =
plotyy(1:16384,angleI,1:16384,angleU,'plot');
% grid
```

Figure A.8.: Matlab Frequency Domain for 3RC-Elements

```
% title('FFT Angle Shifts')
% axes(haxes(1))
% ylabel('Current Angle in Degree')
% axes(haxes(2))
% ylabel('Voltage Angle in Degree')
% xlabel('Frequency')
% end

if 1 <= cell && cell <= 11
    fa = speicher_frequenz(cell)* 2^(2+cell);
    fa_dependence(cell) = speicher_frequenz(cell)*
2^(2+cell);
    points_per_period(cell) = 2^(2+cell);
end
if cell >= 12
    fa = speicher_frequenz(cell)*16384;
    fa_dependence(cell) = speicher_frequenz(cell)*16384;
    points_per_period(cell) = 16384;
end
df = fa/N;
fn = fa/2;
x_fa = 0 : df : fa-df;
x_fn = 0 : df : fn-df;

amplitudengangI = [amplI(1)/N amplI(2:N/2)/(N/2)]; % DC-Bin
in N normalization
% figure
% stem(x_fn, amplitudengangI, 'b.-')
% title('Current Amplitude Response')
% ylabel('Current Amplitude in Ampere')
% xlabel(['Resolution: ',num2str(df),' Hz ... Frequency in
Hz'])
% grid

amplitudengangU = [amplU(1)/N amplU(2:N/2)/(N/2)]; % DC-Bin
in N normalization
% figure
% stem(x_fn, amplitudengangI, 'b.-')
% title('Voltage Amplitude Response')
% ylabel('Voltage Amplitude in Volt')
% xlabel(['Resolution: ',num2str(df),' Hz ... Frequency in
Hz'])
```

Figure A.9.: Matlab Frequency Domain for 3RC-Elements

```
% grid

Imax = max(amplitudengangI);
Umax = max(amplitudengangU);

% for plotting amplitudes
Iamp(cell) = max(amplitudengangI);
Uamp(cell) = max(amplitudengangU);

Imaxcheck = max(speicher_strom{:,cell});
Umaxcheck = max(speicher_spannung{:,cell});

%computation Z
Z_absolute = sqrt(Umax^2 / Imax^2);

%computation phi
i=0;

for i=1:N
    if amplitudengangI(i) > 0.1
        break;
    end
end

phi = (angleU(i) - angleI(i)) *180/pi;

%check solution
% for i=1:N
%     Isin(i) = Imax*sin(2*pi*speicher_frequenz(cell)*i);
% end

Zreal1(cell) = Z_absolute * cos(phi*pi/180);
Zimg1(cell) = Z_absolute * sin(phi*pi/180);
end

% Plot Fa

% figure
% plot(points_per_period);
% title('Measurement Points per Signal Period')
% ylabel('Number of Measurement Points')
% xlabel('Data Set, from high to low Frequency')
```

Figure A.10.: Matlab Frequency Domain for 3RC-Elements

```
% grid
%
% figure
% plot(fa_dependence);
% title('Sampling Rate')
% ylabel('Number of Measurement Points')
% xlabel('Data Set, from high to low Frequency')
% grid

% Plot Amplitudes

figure
plot(Iamp);
title('Currtent Amplitudes')
ylabel('Current [A]')
xlabel('Data Set, from high to low Frequency')
grid

figure
plot(Uamp);
title('Voltage Amplitudes')
ylabel('Voltage [V]')
xlabel('Data Set, from high to low Frequency')
grid

%PLOT ONE SIGNAL

fa = speicher_frequenz(7)* 2^(2*5);
ta = 1/fa; %sampling rate

%x-axes
for i = 1:length(speicher_strom{:,5})
    time(i) = i*ta;
end

Umean = mean(speicher_spannung{:,5});
Usignal = speicher_spannung{:,5} - Umean;

Fontsize = 20;
figure1 = figure();
[haxes,hline1,hline2] =
plotyy(time,speicher_strom{:,5},time,Usignal,'plot');
```

Figure A.11.: Matlab Frequency Domain for 3RC-Elements

```
grid
title('Current - Voltage Signals')
axes(haxes(1))
ylabel('Current in Ampere')
axes(haxes(2))
ylabel('Voltage in Volt')
xlabel('Time in Seconds')

%Ri
found=0;
Ri=0;
for i=startmeas:endmeas
    if (Zimg1(i)<=0 && found==0)
    Ri=Zreal1(i);
    found=1;
    end
end


global Ri KR1 KR2 KR3 KC1 KC2 KC3 KL
global Zimg1 Zreal1
cnt1 = 0;
No_Coeff = 8; % 8 Coefficients are unknown ...
C1,C2,R1,R2,Ri ...

optims=optimset('fminsearch');
optims.MaxIter = 10000000000;
optims.MaxFunEvals = 10000000000;
optims.TolX=1e-10;
optims.TolFun=1e-10;

start=[1;1;1;1;1;1;1];

%Initial Seed
KR1=0.0033;
KR2=0.007;
KR3=0.08;
KC1=0.5314;
KC2=2050;
KC3=8000;
KL=1.1459e-008;
```

Figure A.12.: Matlab Frequency Domain for 3RC-Elements

```
parameters=repmat(start,1,endmeas);

parameters(:,1) =
fminsearch('impedanz1011Ri',parameters(:,1),optims);

% plot of the result
imagt=zeros(1,endmeas);
realt=zeros(1,endmeas);


for i=startmeas:endmeas
    w=speicher_frequenz(i)*2*pi;
    R1=parameters(1,1);
    R2=parameters(2,1);
    R3=parameters(3,1);
    C1=parameters(4,1);
    C2=parameters(5,1);
    C3=parameters(6,1);
    L =parameters(7,1);
Z1 = Ri;
Z2 = ((R1*KR1)/(1i*w*(C1*KC1)))/((R1*KR1)+1/
(1i*w*(C1*KC1)));
Z3 = ((R2*KR2)/(1i*w*(C2*KC2)))/((R2*KR2)+1/
(1i*w*(C2*KC2)));
Z4 = ((R3*KR3)/(1i*w*(C3*KC3)))/((R3*KR3)+1/
(1i*w*(C3*KC3)));
Z5 = 1i*w*(L*KL);
zg = Z1 + Z2 + Z3 + Z4 + Z5;
realt(i) = real(zg);
imagt(i) = imag(zg);
end


    Ri
    R1=(parameters(1,1))*KR1
    R2=(parameters(2,1))*KR2
    R3=(parameters(3,1))*KR3
    C1=(parameters(4,1))*KC1
    C2=(parameters(5,1))*KC2
    C3=(parameters(6,1))*KC3
    L =(parameters(7,1))*KL
% figure
```

Figure A.13.: Matlab Frequency Domain for 3RC-Elements

```
figure
 plot (parameters(1,:))
figure
plot(realt(startmeas:endmeas),-imagt(startmeas:endmeas))
hold
plot(Zreal1,-Zimg1,'r.')
```

Figure A.14.: Matlab Frequency Domain for 3RC-Elements

```
function e=impedanz1011Ri(p)

global speicher_frequenz Zimg1 Zreal1 cnt1


R1=p(1);
R2=p(2);
R3=p(3);
C1=p(4);
C2=p(5);
C3=p(6);
L =p(7);


global Ri KR1 KR2 KR3 KC1 KC2 KC3 KL


e = 0;

for cnt1 = 1:24

w = speicher_frequenz(cnt1)*2*pi;
Z1 = Ri;
Z2 = ((R1*KR1)/(1i*w*(C1*KC1)))/((R1*KR1)+1/
(1i*w*(C1*KC1)));
Z3 = ((R2*KR2)/(1i*w*(C2*KC2)))/((R2*KR2)+1/
(1i*w*(C2*KC2)));
Z4 = ((R3*KR3)/(1i*w*(C3*KC3)))/((R3*KR3)+1/
(1i*w*(C3*KC3)));
Z5 = 1i*w*(L*KL);
zg = Z1 + Z2 + Z3 + Z4 + Z5;
realteil = real(zg);
imagteil = imag(zg);
a = 1/((Zreal1(cnt1))^2 + (Zimg1(cnt1))^2);


e = e + a * ((realteil-Zreal1(cnt1))^2+(imagteil-
Zimg1(cnt1))^2);
end
```

Figure A.15.: Matlab Frequency Domain for 3RC-Elements - Least Squares Fit

A.3. Matlab Computation Time Domain

```
clear all variables
close all

load ('12-10-22__15-02_t_u_i_a123_2300mah')

global startmeas endmeas Icom Ucom

global KRi KR1 KR2 KC1 KC2


% MANUAL DATA EXTRACTION

% 10 different SOC setpoints; 05% aborded

% U_SOC95 = data(1:734324,2) * 1.004;
% U_SOC85 = data(734324:1342400,2) * 1.004;
% U_SOC75 = data(1342400:1950700,2) * 1.004;
% U_SOC65 = datar(1950700:2559100,2) * 1.004;
% U_SOC55 = data(2559078:3167600,2) * 1.004;
% U_SOC45 = data(3167600:3776200,2) * 1.004;
% U_SOC35 = data(3776200:4385000,2) * 1.004;
U_SOC25 = data(4385000:4993900,2) * 1.004;
% U_SOC15 = data(4993900:5602900,2) * 1.004;
% U_SOC05 = data(5602900:5633912,2) * 1.004;



% SQUARES

%95
% U_Square = U_SOC95(342433:349630);
% Imeas = data(1:734324,1) * 4.8;
% Icom = 1.286;
%
% U1ocv = 3.3313;
% U2ocv = 3.3277;

%85
% U_Square = U_SOC85(216166:223350);
%
% Imeas = data(734324:1342400,1) * 4.8;
% Icom = 1.286;
```

Figure A.16.: Matlab Time Domain for 2RC-Elements

```
%
% U1ocv = 3.3254;
% U2ocv = 3.324;

%75
% U_Square = U_SOC75(216264:223455);
%
% Imeas = data(1342400:1950700,1) * 4.8;
% Icom = 1.286;
%
% U1ocv = 3.3055;
% U2ocv = 3.2984;

%65
% U_Square = U_SOC65(216253:223450);
%
% Imeas = data(1950700:2559100,1) * 4.8;
% Icom = 1.286;
%
% U1ocv = 3.2870;
% U2ocv = 3.2868;

%55
% U_Square = U_SOC55(216284:223480);
%
% Imeas = data(2559078:3167600,1) * 4.8;
% Icom = 1.283;
%
% U1ocv = 3.2851;
% U2ocv = 3.2848;

%45
% U_Square = U_SOC45(216305:223480);
%
% Imeas = data(2559078:3167600,1) * 4.8;
% Icom = 1.286;
%
% U1ocv = 3.2824;
% U2ocv = 3.2804;

% 35
% U_Square = U_SOC35(216387:223357);
```

Figure A.17.: Matlab Time Domain for 2RC-Elements

```
%
% Imeas = data(3776200:4385000,1) * 4.8;
% Icom = 1.286;
%
% U1ocv = 3.2544;
% U2ocv = 3.24945;

%25
U_Square = U_SOC25(216428:223357);

Imeas = data(4385000:4993900,1) * 4.8;
Icom = 1.286;

U1ocv = 3.2234;
U2ocv = 3.2185;

%15
% U_Square = U_SOC15(216474:223660);
%
% Imeas = data(4993900:5602900,1) * 4.8;
% Icom = 1.2875;
%
% U1ocv = 3.1853;
% U2ocv = 3.1656;

%05 aborded



startmeas = 1;
endmeas = length(U_Square); %squarelength

%start square
t1 = startmeas;
%end square
t2 = endmeas;

%OCV curve

for i=t1:t2
    Uocv(i) = U1ocv -((i-t1)*(U1ocv-U2ocv)/(t2-t1));
end
```

Figure A.18.: Matlab Time Domain for 2RC-Elements

```
for i = startmeas:endmeas
    Ucom(i) = U_Square(i) - Uocv(i);
end


    %%%ACTUAL CURVE FITTING%%%

% editing Ucom to fit
Ucom = -Ucom;


No_Coeff= 5; %5 Coefficients are unknown ...
C1,C2,R1,R2,Ri...


optims=optimset('fminsearch');
optims.MaxIter = 10000000000;
optims.MaxFunEvals = 10000000000;
optims.TolX=1e-10;
optims.TolFun=1e-10;

start=[1;1;1;1;1];

%Initial Seed
KRi=0.45;
KR1=0.0055;
KR2=0.0151;
KC1=1000;
KC2=1.9317e+003;


parameters=repmat(start,1,endmeas);

parameters(:,1) =
fminsearch('Timpedanz23112RC',parameters(:,1),optims);



Ri=(parameters(1,1))
R1=(parameters(2,1))
R2=(parameters(3,1))
```

Figure A.19.: Matlab Time Domain for 2RC-Elements

```
C1=(parameters(4,1))
C2=(parameters(5,1))


%%plot of the result

for t=startmeas:endmeas
    Ri=parameters(1,1);
    R1=parameters(2,1);
    R2=parameters(3,1);
    C1=parameters(4,1);
    C2=parameters(5,1);
URi = (Ri*KRi)*Icom;
URC1(t) = (R1*KR1)*Icom *(1 - exp(-t/
(100*(R1*KR1)*(C1*KC1))));
URC2 = (R2*KR2)*Icom*(1 - exp(-t/(100*(R2*KR2)*(C2*KC2))));
U1(t) = URC1(t) + URC2;
U(t) = URi + URC1(t) + URC2;
end


    Ri = (parameters(1,1))*KRi
    R1 = (parameters(2,1))*KR1
    R2 = (parameters(3,1))*KR2
    C1 = (parameters(4,1))*KC1
    C2 = (parameters(5,1))*KC2
    tau1 = R1*C1
    tau2 = R2*C2
% figure
% plot (parameters(1,:))
figure
hold
plot((startmeas:endmeas)/100,U,'b')
title('Least Squares Fit - Time Domain')
ylabel('Voltage [V]')
xlabel('Time [s]')
plot((startmeas:endmeas)/100,URC1,'c')
plot((startmeas:endmeas)/100,U1,'g')
plot((startmeas:endmeas)/100,Ucom,'r')

% FOR SIMULATION ONLY
```

Figure A.20.: Matlab Time Domain for 2RC-Elements

```
% figure
% Simulation_Voltage_25 = U_SOC25(306433:342433);
% plot((1:36001)/100,Simulation_Voltage_25)

% Simulation_Voltage_45 = U_SOC45(306312:343302);
% plot((1:36991)/100,Simulation_Voltage_45)

% Simulation_Voltage_55 = U_SOC55(306289:342289);
% plot((1:36001)/100,Simulation_Voltage_55)

% Simulation_Voltage_85 = U_SOC85(306170:342170);
% plot((1:36001)/100,Simulation_Voltage_85)

% hold
% plot((1:360001)/1000,Output_Voltage.signals.values)
% plot((1:360001)/1000,Output_Voltage1.signals.values)
```

Figure A.21.: Matlab Time Domain for 2RC-Elements

```
function e=Timpedanz23112RC(p)

global startmeas endmeas Icom Ucom


Ri=p(1);
R1=p(2);
R2=p(3);
C1=p(4);
C2=p(5);



global KRi KR1 KR2 KC1 KC2

e = 0;

for t = startmeas:endmeas

URi = (Ri*KRi)*Icom;
URC1 = (R1*KR1)*Icom *(1 - exp(-t/
(100*(R1*KR1)*(C1*KC1))));
URC2 = (R2*KR2)*Icom *(1 - exp(-t/
(100*(R2*KR2)*(C2*KC2))));
U = URi + URC1 + URC2;

e = e + (U - Ucom(t))^2;


if Ri < 0 || R1 < 0 || R2 < 0 || C1 < 0 || C2 < 0
    e = e + 10;
end
end
```

Figure A.22.: Matlab Time Domain for 2RC-Elements - Least Squares Fit

```
clear all variables
close all

load ('12-10-22__15-02_t_u_i_a123_2300mah')

global startmeas endmeas Icom Ucom

global KRi KR1 KR2 KR3 KC1 KC2 KC3

% MANUAL DATA EXTRACTION

% 10 different SOC setpoints; 05% aborded

% U_SOC95 = data(1:734324,2) * 1.004;
% U_SOC85 = data(734324:1342400,2) * 1.004;
% U_SOC75 = data(1342400:1950700,2) * 1.004;
% U_SOC65 = data(1950700:2559100,2) * 1.004;
U_SOC55 = data(2559078:3167600,2) * 1.004;
% U_SOC45 = data(3167600:3776200,2) * 1.004;
% U_SOC35 = data(3776200:4385000,2) * 1.004;
% U_SOC25 = data(4385000:4993900,2) * 1.004;
% U_SOC15 = data(4993900:5602900,2) * 1.004;
% U_SOC05 = data(5602900:5633912,2) * 1.004;



% SQUARES

%95
% U_Square = U_SOC95(342433:349630);
% Imeas = data(1:734324,1) * 4.8;
% Icom = 1.286;
%
% U1ocv = 3.3313;
% U2ocv = 3.3277;

%85
% U_Square = U_SOC85(216166:223350);
%
% Imeas = data(734324:1342400,1) * 4.8;
% Icom = 1.286;
%
```

Figure A.23.: Matlab Time Domain for 3RC-Elements

```
% U1ocv = 3.3254;
% U2ocv = 3.324;

%75
% U_Square = U_SOC75(216264:223455);
%
% Imeas = data(1342400:1950700,1) * 4.8;
% Icom = 1.286;
%
% U1ocv = 3.3055;
% U2ocv = 3.2984;

%65
% U_Square = U_SOC65(216253:223450);
%
% Imeas = data(1950700:2559100,1) * 4.8;
% Icom = 1.286;
%
% U1ocv = 3.2870;
% U2ocv = 3.2868;

%55
U_Square = U_SOC55(216284:223480);

Imeas = data(2559078:3167600,1) * 4.8;
Icom = 1.283;

U1ocv = 3.2851;
U2ocv = 3.2848;

%45
% U_Square = U_SOC45(216305:223480);
%
% Imeas = data(2559078:3167600,1) * 4.8;
% Icom = 1.286;
%
% U1ocv = 3.2824;
% U2ocv = 3.2804;

% 35
% U_Square = U_SOC35(216387:223357);
%
```

Figure A.24.: Matlab Time Domain for 3RC-Elements

```
% Imeas = data(3776200:4385000,1) * 4.8;
% Icom = 1.286;
%
% U1ocv = 3.2544;
% U2ocv = 3.24945;

%25
% U_Square = U_SOC25(216428:223357);
%
% Imeas = data(4385000:4993900,1) * 4.8;
% Icom = 1.286;
%
% U1ocv = 3.2234;
% U2ocv = 3.2185;

%15
% U_Square = U_SOC15(216474:223660);
%
% Imeas = data(4993900:5602900,1) * 4.8;
% Icom = 1.2875;
%
% U1ocv = 3.1853;
% U2ocv = 3.1656;

%05 aborded



startmeas = 1;
endmeas = length(U_Square); %squarelength

%start square
t1 = startmeas;
%end square
t2 = endmeas;

%OCV curve


for i=t1:t2
    Uocv(i) = U1ocv -((i-t1)*(U1ocv-U2ocv)/(t2-t1));
end
```

Figure A.25.: Matlab Time Domain for 3RC-Elements

```
for i = startmeas:endmeas
    Ucom(i) = U_Square(i) - Uocv(i);
end


    %%%ACTUAL CURVE FITTING%%%

% editing Ucom to fit
Ucom = -Ucom;



No_Coeff= 7; %7 Coefficients are unknown ...
C1,C2,C3,R1,R2,R3,Ri...


optims=optimset('fminsearch');
optims.MaxIter = 10000000000;
optims.MaxFunEvals = 10000000000;
optims.TolX=1e-10;
optims.TolFun=1e-10;

start=[1;1;1;1;1;1;1];

%Initial Seed
KRi=0.45;
KR1=0.00055;
KR2=0.0151;
KR3=0.0151;
KC1=0.0931;
KC2=1.9317e+003;
KC3=1.9317e+003;


parameters=repmat(start,1,endmeas);

parameters(:,1) =
fminsearch('Timpedanz11123RC',parameters(:,1),optims);
```

Figure A.26.: Matlab Time Domain for 3RC-Elements

```
Ri=(parameters(1,1));
R1=(parameters(2,1));
R2=(parameters(3,1));
R3=(parameters(4,1));
C1=(parameters(5,1));
C2=(parameters(6,1));
C3=(parameters(7,1));


%%plot of the result

for t=startmeas:endmeas
    Ri=parameters(1,1);
    R1=parameters(2,1);
    R2=parameters(3,1);
    R3=parameters(4,1);
    C1=parameters(5,1);
    C2=parameters(6,1);
    C3=parameters(7,1);
URi = (Ri*KRi)*Icom;
URC1(t) = (R1*KR1)*Icom *(1 - exp(-t/
(100*(R1*KR1)*(C1*KC1))));
URC2 = (R2*KR2)*Icom*(1 - exp(-t/(100*(R2*KR2)*(C2*KC2))));
URC3 = (R3*KR3)*Icom*(1 - exp(-t/(100*(R3*KR3)*(C3*KC3))));
U1(t) = URC1(t) + URC2;
U2(t) = URC1(t) + URC2 + URC3;
U(t) = URi + URC1(t) + URC2 + URC3;
end


    Ri = (parameters(1,1))*KRi
    R1 = (parameters(2,1))*KR1
    R2 = (parameters(3,1))*KR2
    R3 = (parameters(4,1))*KR3
    C1 = (parameters(5,1))*KC1
    C2 = (parameters(6,1))*KC2
    C3 = (parameters(7,1))*KC3
    tau1 = R1*C1
    tau2 = R2*C2
    tau3 = R3*C3
% figure
% plot (parameters(1,:))
```

Figure A.27.: Matlab Time Domain for 3RC-Elements

```
figure
hold
plot((startmeas:endmeas)/100,U,'b')
title('Least Squares Fit - Time Domain')
ylabel('Voltage [V]')
xlabel('Time [s]')
plot((startmeas:endmeas)/100,URC1,'c')
plot((startmeas:endmeas)/100,U1,'c')
plot((startmeas:endmeas)/100,U2,'g')
plot((startmeas:endmeas)/100,Ucom,'r')


% FOR SIMULATION ONLY

% figure
% Simulation_Voltage_25 = U_SOC25(306433:342433);
% plot((1:36001)/100,Simulation_Voltage_25)

% Simulation_Voltage_45 = U_SOC45(306312:343302);
% plot((1:36991)/100,Simulation_Voltage_45)

% Simulation_Voltage_55 = U_SOC55(306289:342289);
% plot((1:36001)/100,Simulation_Voltage_55)

% Simulation_Voltage_85 = U_SOC85(306170:342170);
% plot((1:36001)/100,Simulation_Voltage_85)


% hold
% plot((1:360001)/1000,Output_Voltage.signals.values)
% plot((1:360001)/1000,Output_Voltage1.signals.values)
```

Figure A.28.: Matlab Time Domain for 3RC-Elements

```
function e=Timpedanz11123RC(p)

global startmeas endmeas Icom Ucom


Ri=p(1);
R1=p(2);
R2=p(3);
R3=p(4);
C1=p(5);
C2=p(6);
C3=p(7);



global KRi KR1 KR2 KR3 KC1 KC2 KC3

e = 0;

for t = startmeas:endmeas

URi = (Ri*KRi)*Icom;
URC1 = (R1*KR1)*Icom *(1 - exp(-t/
(100*(R1*KR1)*(C1*KC1))));
URC2 = (R2*KR2)*Icom *(1 - exp(-t/
(100*(R2*KR2)*(C2*KC2))));
URC3 = (R3*KR3)*Icom *(1 - exp(-t/
(100*(R3*KR3)*(C3*KC3))));
U = URi + URC1 + URC2 + URC3;

e = e + (U - Ucom(t))^2;


if Ri < 0 || R1 < 0 || R2 < 0 || R3 < 0 || C1 < 0 || C2 < 0
|| C3 < 0
    e = e + 10;
end
end
```

Figure A.29.: Matlab Time Domain for 3RC-Elements - Least Squares Fit